AN ABSTRACT OF THE DISSERTATION OF

D. James Minick for the degree of Doctor of Philosophy in Toxicology presented on January 17, 2018

Title: Advancement of Passive Sampling Applications for Assessing Contaminant Transport, Bioaccumulation, and Toxicity

Abstract approved:

Kim A. Anderson

In the environment, it is the unbound fraction of chemical (C_{free}) which is able to diffuse across environmental interfaces and biological membranes. It is therefore C_{free} which drives many important biological-environmental processes including contaminant transport, bioaccumulation and toxicity. Passive sampling devices (PSDs) offer a simplified and more accurate approach for measuring C_{free} compared to traditional methods. The chapters of this dissertation extend the applications of passive sampling for answering questions related to the transport, bioaccumulation, and toxicity of contaminants, specifically polycyclic aromatic hydrocarbons (PAHs). In Chapter 1, using PSDs, we measured the diffusive flux of PAHs between sediment, water, and air at the Portland Harbor Superfund site (PHSS). Data indicated that modern (atmospheric) sources of 2- and 3-ring PAHs were more significant than legacy (sediment) sources. Additionally, the data pointed toward PHSS sediments as potential atmospheric sources of 4-ring and larger PAHs through diffusion. This result may have significant health risk implications for those living near the PHSS and other contaminated sites. Ultimately, data generated by this study was used to make a regulatory decision at the McCormick and Baxter Superfund site, highlighting the growing acceptance and applicability of passive sampling

devices. Transport of contaminants may lead to exposure and bioaccumulation in humans and organisms. When organisms are consumed by humans, measuring bioaccumulation of contaminants in those organisms is essential for assessing human health risk. This is especially true for subsistence consumers who have elevated ingestion rates including Native American tribes. Traditional predictive methods for bioaccumulation in benthic organisms are often inaccurate because of reliance on poorly characterized and understood site specific sediment characteristics. Passive sampling devices directly measure C_{free} and therefore inherently account for these site specific differences. In Chapter 2, sediment PSDs were used to build a model for predicting PAH concentrations in traditionally harvested clams on Native American tribal land in the Puget Sound region of the Salish Sea. The model was able to predict PAH concentrations in butter clams (*Saxidomus giganteus*) within a factor of 1.9 ± 0.2. This model will provide a more accurate and simplified method to monitor PAH concentrations in clams without having to remove clams from the environment. Additionally, data from this study highlighted spatial differences in carcinogenic risk associated with the consumption of clams and was used to inform local communities. Bioaccumulation of PAHs may result in health effects if the PAHs are toxic. In the environment PAHs exist as mixtures and it is therefore essential to consider the toxicity of relevant environmental PAH mixtures. There is growing evidence for developmental effects (morphological and neurological) from PAH exposure. In Chapter 4, data from passive sampling devices deployed in surface water at the PHSS was used to construct a surrogate mixture of the 10 most abundant PAHs (Supermix10). Using the zebrafish model, we assessed the developmental toxicity of Supermix10 (SM10), its toxic (Supermix3) and non-toxic (Supermix7) sub-fractions, and the 10 individual PAHs. Data indicated that the general additivity model may be sufficient for explaining the overall developmental effects caused by these PAH mixtures. However, we showed that individual PAH toxic endpoints may not be predictive of the toxic

endpoints in PAH mixtures. Finally, SM10 caused behavioral effects in adult fish following exposure during development at concentrations below those which caused overt morphological effects. Ultimately the work in this dissertation advances the application of passive sampling technologies toward a better understanding of PAH transport, bioaccumulation, and toxicity.

Advancement of Passive Sampling Applications for Assessing Contaminant Transport, Bioaccumulation, and Toxicity

by
D. James Minick

A DISSERTATION

submitted to

Oregon State University

in partial fulfillment of
the requirements for the
degree of

Doctor of Philosophy

Presented January 17, 2018
Commencement June 2018

Doctor of Philosophy dissertation of D. James Minick presented on January 17, 2018.

Approved:

Major Professor, representing Toxicology

Head of the Department of Environmental and Molecular Toxicology

---

Dean of the Graduate School

I understand that my dissertation will become part of the permanent collection of Oregon State University libraries. My signature below authorizes release of my dissertation to any reader upon request.

D. James Minick, Author

ACKNOWLEDGEMENTS

First, I would like to thank my advisor, Dr. Kim Anderson. The opportunity to be part of the Food Safety and Environmental Stewardship (FSES) Lab has been a wonderful opportunity and experience. Thank you for your patience and guidance through the course of my time in the lab. I also would like to extend my thanks to the faculty and staff of the Department of Environmental and Molecular Toxicology for the wonderful learning opportunities you have given me. A special thanks to my committee: Dr. Staci Simonich, Dr. Susan Tilton, Dr. Robert Tanguay, and Dr. Michelle Odden. I'd also like to thank my undergraduate professors: Dr. Jeffrey Peloquin, Dr. Kristen Mitchell, and Dr. Ken Cornell whom inspired me to pursue science and strive for excellence.

To all of the staff in the FSES lab; thank you for your support through the good times, and the difficult times. To Blair Paulik, Carey Donald, Alan Bergman, Holly Dixon, Gary Points, Kevin Hobbie, Carolyn Poutasse, Pete Hoffman, Josh Willmarth, Glenn Wilson, Christine Ghetu, Steven O'Connell, and everyone else, thank you. I would also like to say thank you to collaborators at the Sinhueber Aquatic Research Laboratory at Oregon State University including Dr. Robert Tanguay, Mitra Geier, and Lisa Truong. Finally, I would like to say thank you to the Native American tribes who were the driving force behind the work in Chapter 3 and from whom I learned so much.

To my friends and family, thank you for all your support. To Dr. Grant Meredith and Alicea Meredith, thank you for being my second family in Corvallis. To Dr. Matt Perkins, Barrett Welch, Greta Fey, Pepa Roth and all the rest of my truly wonderful friends- thank you for the exciting adventures and hardy laughs. To my parents; I am completely sure that I wouldn't have accomplished this without your support and guidance through the years, so thank you. Thank you Jessica and Josie for being equally awesome sisters.

CONTRIBUTION OF AUTHORS

Dr. Kim Anderson's contributions can be seen throughout the entirety of this work.

In Chapter 2, multiple members of the FSES lab contributed to the field work and sample processing including Blair Paulik, Carey Donald, Alan Bergman, Lane Tidwell, Steven O'Connell, Holly Dixon, and Gary Points. Steven O'Connell and Lane Tidwell were also highly involved in the design of the passive sampling equipment used in this work.

In Chapter 3, Dr. Blair Paulik was responsible for study design including collection of clams and deployment and extraction of passive samplers. Dr. Brian Smith was involved with data analysis and interpretation. Richard Scott assisted with sample processing and provided analytical expertise. Dr. Molly Kile and Dr. Diana Rohlman were primarily responsible for communicating with the Native American tribes in the study.

In chapter 4, Dr. Mitra Geier was an equal contributor and was involved with all phases of the work including study design, data interpretation, and writing. Dr. Lisa Truong assisted with study design, data analysis and writing. Dr. Susan Tilton assisted with writing and provided expertise in mixture toxicity. Dr. Robert Tanguay contributed to all aspects of this work.

TABLE OF CONTENTS

Page

TABLE OF CONTENTS (Continued)

Page

LIST OF FIGURES

LIST OF TABLES

LIST OF APPENDIX FIGURES

LIST OF APPENDIX TABLES

Advancement of Passive Sampling Applications for Assessing Contaminant Transport, Bioaccumulation, and Toxicity

CHAPTER 1 – INTRODUCTION

The freely dissolved fraction

Spontaneous chemical processes in the environment including diffusion across environmental compartments and biological membranes are driven by chemical activity[1]. Chemical activity is determined by the concentration of chemical which is not bound to particles or to dissolved organic carbon, but rather, is freely dissolved (C_{free}) [2, 3]. For this reason, C_{free} is often a better indicator of contaminant bioavailability and bioaccumulation, and subsequently toxicity compared to total chemical concentration [4-9]. Determination of C_{free} is therefore critical for answering a wide range of questions related to the potential impact of contaminants on humans and organisms in the environment.

Traditional methods for quantifying C_{free} are problematic because of the large sample sizes required and the highly involved laboratory procedures which may artificially alter the sampled matrix [10]. Meanwhile, passive sampling devices (PSDs) accumulate hydrophobic contaminants in a similar manner to organisms; through chemical activity driven, diffusional processes[11]. Passive sampling therefore offers a direct, simple approach to measure C_{free} in environmental matrices. Work over the last 30 years has resulted in a wide range of passive sampling devices and techniques to measure hydrophobic contaminants in sediments, water, and air [12-14]. These studies have shown that passive sampling devices offer a more accurate, simpler, and therefore cheaper way to determine C_{free} and to measure chemical transport and to predict bioaccumulation and toxicity [15].

The work described in this dissertation takes advantage of the ability of passive sampling devices to accurately and easily measure C_{free}. Specifically, we demonstrate an expansion of passive sampling applications to answer questions regarding the transport, bioaccumulation, and toxicity of the environmental contaminants, polycyclic aromatic hydrocarbons (PAHs). Traditionally, concern regarding the health effects of PAHs were focused on their carcinogenicity[16]. However, several studies have reported neurological and morphological effects caused by developmental exposure to PAHs in both humans and fish[17-22]. Ultimately this work will serve to protect the health of humans and organism in the environment from the impact of chemical contaminants.

Transport

Understanding contaminant transport in this environment is important for determination of potential chemical risk and for informing remediation and management decisions of contaminated sites[12, 23]. Of environmental chemical transport processes, diffusion is the only continuously active process and has been used as a baseline for total flux[24]. Previous studies have shown that the diffusive flux of PAHs between water and air may play a large role in controlling total PAH load [25, 26]. In addition, the sediment may be an important source of PAHs to the overlying water and the air[27]. This raises concern over the potential PAH exposure for residents living near a PAH contaminated Superfund site. Although studies have investigated both sediment-water and water-air flux independently, in Chapter 2, for the first time we used PSDs to measure the diffusive flux of PAHs between sediment porewater and water-air concurrently. Data from this study was used to gain insight into the relative importance of both atmospheric and sediment sources of PAHs at the Portland Harbor Superfund Site (PHSS) and the McCormick and Baxter Superfund site (MCBSS) near Portland, Oregon. We showed that the atmosphere is generally a larger source of 2- and 3-ring PAHs to the water than contaminated sediments while the reverse is true for 4-ring PAHs and larger. In addition, the data indicates that contaminated sediments in the PHSS may ultimately lead to inhalation exposure for residents through diffusional flux from sediments to the water and from the water to the air. This study and similar types of studies will play an important role in informing remediation efforts, highlighting cleanup priorities, and bringing to light potential contamination sources which might ultimately undermine those efforts[23]. Indeed, data from the study at the MCBSS was used by the Oregon Department of Environmental Quality (ODEQ) to determine that the sediment cap continues to be effective in containing contaminants from entering into the overlying water[28]. This decision by ODEQ highlights the growing acceptance of passive sampling in the regulatory world.

Bioaccumulation

Transport of chemicals in the environment may result in exposure and bioaccumulation in both humans and other organisms [9]. When organisms are a food source for humans, assessing bioaccumulation in those organisms is important for quantifying human health risk. This is true for subsistence consumers such as Native American tribes of the Pacific Northwest[29]. Measuring contaminant concentrations directly in organisms is difficult, may deplete an important cultural/subsistence food, and has negative impact on the ecosystem[30]. For benthic organisms, this

has given rise to predictive tools using total sediment concentrations but these are often inaccurate due to the presence of highly hydrophobic types of organic carbon which vary between locations [31, 32]. Passive sampling directly measures C_{free} and studies have shown that passive sampling predictive methods are often more accurate for benthic organisms [6, 10]. In Chapter 3, a model was built using passive sampling derived sediment porewater PAH concentrations to predict PAH concentrations in butter clams (*Saxidomus giganteus*) from adjudicated usual and accustomed Native American tribal fishing grounds and stations in the Salish Sea located in the Pacific Northwest. The model was able to predict PAH concentrations in butter clams within a factor of 2 highlighting its applicability for monitoring of this important food source. Additionally, the data showed high spatial variability in PAH concentrations and carcinogenic risk and this was communicated back to the communities to inform subsistence harvesters.

Mixture Toxicity

Ultimately, health effects resulting from chemical exposure and bioaccumulation may occur if the chemicals are toxic. In the environment, exposure to chemicals occurs almost exclusively to mixtures of chemicals rather than to individual chemicals [33, 34]. Component based approaches for mixture toxicity are limited to individual chemicals with detailed mechanistic data while whole mixture approaches are difficult because of the nearly infinite number of potential whole chemical mixtures. Another approach which may represent a compromise between these existing approaches is the sufficiently similar, or representative mixture approach. This approach is based on the idea that the relative ratios of chemicals from sources are similar and that preservation of those ratios in a surrogate mixture allows for assessment of toxicity[35]. In Chapter 4 of this dissertation, using passive samplers to measure C_{free} in the water, we demonstrate the use of the representative mixture approach to assess the developmental toxicity of a mixture of the 10 most abundant PAHs (Supermix10) in the PHSS. The zebrafish developmental toxicity model was used to determine the potential hazard of Supermix10 (SM10), its toxic (Supermix3) and non-toxic sub fractions (Supermix7), and the individual PAH components. Importantly, this data showed that although the overall developmental toxicity of SM10 may be predicted from the individual components using the general additivity model, the individual toxic endpoints differ compared to the mixture. Additionally, we showed that developmental exposure to SM10 may result in neurobehavioral impacts in adulthood even in the absence of morphological impacts.

The work presented in this dissertation represents an advancement in the applications of passive sampling technologies toward understanding the transport, bioaccumulation, and toxicity of PAHs.

Chapter 2 –DIFFUSIVE FLUX OF PAHS ACROSS SEDIMENT-WATER AND WATER-AIR INTERFACES AT URBAN SUPERFUND SITES

D. James Minick and Kim A. Anderson

Department of Environmental and Molecular Toxicology, Oregon State University, ALS 1007, Corvallis, OR, 97331

Accepted: Environmental Toxicology and Chemistry

SETAC Press

2017, Vol. 36, No. 9, pp. 2281-2289

Abstract

Superfund sites may be a source of polycyclic aromatic hydrocarbons (PAHs) to the surrounding environment. These sites can also act as PAH sinks from present day anthropogenic activities especially in urban locations. Understanding PAH transport across environmental compartments helps to define the relative contributions of these sources and is therefore important for informing remedial and management decisions. In the present study, paired passive samplers were co-deployed at sediment-water, and water-air interfaces within the Portland Harbor Superfund site (PHSS) and the McCormick and Baxter Superfund Site (MCBSS). These sites, located along the Willamette River in Portland, Oregon, have PAH contamination from both legacy and modern sources. Diffusive flux calculations indicate that the Willamette River acts predominately as a sink for low molecular weight PAHs from both the sediment and the air. The sediment was also predominately a source of 4 and 5 ring PAHs to the river and the river was a source of these same PAHs to the air, indicating that legacy pollution may be contributing to PAH exposure for residents of the Portland urban center. At the remediated MCBSS flux measurements highlight locations within the sand and rock sediment cap where contaminant breakthrough is occurring.

Introduction

Polycyclic aromatic hydrocarbons (PAHs) are a widespread class of persistent chemicals arising from both natural sources and anthropogenic activities [36]. In addition to the carcinogenic potential of some PAHs which are thought traditionally to drive health risks [16], PAHs have also been shown to be toxic in developing fish [37], and evidence is emerging for their neurotoxicity and negative impact on pulmonary function in humans [21, 38].

A lack of regulation on industrial discharge into water bodies before The Clean Water Act of 1972 has left many urban water bodies in the USA with highly contaminated sediments [39, 40]. These sediments may be a continual source of contaminants, including PAHs, to the overlying water and surrounding environment long after cessation of direct discharge [41]. Additionally, with a continued reliance on fossil fuels and expanding urban populations, urban water bodies are subject to an increase in PAH load from non-point sources such as vehicle exhaust and storm water runoff [42-44].

Understanding the direction and magnitude of contaminant transport at these locations is important for determining the relative contribution from modern and legacy sources and subsequently for informing remedial and management decisions [23]. The exchange of contaminants between sediment and water may occur through several processes including the transport of colloids, particle resuspension/deposition, gas ebullition, advective flow, bio-irrigation, and diffusion. Meanwhile, chemical water-air exchange may result from particle deposition as well as diffusion [45]. Of these processes, diffusive flux is the only process which occurs in every system and is therefore a conservative standard baseline for total flux. Additionally, diffusive exchange has been shown to be a prominent factor for controlling urban water concentrations and measurements can provide insight into the relative contributions from other chemical exchange mechanisms [24, 25]. Diffusive flux is dependent upon the freely-dissolved (C_w) concentration gradients across environmental compartments [24]. These freely-dissolved fractions are also a better indicator for bioavailability, bioaccumulation, bio-concentration and toxicity in both water and sediment [5, 6, 23].

To measure freely dissolved and vapor phase PAH concentrations, traditional active sampling combined with filtration and/or centrifugation have been used, but can be cumbersome [25, 46, 47]. Sediment equilibrium models for porewater measurements have been shown to be highly inaccurate due to their reliance on poorly described and often highly heterogeneous sediment characteristics [48]. Passive sampling allows for a direct measurement of C_w and C_a, avoiding filter bias and providing a time-weighted average incorporating episodic events [49]. Several studies have demonstrated the use of passive samplers to measure the diffusive flux of PAHs across air-water interfaces[25, 26, 46, 50-53]. Fewer studies have utilized passive samplers to measure the diffusive flux of PAHs between porewater and water [27, 54, 55]. To the author's knowledge, the present study is the first to measure PAH diffusive flux across both interfaces concurrently.

The Portland Harbor is located along the Willamette River in Portland, Oregon, USA and is a typical urban harbor with a history of industrial pollution dating back to the 19th century. Industrial processes including gas manufacturing, wood treatment and bulk fuel processing have resulted in high levels of contaminants including PAHs, PCBs, and metals in sediment and shoreline along much of the harbor. Subsequently, an approximately 11-mile section of the river, the Portland Harbor Superfund site (PHSS) was added to the U.S. EPA's National Priorities List

in 2000 [56]. With a surrounding metropolitan population of over 2 million people, modern non-point sources such as vehicle emissions are also likely a major source of PAHs to the Portland Harbor.

Here we demonstrate the deployment of passive samplers across both the sediment-water and water-air interfaces to better understand the relative contributions from legacy and modern day pollution using the Portland Harbor as a model urban aquatic system as depicted in Figure 1. Larsson [57] showed that aquatic sediments have the potential to be a source of hydrophobic organic pollutants to the air and residents of the Portland Harbor area have voiced concerns over fumes and vapors arising from the PHSS [58]. The study design presented here helps to inform about PAH fate for residents living near the Portland Harbor and may be applied to other contaminated urban waterways. Diffusive flux of 61PAHs was determined across both interfaces at 6 different locations including upriver, downriver, and within the PHSS. Additionally, diffusive flux was determined across the sediment-water interface at 14 locations within the McCormick and Baxter Superfund Site (MCBSS) where a sediment cap was placed in 2005 to contain creosote plumes from entering the river [59]. Using a novel sediment probe design, we present the first published work of PAH diffusive flux at a remediated Superfund Site to assess sediment cap effectiveness. This probe allowed for measurement of porewater concentrations at discrete depths both within and below the sediment cap to assess the performance of the cap and assess the implications of cap failure. This probe has the potential to be used in a wide variety of soils and setting because of its durability, ease of deployment, and ability to measure discrete porewater

Materials and Methods

Study Area

The PHSS is located on the Willamette River as it flows north through the city of Portland, Oregon from River Mile (RM)1.9 to RM11.8 as measured upstream of the Columbia River, shown in Figure 2. Several locations within the Superfund site were termed “early action areas”. These locations include the eastern shore at RM11 (RM11E) due to high levels of PCBs and PAHs, and RM6.5W, home to a former gas manufacturing plant where a large tar ball was removed in 2005.

The MCBSS was added to the Superfund National Priorities List in 1994 and is located within the PHSS at RM7E where the McCormick and Baxter Creosote Company operated from 1944-1991 [59]. In 2005, approximately 22 acres of contaminated sediment was capped with sand, organoclay, and a concrete/rock armoring to contain creosote seeps and prevent release of contaminants, including PAHs and pentachlorophenol from sediments. Additionally, construction was completed on an 18-acre subsurface barrier wall extending 14 to 24 meters below the surface to eliminate potential for upland contaminant migration into the river.

Sampling methodology

Deployment of PSDs occurred in September and October of 2015 at 14 locations within the MCBSS, 4 locations within the PHSS (RM11E, RM7E, RM6.5W, RM3.5W), 1 upstream (RM18.5E), and 1 downstream location (RM1E) (Figure 2.2).

At RM18.5E, RM11E, RM7E, RM6.5W, RM3.5W, and RM1E pairs of PSDs were co-deployed across sediment-water and water-air interfaces. For determination of water-air flux, PSDs were deployed from Dock-Blocks® platforms. Air cages containing 5 LDPE strips were placed 1m above the surface of the water. Below each platform, a cage containing 5 LDPE strips was deployed from a steel cable 1m below the surface of the water ($1m_{surface}$). The anchoring mechanism allowed for approximately 20 meters of platform movement in the river. These platforms were co-located with paired sediment and water PSDs at RM18.5E, RM11E, RM 7E, RM6.5W, RM3.5W, and RM1E (Figure A2). Novel sediment probes to measure porewater were driven into the sediment until flush with the sediment surface (Figure A4). Briefly, these 25cm long probes consist of stainless steel casing and mesh windows coupled with a slide hammer adapter allowing for easy deployment into sediments from a standing position or by divers. An aluminum or steel insert is placed inside the probe around which LDPE strips are wrapped and secured. Similarly designed 25cm long extensions can be connected allowing for sampling at multiple depths with no concern of vertical contaminant migration (Figure A4). Water cages were deployed 0.3m above the surface of the sediment ($0.3m_{bottom}$) on a steel cable attached to a submerged buoy to ensure stability within the water column.

Within the MCBSS, paired sediment and water PSDs only were deployed at 14 locations. These samplers were placed into the cap with the help of EPA divers as part of a 10-year sediment cap effectiveness assessment conducted by the Oregon DEQ. At sampling locations 1 (MCB-1),

MCB-2, MCB-3, and MCB-4 a probe extension was used to measure porewater from 0-25cm (armoring) and 25-50 cm below the surface (inter-armoring). In the case of MCB-1 and MCB-2, the articulated concrete cap was removed and sediment probes were placed directly into the sand layer of the cap. For the remaining 12 locations the sediment probes were placed into the top layer of the cap which consisted of rock, sand, and deposited sediment.

Samplers within the McCormick and Baxter superfund site were deployed for approximately three weeks (September 15-16, 2015-October 6, 2015). The remaining samplers were deployed for 5 weeks (September 14, 2015-October 19, 2015). Environmental conditions and deployment are described in detail in supplemental data (Table A4).

PSD preparation and extraction

Additive free low-density polyethylene (LDPE) passive sampling devices (PSDs) were constructed in 1-meter-long strips as described in Anderson et al. [60]. Three performance reference compounds (fluorene-d10, pyrene-d10, and benzo[b]fluoranthene-d12) were added to the samplers prior to deployment for determination of *in situ* uptake rates. Analyte sampling rate was derived from PRC loss using only PRCs with dissipation greater than 10% and less than 90%. In this way, pyrene-d10 was used for all water and air calculations, and fluorene-d10 was used for all sediment calculations. At location MCB-3, fluorene-d10 depletion was less than 10% for both porewater measurements and data therefore should be considered to having higher error. PRC dissipation is shown in Appendix A (Table A13).

LDPE strips were transported back to the lab in glass jars placed in coolers, within 12 hours, and stored at -20°C prior to sample processing. Sample processing is described in detail by Allan et al. [61], but briefly, PSDs were spiked with 7 deuterated surrogate extraction standards followed by dialysis in n-hexane and quantitative concentration. Surrogate extraction standards included: naphthalene-d8, acenaphthylene-d8, phenanthrene-d10, fluoranthene-d10, chrysene-d12, benzo[a]pyrene-d12 and benzo[ghi]perylene-d12. Surrogate recoveries ranged from 51% for naphthalene-d12 (RSD 13.8%) to 92% for benzo(a)pyrene-d12 (RSD 5.8%). Perylene-d12 was used as the instrumental internal standard. Transport stability studies performed by Donald et al. [62] verified that the transport times (12 hours) and temperatures (<20C) should not result in loss of PAHs. All solvents used were Optima grade or better (Fisher Scientific), and standards were purchased at purities ≥ 97%.

Chemical analysis

Samples were analyzed for 61 PAHs (Table A1) using an Agilent 7890A gas chromatograph (GC) with an Agilent 7000C MS/MS as described in Anderson et al. 2015 [63]. Use of an Agilent Select PAH column (30m x 250µm x 0.15µm) allowed for enhanced separation of compounds. For all PAHs at least a 5-point calibration was employed with correlations ≥0.98. GC oven and MS parameters along with a comprehensive list of method detection limits (MDLs) can be found in Appendix A.

Quality control

Quality control samples including field, trip, instrument, cleaning, reagent, and laboratory blanks as well as laboratory duplicates and over-spikes accounted for over 30% of the total samples run. Blanks contained quantifiable levels of several low molecular weight PAHs (Table A5) making up less than 1% of all PAHs measured. Samples were corrected for background concentrations by adding the average extract value for field and cleaning blanks and subtracting this value from sample extract values. To assess field variability, relative standard deviation was calculated (Table A6) from samplers deployed in triplicate in each of the three matrices (sediment, water, air) at RM 6.5. Due to the high heterogeneity of sediment, the triplicate porewater samplers at RM6.5 (RM6.5-1, RM6.5-2, RM6.5-3) will be referred to as 'approximates'. To ensure instrument consistency over the course of analysis, continuing calibration verification samples were run and in all cases met data quality objectives. Further details can be found in Appendix A.

Calculations

We calculated the freely dissolved (C_w) and vapor phase (C_a) PAHs on both sides of the sediment-water and water-air interfaces using PSDs and an empirical uptake model with PRC derived sampling rates described by Huckins et al. [11]. Further details can be found in Appendix A.

Calculations for diffusive flux (F_x), expressed in units of mass/(area x time), followed the basic form of Fick's First law where a negative flux value is defined as deposition and a positive flux value is defined as release or volatilization. Here, flux is represented as a function of the concentration gradient (C) across the x-axis (environmental interface) and the molecular diffusion coefficient (D) which is determined by both the specific properties of the chemical and environmental conditions [45].

$$F_x = D\left(\frac{dC}{dx}\right) \quad (1.1)$$

Diffusive flux across the air-water interface ($F_{w\text{-}a}$) followed a Whitman 2 film model, as described in Bamford et al. [25], which defines transport rate as being limited by movement across 2 thin stagnant layers at the air-water interface described by the total mass transfer coefficient (K_{ol}) as shown below in *Equation 2 (Equation 2)*.

$$F_{w-a} = K_{ol}(C_w - \frac{C_a}{H_T'}) \quad (1.2)$$

In this equation, $H_{(T)}$' is the unitless Henry's law constant, corrected for temperature using the Van't Hoff equation *(Appendix A, equation A14)*. The total mass transfer coefficient consists of air-side and water-side mass transfer coefficients which are a function of wind speed, temperature, and specific chemical characteristics (*Appendix A, equation A11-A13*).

Diffusional flux ($F_{s\text{-}w}$) across the sediment-water interface is assumed to be rate limited by a thin layer of stagnant water called the boundary layer (δ_L). Calculations followed a similar method to Fernandez et al. [24] as shown in Equation 3 (Equation 3).

$$F_{s-w} = -\frac{D_w}{\delta_L}\left(C_w - C_{pw}\right) \quad (1.3)$$

In this equation, C_{pw} is the freely dissolved concentration in porewater and D_w (cm^2/s) is the compound specific diffusion coefficient in water.

$$D_w = \frac{13.26\ x\ 10^{-5}}{\eta^{1.14}\ V^{.589}} \quad (1.4)$$

In Equation 1.4 , V is the molar volume of the chemical as a liquid (cm^3/mol) calculated using the *LeBas method* and η is the viscosity of water (10^{-2}g/cms) at the average water temperature during deployment. Equation 1.4 is based on a pseudo-empirical relationship and must be used with the defined units [64]. Determination of diffusional flux between the armoring (0-25cm) and sub armoring (25-50cm) is discussed further in Appendix A.

Accurately estimating δ_L depth is important for describing the magnitude of diffusional flux. Boundary layer thickness decreases with increasing flow and increases with sediment surface roughness. Several studies have attempted to measure δ_L thickness and have reported similar

values. Jorgensen et al. [65] used microelectrodes to measure oxygen gradients in a controlled laboratory environment and determined δ_L to be 0.025 and 0.05cm for rough and smooth sediment respectively with flow velocity between 10 and 20 cm/s. Santchi et al. [66] reported δ_L thicknesses of 0.019 and 0.013 for flows of 8.4 and 15.3 cm/s based on gypsum dissolution rates while Eek et al. [27] replicated these measurements but in a stagnant environment and calculated a boundary layer of 0.17cm. Koelmans et al. [54] took a different approach to measure PAH flux between sediment and water by directly measuring the mass transfer coefficient (Kl), equal to D_w/ δ_L if transport is assumed to be controlled by the water side resistance and no gradient exists in the sediment. A laboratory measured Kl of 0.024 m/d was applied to PAH gradients between sediment and water in lakes, canals, and harbors in the Netherlands. This number is similar to the mass transfer coefficients used by Eek et al. [27] (0.020 m/d- 0.027 m/d) to measure flux of PAHs from sediment to water in Norway based on a stagnant water boundary layer.

Near its terminus, the tidally influenced Willamette River runs through a smooth, homogenous river channel and therefore, only minor differences are expected in flow or sediment type between sampling locations. During the course of the 5-week deployment in Portland Harbor, the average absolute flow velocity was 14.5 cm/s as measured by a USGS station downtown Portland. This flow velocity typically corresponds with a smooth river bottom composition of silt, mud and small organic debris and falls within the range of measured boundary layer thicknesses reported by Santchi et al. and Jorgensen et al. [65, 66]. Considering the homogeneity of the river channel and the flow rate, it was determined to be both practical and valid to use a single δ_L thickness of 0.02 cm for all flux calculations. The subsequent mass transfer coefficient values are therefore approximately an order of magnitude higher (0.18 to 0.29 m/d) than the values used by Koelmans et al. and Eek et al. [27, 54]. However, the aforementioned studies were based on stagnant water boundary layers and we would therefore expect a much higher mass transfer coefficient with higher flows and resultant smaller boundary layers for locations in the present study.

Statistics

Analytes below method quantification limits were assigned values of one-half method quantitation limits (MQLs) (Table A1). Relative standard deviation was calculated based on n=3 replicates in water, and air and on n=3 ‘approximates’ in sediment at RM6.5W (RM6.5(1), RM6.5(2), RM6.5(3)) as displayed in Table A6. Propagation of error in flux across the water-air

interface followed Liu et al. [67] assuming relative uncertainties of 30% and 50% for air-water mass transfer velocities and Henry's law constants respectively. Uncertainty in temperature was determined from temperature measurements at RM6.5W. Error in flux across the sediment-water interface was calculated in a similar manner assuming a relative uncertainty of 30% in the mass transfer velocity. Flux uncertainty calculations here are therefore conservative as compared to others such as Bamford et al. [25] who have not included uncertainty in Henry's law constants.

Results and Discussion

Sediments, a source of vapor phase PAHs

Throughout the PHSS results indicate that the Willamette River is largely a sink for 2 and 3-ring (low molecular weight) PAHs from the air while being a source for many 4-ring and larger (high molecular weight) PAHs especially at locations within and below the PHSS. Phenanthrene was in deposition across the water-air interface at all locations ranging from -280 (± 220) ng/m^{2}d at RM1E to -2400 (± 1900) ng/m^{2}d at RM7E. These values fall within the range of values for phenanthrene reported by McDonough et al. [51] at both urban and rural locations in the Great Lakes region. In a similar manner to McDonough et al., there was no correlation in the present study between water and air concentrations for phenanthrene suggesting that diffusive exchange is not the only mechanism influencing aqueous concentrations of phenanthrene.

The greatest volatilization fluxes determined in the study area were for pyrene and retene. In the case of pyrene, the magnitude of volatilization downstream of the PHSS at RM1E was more than a factor of 4 greater than upstream of the PHSS at RM18.5E indicating that the PHSS is likely a source of vapor phase pyrene in the atmosphere even after the river passes through the site. This difference was driven by an increase in dissolved water concentration. Pyrene also showed high volatilization in the Great Lakes region, though the magnitudes of volatilization were up to a factor of 7 greater than reported here [51].

At the sediment-water interface greatest PAH release from sediment was determined at locations within the PHSS and MCBSS with high individual PAH and location variability reflecting the heterogeneity of the sediment. Hydrophobic contaminants in the sediment have the ability to be a source to the overlying water and ultimately to the air as shown by Larsson [57] and more recently proposed to be the case in the sediment plume of the Yangtze River in China [68]. Examination of

individual PAH flux patterns here showed several cases supporting the possibility of sediments being a source to the air. In the case of acenaphthylene, we determined volatilization to be occurring at RM6.5 and downstream locations coupled with large release from the sediment at RM6.5(1) and locations MCBJ and MCB2 as seen in Figure 2.3 and Figure 2.4. Pyrene exhibited deposition into the sediment above and below the PHSS while being released out of the sediment at locations within the PHSS and MCBSS coupled with high volatilization within the PHSS. Additionally, a greater number of instances of positive flux across both interfaces occurred within the PHSS compared to outside of the site. Of 61 PAHs analyzed, an average of 17 individual PAHs were diffusing from sediment to water and from water to air for locations within the PHSS compared to 2 outside of the PHSS.

While not definitive, these results support the hypothesis that legacy contaminated sediments are a source of PAHs to the air. This is potentially of concern for those living near Superfund sites and warrants further investigation. Indeed, it is estimated that approximately 53 million Americans, or approximately 17% of the U.S. population, live within 3 miles of a Superfund Site [69]. Furthermore, these data illustrate a process by which legacy contamination may be redistributed through transport on both a regional and global scale.

Comparison of flux magnitudes

A comparison of flux magnitudes in the present study shows that diffusive flux from air to water for low molecular weight (LMW) PAHs was generally greater than LMW PAH exchange across the sediment-water interface throughout the study area. Assuming a historical origin of sediment PAHs, a comparison of flux magnitudes across sediment-water and water-air interfaces can provide insight into the relative PAH contributions from both legacy sources as well as modern anthropogenic activities in urban aquatic systems. Following this logic, the results in the present study point toward modern anthropogenic activity being a larger source of LMW PAHs than legacy pollution. This was reflected by generally higher vapor phase PAH concentrations at locations downwind and closer to downtown Portland (RM7E, RM11E, RM18.5E). Bamford et al. [25] also showed that emissions from an urban center drove deposition of vapor phase phenanthrene into an adjacent water body, Chesapeake Bay, and estimate that diffusive exchange contributed greater than 90% of total loadings of PAHs from the atmosphere.

Conversely, legacy pollution in sediment appears to be a greater source of dissolved HMW PAHs to the Willamette River compared to vapor phase PAHs from modern anthropogenic activity. In cases where these HMW PAHs were volatilizing within the PHSS, the magnitude was lower than flux from sediments suggesting that many of these freely dissolved HMW PAHs are transported downstream and deposited. This is supported by the determination that dissolved concentrations of HMW PAHs below the PHSS at RM1E (5.6ng/L) were more than double the concentration above the PHSS at RM18.5E (2.5ng/L). However, redistribution of contaminants may also be occurring on a local scale which is demonstrated by the replicates at RM6.5W. Sediment release of contaminants occurred at RM6.5W(1) and RM6.5W(2) while deposition occurred at RM6.5W(3) with a distance of less than 1m separating the samplers. The small magnitudes of HMW PAH transfer across the air-water interface may also be due to the low fraction of vapor phase HMW PAHs in the atmosphere. Indeed, particulate bound HMW PAHs may be an important contributor to PAH load, a question beyond the scope of the present study.

The study design presented here demonstrates how passive samplers may be co-deployed across environmental interfaces to better understand the relative contributions from sources at urban locations. Such knowledge may help to prioritize remediation strategies and is a critical piece for management decisions at sites such as the PHSS [23].

Flux measurements highlight seepage areas in sediment cap

Flux measurements on the MCBSS sediment cap show a highly dynamic area with instances of both PAH release and deposition as seen in Figure 2.4. The sediment cap was constructed in 2005 and consists of sand with organoclay in spots, on top of which lies a rock armoring with concrete in areas subject to erosional processes. The newly described sediment probe (described further in Appendix A) was placed into the rock armoring at 10 locations. At 4 locations, an extension was used to measure porewater at discrete depths below the armoring to assess the potential for future cap failure, called “early warning locations”. This probe has the potential to be used in a wide variety of soils and settings because of its ruggedness, durability, and ability to measure discrete porewater depths.

At two of the locations Σ61PAH diffusive flux from the sediment was nearly two orders of magnitude higher than any other flux measurements in the PHSS. These included MCB-j (3,900,000 ng/m^{2}d) and MCB-2 (4,000,000 ng/m^{2}d), with the latter being an early warning

location at which the concrete armoring was removed and the sediment probe was placed directly into the sand cap. Flux measurements at MCB-2 therefore give insight into the implications of cap failure and show that concrete is likely preventing large amounts of PAHs from entering the river. However, the contaminants appear to be moving through the cap at other locations including MCB-j, MCB-c, and MCB-d indicating that the contaminated sediment at MCBSS continues to be a source of PAHs to the Willamette River. Interestingly, the largest magnitude of Σ61PAH deposition occurred at locations directly downstream from MCB-j including MCB-i, MCB-3, and MCB-g indicating that these hotspots may be redistributing PAHs on a local scale.

Historically, creosote was the main source of PAHs to the Willamette River at the MCBSS and PAH profiles in the present study point toward creosote derived PAHs as a continual source of PAHs [70]. Creosote is produced through the distillation of coal tar and is comprised primarily of LMW PAHs, in particular acenaphthene, naphthalene, and alkyl naphthalenes. At locations of PAH release from the sediment the percentage of LMW PAHs was inflated as seen in Figure 2.5. Specifically, LMW PAHs made up on average 92% of total PAHs in the porewater at locations with net Σ61PAH release from sediment compared to 68% at locations with movement into sediment. In particular, acenaphthene accounted for 59% and 23% of Σ61PAHs in porewater at locations of net Σ61 PAH release and deposition from sediment respectively.

Utilizing multiple depth measurements of pore-water at four locations in the MCBSS, we calculated the flux due to diffusion across the boundary of the armoring and inter-armoring (Table A14). We determined downward diffusional flux of LMW PAHs at MCB-1 and MCB-2 and postulate that this may be due to pooling of non-aqueous phase liquids (NAPLs) underneath the cap. Conversely, at locations MCB-3 and MCB-4, where there is no concrete cap, we determined the diffusional flux of PAHs to be directed upwards from the sand layer into the armoring. Future studies would benefit from an increased spatial resolution of contamination concentrations through the cap.

With the exception of the extreme flux seen at MCB-j and MCB-2, flux measurements reported here are comparable to other flux studies in urban harbors. Koelmans et al. [54] estimated Σ12PAH flux from sediments of 43,000 ng/m^{2}d at the most contaminated site sampled in the Ijmuiden Harbor of the Netherlands. Eek et al. [55] reported porewater-water Σ15PAH flux of 3,800 ng/m^{2}d and 32ng/m^{2}d for uncapped and capped sediments respectively in the Oslo Harbor of Norway.

While flux measurements here indicate some breakthrough in the sediment cap, a 10-year remedial effectiveness assessment conducted by the Oregon Department of Environmental Quality (ODEQ) concluded that the cap meets its original remedial action objectives. A major driver for this decision was measured PAH surface water concentrations from this study which were lower than federal and state ambient water criteria [28].

Temporal extrapolations

The direction and magnitude of diffusive exchange across environmental compartments is significantly affected by environmental conditions including air temperature, precipitation, wind velocity, and flow velocity which can vary dramatically over the course of a year [25]. Data collected in the present study is therefore limited in its temporal scope though general statements based on average climatic parameters can be made. Previous studies in temperate environments have shown that higher temperatures and lower precipitation during summer months favor volatilization of PAHs [25, 51, 53]. Sampling in the present study occurred from approximately middle of September to the middle of October, typically a period of climatic transition from dry/hot to wet/cool in Western Oregon. For the 5-week deployment, 9 days of measurable precipitation were recorded for a total of 3.8 cm, approximately 4% of the annual average precipitation. Additionally, the average atmospheric temperature was 16.85°C, well above the annual average temperature of 12.5°C. Sower and Anderson, 2008 [71] reported insignificant differences in dissolved PAH concentrations at locations in the PHSS during the wet season (winter) compared to the dry season (summer). With weather conditions favoring volatilization compared to a yearly average and consistent PAH levels it is reasonable to conjecture that the PAH deposition determined in the present study is likely occurring over the entire year. Conversely, it is possible that for compounds in volatilization, we may see deposition in winter months. Further, the magnitudes of both diffusive exchanges may be subject to high variation due to changes in wind-speed and river flow velocity with typically higher wind speeds and flow velocities in winter months increasing the diffusive exchange.

Considerations

Only PAHs in the porewater directly at the sediment-water interface may exchange with the overlying water. In the present study, we assigned porewater at 25cm sampling intervals a single

value and therefore did not account for the possibility of an existing concentration gradient which may exist in the vertical profile of contaminated sediments and sediment caps [24].

Additionally, the present study utilized passive sampling devices which sequester only the freely dissolved or vapor phase fractions of contaminants. Accordingly, the present study does not address transport processes including dry and wet particle deposition, bioturbation, and other resuspension events that may play an important role in total contaminant movement.

Along the same lines, concentration gradients may also exist from the sediment surface vertically up into the water column and thus the most accurate water measurement for flux calculations would be as close as possible to the sediment-water interface. However, Fernandez et al. [24]showed very minor vertical concentration gradients from the sediment surface to 24cm above in an ocean environment. In this study, passive samplers were placed 30cm above the surface of the sediment in a river system with constant water movement where we might expect this gradient to be even less important. Indeed, even between the surface and bottom water samplers in the present study we see in most cases PAH concentrations are within 20% of each other. An exception was RM6.5W where PAH concentrations were higher closer to the bottom, possibly reflecting sediment as a significant source of PAHs to the water column at this location. Finally, measurements in the present study are discrete points and spatial interpolations are not valid.

Conclusions

This works describes the first application of passive samplers to measure the diffusive flux of contaminants across sediment-water and water-air interfaces concurrently. Such work highlights how these tools may be applied to gain insight into PAH transport at locations with inputs from multiple PAH sources. Data from studies such as this may provide information to predict the fate and exposure to contaminants and ultimately be used to inform remedial and management decisions at contaminated urban locations.

Acknowledgment

The present study was supported in part by award numbers P42 ES016465. The content is solely the responsibility of the authors and does not necessarily represent the official views of any funding organizations. We are highly appreciative of the EPA region 10 divers, in addition to E. Hughes and H. Blischke for assistance at the McCormick and Baxter Superfund Site. We are

grateful to our boat captain J. Pierce and field assistance from L. Tidwell, C. Donald, A. Bergmann, H. Dixon, K. Hobbie, and S. O'Connell. In addition, we are thankful for analytic expertise and other contributions from G. Wilson, R. Scott, and G. Points and P. Hoffman. We also thank S.Carver for his graphical design expertise.

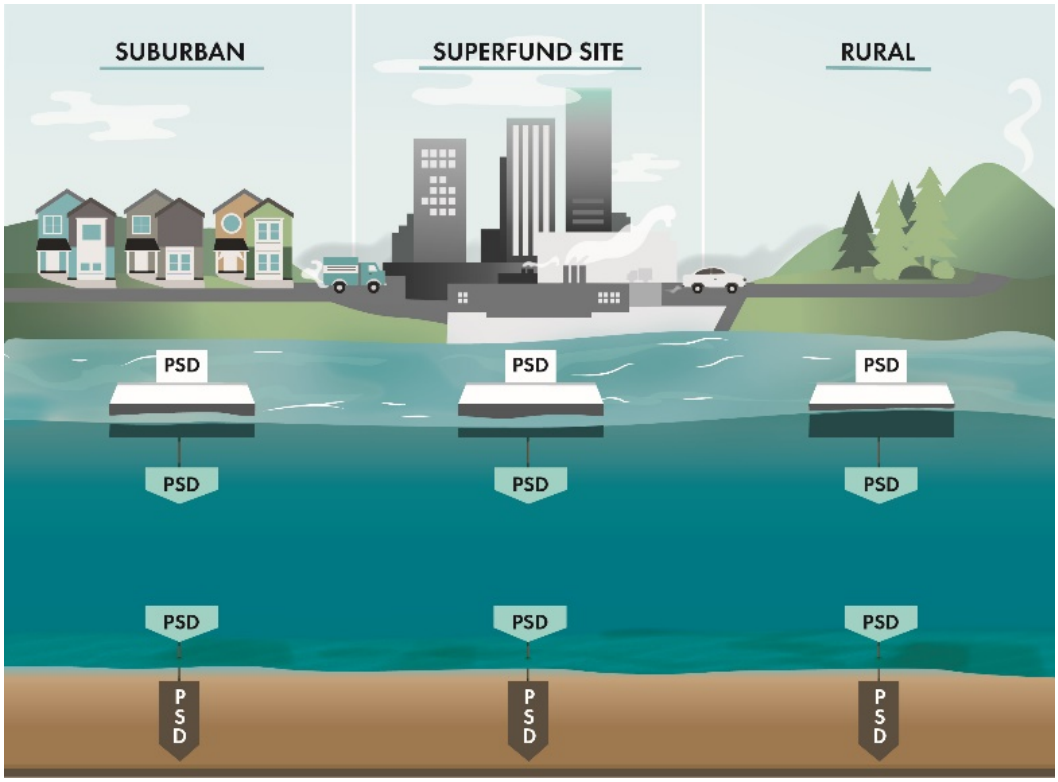

Figure 2.1. Graphical abstract of sampling methodology. Passive sampling devices (PSDs) were deployed in pairs across sediment-water and water-air interfaces at upstream, downstream and locations within the Portland Harbor Superfund site. Subsequently, diffusive flux was determined across both interfaces.

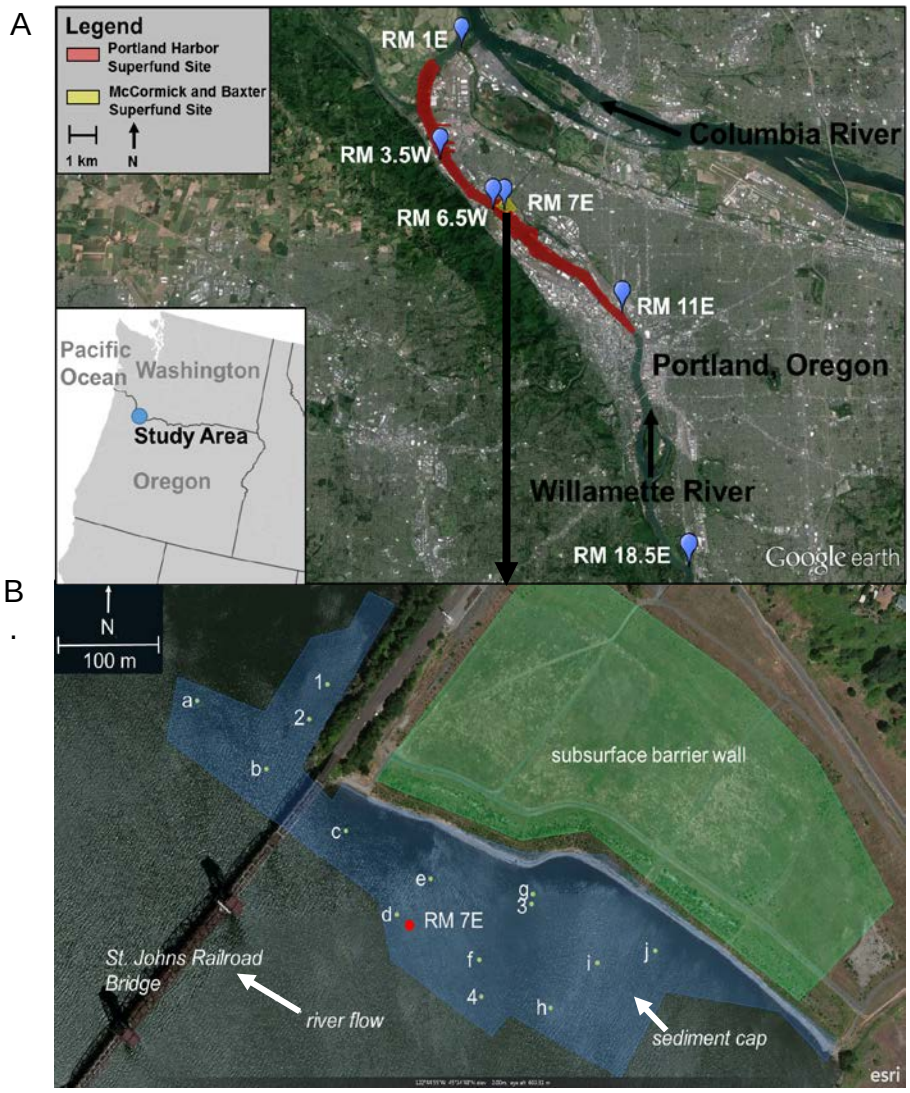

Figure 2.2. (a) Portland Harbor Superfund site. Sampling locations are denoted by blue pins at 6 river mile (RM) locations as measured upstream from the confluence of the Columbia and Willamette Rivers. (b) McCormick and Baxter Superfund Site. Sampling locations with letters (a-j) indicate porewater measurement within the sediment cap armoring, from 0-25cm below the sediment water-interface. Numbers (1-4) indicate placement both within and below the armoring, from 0-25cm and 25-50cm below the sediment-water interface.

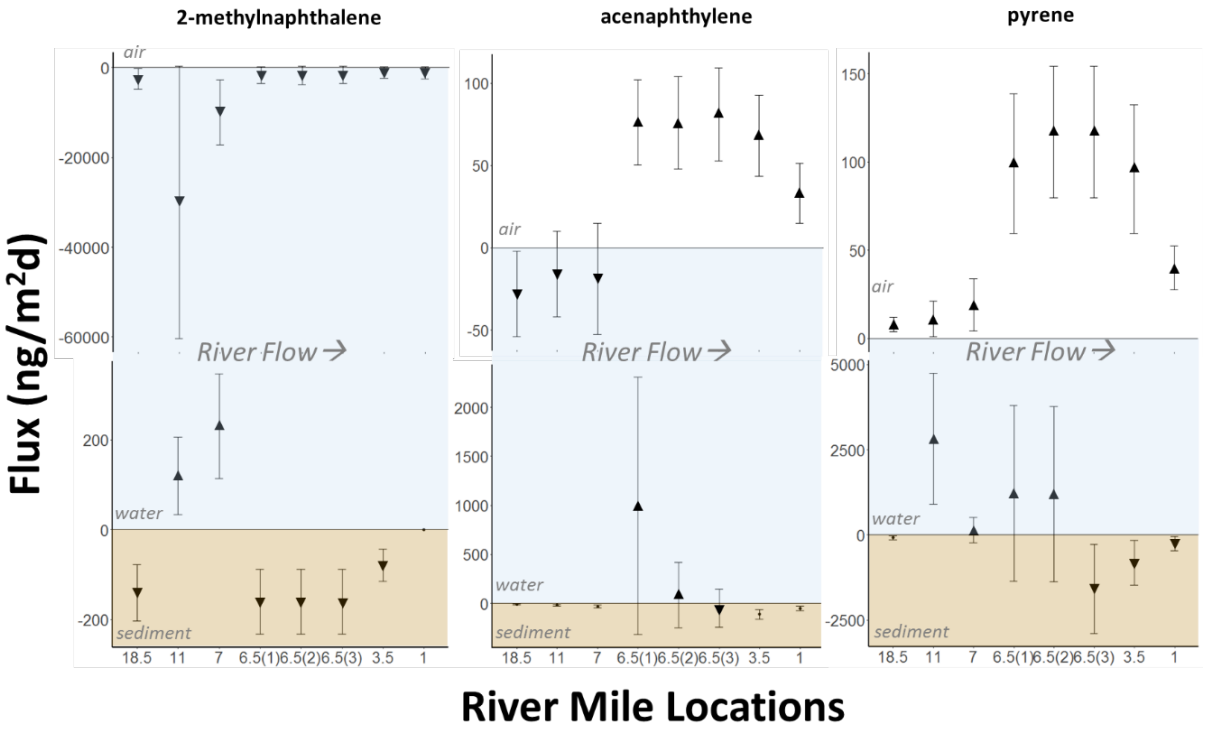

Figure 2.3. Diffusive flux (ng/m^{2}d) across both sediment-water and water-air interfaces for 2-methylnaphthalene, acenaphthylene and pyrene at river mile locations 18.5E, 11E, 7E, 6.5W (replicates 1-3), 3.5W, and 1E. Error bars represent 1 standard deviation after propagation of error.

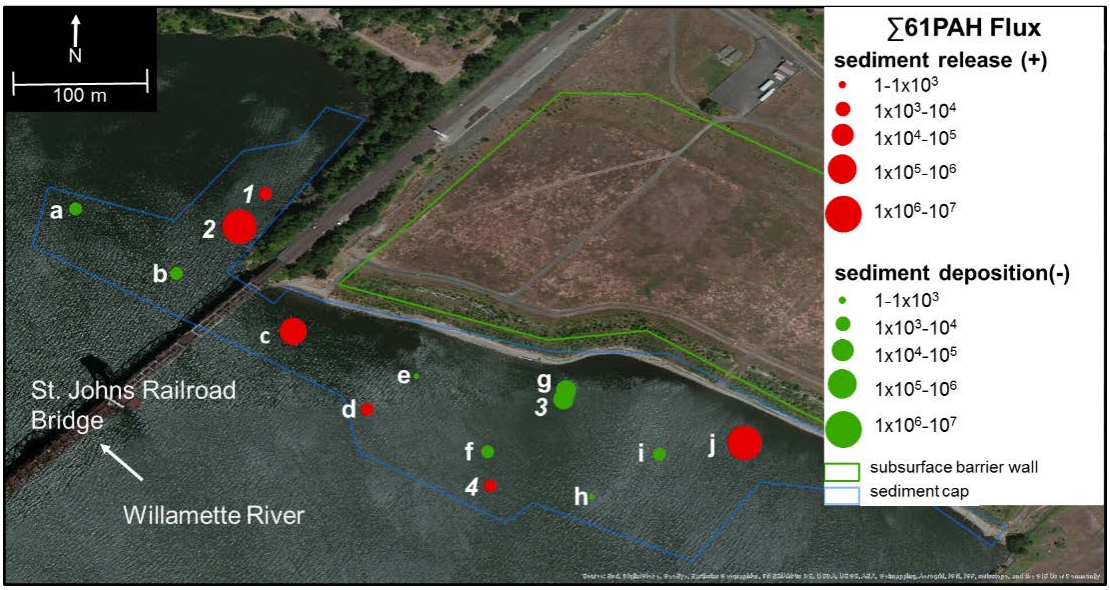

Figure 2.4. Diffusive flux measurements across the McCormick and Baxter Superfund Site for 61PAHs. Sampling locations with letters (a-j) indicate porewater measurement within the sediment cap armoring from 0-25cm below the sediment water interface. Numbers (1-4) indicate placement both within and below the armoring from 0-25cm and 25-50cm below the sediment water interface. Red values indicate positive flux from the porewater to water while green values indicate negative flux from the water to porewater. Green and blue lines indicate the approximate boundaries of the sediment cap and upland barrier wall respectively.

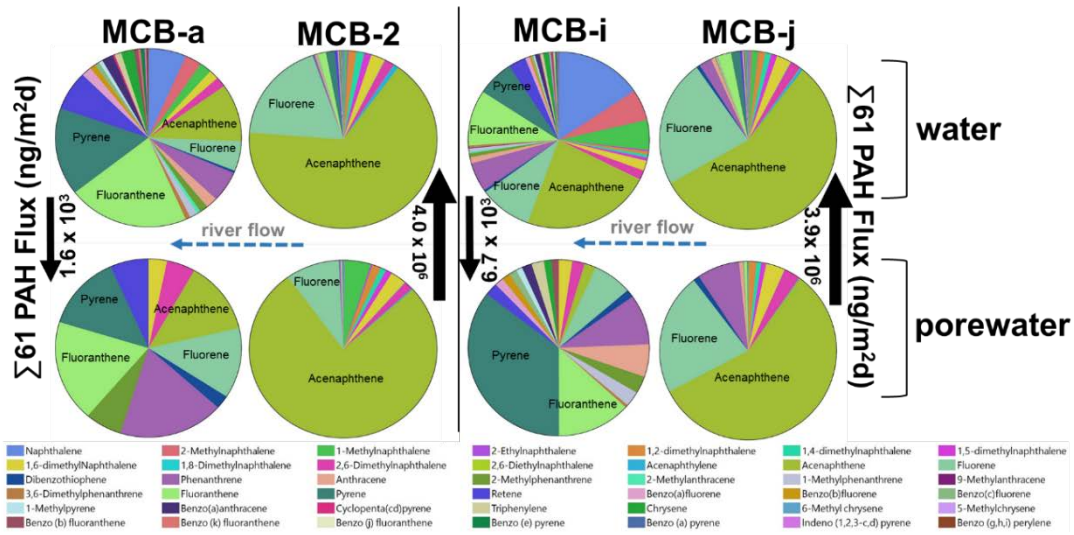

Figure 2.5. Polycyclic aromatic hydrocarbon (PAH) profiles in porewater and water at locations of elevated PAH movement from sediment to water (MCB-j, MCB-2) and at associated downstream locations with PAH deposition (MCB-i, MCB-a). Detected PAHs are represented by colors as a fraction of total PAHs. Arrows indicate direction of ∑61 PAH flux between sediment and water in units of ng/m2d.

CHAPTER 3 – A PASSIVE SAMPLING MODEL TO PREDICT PAHS IN BUTTER CLAMS (SAXIDOMUS GIGANTEUS), A TRADITIONAL FOOD SOURCE FOR NATIVE-AMERICAN TRIBES OF THE SALISH SEA REGION

D. James Minick*, L. Blair Paulik*, Brian W. Smith*, Richard P. Scott*, Molly L. Kile[#], Diana Rohlman[#], Kim Anderson*

*Department of Environmental and Molecular Toxicology, Oregon State University, ALS 1007, Corvallis, OR, 97331

#College of Public Health and Human Services, Oregon State University, Corvallis, OR, 97331

Submitted: Environmental Toxicology and Chemistry

Abstract

Native Americans face disproportionate exposures to environmental pollution including exposures through traditional practices such as subsistence clamming and hunting. Prior studies in the Salish Sea region of the Pacific Northwest have found high levels of contaminants including polycyclic aromatic hydrocarbons (PAHs) in clams. As filter feeders, clams may accumulate contaminants found in sediment and water column. Conventional biomonitoring methods require measuring the contaminants in clam tissues. This approach removes clams from the environment which can affect clam abundance and deplete an important cultural and subsistence food. This can be particularly problematic for long lived species such as the butter clam (*Saxidomus giganteus*) which lives along the Pacific coastline in North America. Traditional predictive methods for contaminant bioaccumulation are often inaccurate because of reliance on site specific sediment characteristics and bulk sediment concentrations. The freely dissolved fraction (C_{free}) of contaminants in sediment porewater is a better predictor of contaminant bioavailability than bulk sediment concentration. Determining C_{free} is therefore critical to estimate bioaccumulation. Passive sampling provides a simple and accurate approach to directly measure C_{free} in porewater. In this study, the collection of butter clams was spatially and temporally paired with deployment of sediment porewater passive samplers at 4 locations in the Puget Sound region of the Salish Sea in the Pacific Northwest, USA, within adjudicated usual and accustomed tribal fishing grounds and stations. Clams and passive samplers were analyzed for 62 individual PAHs. A linear regression model was constructed to predict PAH concentrations in the edible fraction of butter clams from C_{free} in porewater. PAH concentrations can be predicted from the freely dissolved PAH concentration in porewater using the following equation:

$$[PAH]Clam = \sqrt{4.1(\pm 0.1) \times [PAH]porewater}$$

The model predicted clam concentrations of PAHs based only on sediment porewater concentrations within a factor of 1.9 ± 0.2 on average. Carcinogenic risk assessment showed potentially unacceptable risk from consuming clams at one of the locations. This model offers a simplified, cost effective, and low impact approach to assess contaminant levels in butter clams which are an important traditional food.

Introduction

In order to calculate human health risk from seafood ingestion, it is necessary to assess contaminant accumulation in organisms. For Native American tribes of the Salish Sea region of the Pacific Northwest, shellfish have been an integral part of the way of life since time immemorial providing a source of both physical and cultural sustenance[72]. Concerns have arisen regarding the impact of anthropogenic contaminants on the safety of natural resources including clams [73, 74]. Previous work in the Salish Sea region has shown that carcinogenic risk from shellfish consumption may be driven by levels of polycyclic aromatic hydrocarbons (PAHs) in clams[72].

Given the importance of subsistence shellfish consumption, Native American tribes, government agencies, and researchers have been working together to better understand these potential human health risks from shellfish [75]. Furthermore, tribes of the Salish Sea region recognize the importance of protecting and sustaining the environment and the natural resources within the environment to protect the identity of their peoples. Subsequently, they have supported efforts to improve the monitoring of contaminants in shellfish.

Directly measuring contaminant levels in organisms is time and resource intensive because of the difficulty of locating and processing the organisms. Additionally, removing organisms from the environment for testing may deplete populations and could be harmful to ecosystems. These considerations have led to the development of predicative tools for determining contaminant levels in organisms [76, 77]. Conventional predictive methods for benthic organisms use total sediment concentrations and empirically derived biota–sediment accumulation factors (BSAF) [78]. However, these methods are often unreliable likely because of uncertainty in site-specific sediment parameters. For instance, variations in the fraction and type of organic carbon can influence the bioavailable fraction of chemical [32, 79]. Several studies have shown that the presence of black carbon, pitch, and other highly hydrophobic materials in the sediment may result in overestimation of the fraction of the chemical that is bioavailable to sediment-dwelling organisms and thus overestimation of chemical bioaccumulation in those organisms [6, 10, 80].

Compared to total sediment concentration, the freely dissolved fraction of chemical (C_{free}) in the interstitial pore space of sediment (sediment porewater) is a better indicator of bioavailability, bioaccumulation, and toxicity for benthic organisms[4, 5]. Passive sampling devices (PSDs) directly measure C_{free} in sediment porewater thereby inherently accounting for site specific sediment characteristics[11]. PSDs therefore offer an improvement in predictive capabilities for bioaccumulation compared to BSAFs[2, 81-83]. A few studies have used passive sampling devices in water to predict contaminant levels in crayfish and mussels[30, 84, 85]. More studies have used passive sampling derived sediment porewater concentrations to predict accumulation in benthic organisms, primarily in worms[6, 7, 10, 83, 86]. *Muijs and Jonker, 2012* reported that passive sampling methods improved prediction of polycyclic aromatic hydrocarbons (PAHs) in benthic worms

compared to traditional methods using BSAF values and total sediment concentrations[7]. *Fernandez and Gschwend, 2015* measured levels of 3 PAHs in sediment and the muscle portion of steamer clams (*Mya arenaria*) from locations in Massachusetts, USA, and compared the ability of passive samplers to predict levels of these 3 PAHs in the clams to the BSAF method. They found that the passive sampling approach was significantly more accurate than the BSAF method, and that the BSAF method consistently over predicted PAH levels in clams by average factors of 10-44 [6].

In the present study we expand on the work of *Fernandez and Gschwend, 2015* by using sediment porewater passive samplers to predict accumulation of 62 PAHs in the *edible fraction* of butter clams (*Saxidomus giganteus*). Butter clams were selected by tribal governments and collected from 4 locations in the Puget Sound region of the Salish Sea in the Pacific Northwest, USA. Specific sampling locations were selected by the tribes and were within adjudicated usual and accustomed tribal fishing grounds and stations. In addition to building a predictive model, a quantitative human health risk assessment was also performed to determine the potential cancer risk due to PAHs associated with consuming butter clams from this area. Ultimately, the development of a more accurate and relatively simple predictive model could allow for an increased ability to monitor pollutant levels in shellfish without having to remove them from the ecosystem.

Materials and Methods

Study location

Sampling occurred on four separate beaches within the adjudicated usual and accustomed tribal fishing grounds and stations in the Puget Sound region of the Salish Sea in Northwestern Washington, USA. Specific beaches (locations and names withheld at request of tribal governments) were selected with the guidance of local tribal members based on their use as clamming grounds. Beach 1 (B1) and Beach 2 (B2) were located in close proximity to oil refineries while Beach 3 (B3) and Beach 4 (B4) were located within 5km of B1/B2.

Field Sampling

A scientific collection permit was obtained from Washington State (Permit# 14-274). After extensive discussion with tribal leaders, the butter clam was selected as the test species because of its importance to the tribes. Local tribal members worked with the research team to harvest and identify butter clams. At each of the 4 sites, 5 clams were collected for a total of 20 clams. Following collection, clams were rinsed with ambient water followed by deionized water, stored in either an amber glass jar or a sealed Teflon bag, and transported back to the lab on ice. Immediately following removal of the clams, sediment passive sampling devices (PSDs) containing low density polyethylene (LDPE) were placed in the clam holes and deployed for a total of 29 days. These sediment passive sampling devices have been previously described in detail and are shown in Figure A4[87]. The LDPE strips were transported back to the laboratory in glass jars in a cooler. Transport stability studies performed by *Donald et al*. confirm that transport times (<24h) and temperature (<20°C) should not result in the loss of PAHs from LDPE[62].

PSD preparation and extraction

Additive free LDPE strips were constructed as described in *Anderson et al.* [60]. Fluorene-d10 was added to the passive samplers prior to deployment for determination of in-situ sampling rates[11]. PSDs were stored at -20°C prior to sample processing which is described in detail by Allan et al. [61]. In brief, PSDs were spiked with 7 deuterated surrogate extraction standards followed by dialysis in n-hexane and quantitative concentration. Surrogate extraction standards included: naphthalene-d8, acenaphthylene-d8, phenanthrene-d10, fluoranthene-d10, chrysene-d12, benzo[a]pyrene-d12 and benzo[ghi]perylene-d12. Surrogate recoveries ranged from 45% for naphthalene-d8 (RSD 11%) to 110% for benzo[ghi]perylene-D12 (RSD 15%). All solvents used were Optima® grade or better (Fisher Scientific, Pittsburgh, PA), and standards were purchased at purities ≥ 97%. Standards were prepared as singles or simple mixes in ethyl acetate, n-hexane, or isooctane (Fisher Scientific, optima grade) at concentrations typically between 1mg/L and 10mg/L.

Clam processing and extraction

Clam tissue was homogenized via freeze fracture using a Robot Coupe Blixer-2 food processor and liquid N_2. After homogenization, tissue was transferred into an amber glass screw-top jar and stored in the dark at -20°C. Prior to use, and between samples, all equipment was washed with soap and water and then rinsed with high purity water, acetone, and hexane. Extraction of PAHs from clam followed a modified QuECHERS method as described previously [84]. Seven individual extraction surrogates (same as LDPE extraction) were added to 1.0 g (± 2%) wet weight of homogenized clam tissue. Surrogate recoveries were 39%, 49%, 44%, 46%, 61%, 73%, and 68% for naphthalene-d8, acenaphthylene-d8, phenanthrene-d10, fluoranthene-d10, chrysene-d12, benzo(a)pyrene-d12, and benzo(ghi)perylene-d12, respectively.

Chemical Analysis

Samples were analyzed for 62 PAHs (Table B1) using an Agilent 7890A gas chromatograph (GC) with an Agilent 7000C MS/MS as described in Anderson et al. [63]. Use of an Agilent Select PAH column (30m x 250µm x 0.15µm) allowed for enhanced separation of compounds. For all PAHs, at least a 5-point calibration was employed spanning 4 orders of magnitude (1µg/L – 10mg/L) with correlations ≥0.98. GC oven and MS parameters along with a comprehensive list of method detection limits (MDLs) can be found in the Appendix B.

Porewater concentration calculation

The freely dissolved concentration of PAHs in the sediment porewater was calculated from extract concentration using methods described by *Huckins et al*[11]. Briefly, performance reference compounds were utilized to determine chemical specific sampling rates with additional corrections for the effect of temperature and salinity on the partition coefficients between the sampler and water. These calculations are described in detail in Appendix B, equation B1-B8.

Quality control

Quality control samples including field, trip, instrument, cleaning, reagent, and laboratory blanks as well as laboratory duplicates and over-spikes accounted for over 30% of the total samples analyzed. Clam extraction blanks contained measurable amounts of several low molecular weight PAHs making up on average 15% of Σ62PAHs in the clams and are shown in Table B2. Average extraction blank concentrations were subtracted from PAH concentrations measured in clam samples. Field blanks for the passive samplers contained quantifiable levels of several low molecular weight PAHs making up on average 13% of Σ62 PAHs in sediment porewater and are

shown in Table B2. Average field blank levels for the passive samplers were subtracted from PAH concentrations measured in sediment porewater samples. Instrument blanks and reagent blanks were below levels of detection for all analytes. Perylene-d12 was used as the instrumental internal standard. Continuing calibration verifications samples consisting of 51 individual PAHs at 500 µg/L were run every 12 samples or less and all met our data quality objectives where >80% of target analytes must be within 20% of the known value.

Human health risk assessment

The relative potency factor approach, described by the US EPA, was utilized to determine the carcinogenic risk associated with consuming the clams analyzed in this study. Risk assessment was performed for both subsistence consumers and consumers in the general US population[88]. Subsistence consumer ingestion rates (100 g/d) were obtained from a previously reported study based on a tribal community located in the Puget Sound region of the Salish Sea in Washington, USA[72]. Average shellfish ingestion rates for the general adult population in the Pacific region (4.6 g/d) was obtained from the US EPA[89]. Excess lifetime cancer risk was assessed based on the following EPA standardized assumptions for an adult (70 kg) using an exposure frequency of 365 days/year for an exposure duration of 70 years. The average benzo[a]pyrene equivalence (BaPeq) factor for each beach was multiplied by the slope factor of 7.3 mg/kg×d based on the latest US EPA guidance[88]. Detailed equations for these calculations can be found in the Appendix B, equation B9-B11.

Statistical Methods

Statistical analyses of PAH data were performed using Microsoft Excel, 2016 and JMP Pro 13. If individual PAH concentrations were below the limit of detections in either the clam or sediment

porewater, the corresponding limits of detection were substituted for modeling purposes. This occurred in 163 of 436 (37%) individual paired (sediment porewater and clam) PAH measurements. The vast majority (93%) of these were detections of PAHs in the sediment porewater but not in the clams resulting in substitutions of clam detection limits. Of these, 89% were 2- and 3- ring PAHs. Statistical analysis of correlations between PAH concentrations in clams and sediment porewater showed that a regression model with a square root function appeared to be the best fit for the data. Specifically, this regression captured the non-linear form of the line at elevated sediment porewater concentrations. Additional factors were explored including individual site locations, clam size/age, and K_{ow} values.

Results and Discussion

PAH concentrations in sediment and clams

Of the 62 PAHs analyzed, 42 different PAHs were detected in at least one sediment porewater or clam sample. Concentrations of PAHs in sediment porewater and clams were correlated (Table 3.1). PAHs with log K_{ow} values between 4.0 and 5.5 were elevated in both clams and sediment porewater. This indicated that freely dissolved PAHs in the sediment porewater were more likely to bioaccumulate in clams (Figure 3.2). As expected, PAHs with log K_{ow} values greater than 6.0 were rarely detected or detected at low levels in both clam and sediment porewater, illustrating that these high molecular PAHs were likely bound to sediment and not readily available for bioaccumulation.

Concentrations of PAHs in the sediment porewater were highest at B2 (12- 390ng/L). For context, PAH concentrations at B2 were comparable to, and in some cases higher than ∑62 PAH concentrations reported in sediment porewater at a PAH-contaminated Superfund site in Portland, Oregon (24-180ng/L)[87]. Concentrations of PAHs in clams were also highest at B2 (25-81ng/g),

driven largely by 2 individual clams with concentrations of 68 ng/g and 81 ng/g. Of note, these 2 clams were located closest to a creosote covered wooden pier. It is possible that creosote, which contains high concentrations of PAHs, is partially responsible for these elevated levels[70].

Spatial differences in PAH concentrations were noted between the 4 sites, and these differences have important implications for shellfish harvesters. The average ∑62 PAH clam concentration at B2 (48 ng/g) was approximately 3 times higher than the average clam concentration at B1 (15 ng/g) and roughly 10 times higher than the average clam concentration at B3 (4.3 ng/g) and B4 (3.3 ng/g). Similar trends were seen for sediment porewater concentrations. PAH data for all clam and sediment porewater samples can be found in Tables B4 and B5, respectively. B2 is adjacent to petroleum refineries and B1 is approximately 1km away from the refineries. B3 and B4 are approximately 5km from the refineries and in a separate bay. Together, these results suggest a potential impact from the refineries on PAH concentrations in clams collected nearby. However, additional historical sources of PAHs in the area exist, including a non-contained waste facility, petroleum storage, and pulp mill.

PAH profiles

Profiles of PAHs in clams from the 4 different beaches shows high variability (Figure 3.3). At B2, fluoranthene, pyrene, and phenanthrene accounted for approximately half of ∑PAH. Additionally, several 4-ring PAHs were detected in clams from B2, the site nearest to the oil refinery, that were not detected at any of the other beaches. Two of these 4-ring PAHs were benzo[a]pyrene and benzo[c]fluorene. This is noteworthy because larger PAHs are generally more carcinogenic than 2- and 3-ring PAHs. In the case of benzo[c]fluorene, the relative potency factor for cancer risk assessment is 20 times higher than that of benzo[a]pyrene[88]. Detections of

4-6 ring PAHs were lower at B1 compared to B2 and ∑PAH was driven by fluoranthene, naphthalene, and phenanthrene. At B3 and B4, individual PAH profiles were very similar showing mostly 2- and 3-ring PAHs with naphthalene and fluorene accounting for approximately half of ∑PAH. PAH profiles in sediment porewater were similar to PAH profiles in clams, but were comparatively elevated in 2 and 3-ring PAHs.

Diagnostic ratios of PAH isomers in sediment may be used in a weight of evidence approach to identify potential sources[90, 91]. The ratio of fluoranthene/pyrene in B2 sediment porewater indicates a primarily petrogenic source consistent with petroleum or creosote and a primarily pyrogenic source at the other beaches[70, 90, 91]. However, a lack of consistent PAH detections across all beaches limits the number of usable diagnostic ratios and makes any type of conclusive statement of PAH sources overreaching.

Predictive modeling

A linear regression model was generated to predict PAH levels in clams from C_{free} in sediment porewater using the 42 detected PAHs (Figure 3.4). Limits of detection were substituted in the case of detection of a PAH in only 1 of a sediment porewater or clam paired sample. The line of best fit is shown in *Equation 1* below.

$$[PAH]Clam\ \left(\frac{ng}{g}\right) = \sqrt{4.1(\pm 0.1) \times [PAH]porewater\left(\frac{ng}{L}\right)} \qquad \text{(Eq. 1)}$$

The root mean square error (RMSE) of this regression is 0.77. With *Equation 1*, PAH concentration in clams were predicted using only C_{free} in sediment porewater measured with passive samplers. The square root function of this regression is such that as PAH concentration in sediment porewater increases, the rate of PAH accumulation in clams decreases. This attribute is fundamentally different than BSAFs which assume linear rates of bioaccumulation with

increasing sediment concentrations. The non-linear nature of our predictive regression model may represent the induction of detoxifying enzymes, such as the cytochrome P450 enzymes which have been shown to be active in some species of clams[92-94]. Specifically, induction of these enzymes may result in a decreased rate of PAH accumulation in clams at higher PAH concentrations. As such, the regression model described in this study is an improvement over the linear nature of BSAFs which would over predict clam concentrations at elevated sediment porewater concentrations with this data set.

Furthermore, we observed that several of the 2- and 3-ring PAHs in our regression model were over-predicted in clams based on their sediment porewater concentrations. That is to say that these PAHs were at high concentrations in the sediment porewater, but did not appear to accumulate appreciably in the clams. This is likely because smaller PAHs are less hydrophobic (lower K_{ow} values) and thus accumulate less in tissues compared to larger PAHs. To explore this finding, a second predictive model was constructed which included only PAHs with 3 full 6-membered rings and larger (dashed lines in Figure 3.4*)*. In this model, the slope of the best fit equation increased slightly as expected but the overall accuracy remains largely unaffected with an RMSE of 0.78. Because of the minor differences between these best-fit lines, we would recommend using the original model that includes all PAHs.

In order to assess model performance, predicted values from *equation 1* were compared to measured values (Figure 3.5). Factors were calculated by taking a ratio of the predicted and measured values. When calculating factors, it is possible that large factors may exist even when the absolute difference is negligible. For instance, if the predicted value was 1.0 ng/g and the actual value was 0.1 ng/g then the factor is 10 but the absolute difference is less than 1 ng/g. To

increase the meaning of factor analysis, instances where either the predicted or measured clam concentration was less than 1 ng/g were excluded from calculation of factors. Refinement of these calculations resulted in 71 individual factor differences for 13 PAHs. Based on these values, the model predicted average concentrations in clams within a factor of 1.9 ± 0.2 of the measured values (0.2 indicates 2*SE). To illustrate that this process did not unduly lower the factors, when considering all factors, only 3.0% were greater than 3 when the absolute difference was also greater than 3.0 ng/g. All of these instances corresponded to 2- and 3-ring PAHs which were detected in sediment porewater and not in clams. It is possible that these small PAHs do not partition into clams because of their relatively low hydrophobicity compared to larger PAHs. Additionally, when considering all the points, the average absolute difference between predicted and measured clam concentrations was 1.1 ng/g.

Other researchers have used sediment PSDs to predict PAHs in other organisms including other clam species. For instance, *Fernandez and Gschwend, 2015* predicted levels of phenanthrene, pyrene, and chrysene in soft-shell steamer clams (*Mya arenaria*) using low density polyethylene PSDs in sediment. The average ratios of predicted to measured values were 0.43, 3.7, and 1.1 for phenanthrene, pyrene, and chrysene respectively[6]. These numbers correspond to an average factor of 2.4 which is larger than the average factor of 1.9 for the 13 PAHs we reported in this study. Additionally, the standard deviation for the factors in our study (1.0) is less than shown by *Fernandez and Gschwend, 2015* [6]. Using PSD derived sediment porewater concentrations, *Muijs and Jonker, 2012* predicted concentrations of 13 PAHs in benthic worms generally within a factor of 4 [7]. The authors cite the relatively low capacity of SPME passive samplers and the use of generic BAF factors as reasons for higher than expected variability. Compared to the model presented by *Fernandez and Gschwend to* predict PAHs in steamer clams, our model is an

improvement because of the incorporation of additional PAHs and the lower factor differences between measured and predicted concentrations. It's possible that the lower factor differences result from the heterogeneity of sediment and the fact that PSDs were placed directly into the clam holes in this study as opposed to adjacent to the clam holes in the *Fernandez and Gschwend* study. An additional benefit, because we were concerned with the fraction of clam which would be eaten by Native American tribal members, our model considers the entire edible fraction as opposed to only the lipid and protein fraction. Taken together, our approach is preferable as a proxy method for monitoring PAH contamination in shellfish for determination of potential risk through ingestion.

In predictive models for bioaccumulation, over-prediction is preferable and false negatives should be kept at a minimum in order to be protective of health. When considering all data points, only 8.7% of individual PAHs were under predicted by the model. Importantly, individual PAHs were measured in clams but were below limits of detection in the sediment in only 2.5% of samples. In these cases, the model would fail to predict any concentration in clams. The majority of these were large PAHs including retene, coronene, and indeno[1,2,3-cd]pyrene and all the clam concentrations were less than 0.5ng/g. It is possible that these larger, more persistent PAHs reflect historical contamination or slow diffusion rates as butter clams can live up to 20 years. Based on the measured length of clams in this study (70-110mm) the corresponding ages are likely between 7-20 years [95].

Additionally, it is possible that the presence of these larger PAHs represents the ingestion of particle-bound PAHs by the clams. Clams, like other bivalves, are filter feeders and therefore may be exposed to both dissolved and particulate-bound PAHs in both the sediment porewater

and the water column[96, 97]. However, studies have demonstrated that even for organisms whose exposure to contaminants is expected to be through the ingestion of sediment, bulk sediment concentrations often do not correlate well with bioaccumulation [83]. Here, the fact the passive sampler generally measured the same PAHs in the clams seems to indicate that the majority of exposure for clams occurs through PAHs in the freely dissolved phase. This observation is further enforced by the similarity between the PAH profiles in sediment porewater and clams. The passive sampling model presented here enables accurate prediction of PAH concentrations in clams and has applicability for risk assessors and land managers.

Human health risk assessment

A quantitative human health risk assessment was conducted to assess the carcinogenic risk from PAHs associated with ingestion of clams using the relative potency factor approach as described by the U.S. EPA[88]. Cancer risk is expressed as the excess lifetime cancer risk (ECLR) which is defined as a probability of the number of potential cancer cases above background. Table 3.1 shows ELCR estimates for each of the 4 beaches. The acceptable risk level is generally defined by the U.S. EPA as an ECLR of between 10^{-6} (1 in a million) and 10^{-4} (1 in 10,000) [98].

The estimated lifetime cancer risk from consuming shellfish in this study was more than 20 fold higher at beach B2 than at the other 3 locations, and more than 20 fold higher for subsistence consumers compared to the general population. The highest risk was for subsistence consumers at B2 where the ECLR was 1.3 in 10,000 based on the average clam concentration at that site. At B1, carcinogenic risk was lower, but remained above 1 in a million while at B3 and B4 risk levels were below 1 in million. For the general population, the ECLR at B2 was 6 in a million and below 1 in a million at the other locations.

This data demonstrates the importance of site-specific monitoring for making recommendations regarding shellfish consumption even within a small geographical region. It is important to note that the excess cancer risk calculated is based only on PAH concentrations. Additionally, cancer target levels set by the U.S. EPA or state agencies may not be representative of the target cancer levels of individual Native American tribal communities. Each Native American tribe may identify a different level of risk that is acceptable to them. Furthermore, it is essential to balance the risk of consuming potentially contaminated clams with both health and cultural benefits[29].

There are several important limitations to this cancer risk assessment. First, the risk assessment assumes that clams with the same PAH concentrations will be consumed daily for 70 years. Second, it is possible that clam concentrations may change over that time period altering the risk. The risk assessment is also limited by the relatively small numbers of clams which were collected from four locations and which were not chosen by random sample generation. In addition, this risk assessment considers only ingestion exposure to PAHs through the consumption of clams. In reality, total lifetime exposure to PAHs may occur through separate inhalation or dermal routes. This risk assessment only considers PAHs when in reality many other chemicals may contribute to risk. Finally, uncertainty exists in every PAH risk assessment due to interspecies extrapolations which are inherently part of the RPFs and because of the lack of toxicity data for the vast majority of PAHs[88].

Conclusions

This study showed that PAHs in butter clams collected in the Salish Sea vary considerably. It is possible that clams from certain locations within adjudicated usual and accustomed tribal fishing

grounds and stations in the Pacific Northwest contain levels of PAH that are harmful to human health particularly for Native Americans who have higher traditional consumption rates. To improve monitoring of contaminant levels in clams and other shellfish while addressing cultural norms and limiting damage to an already fragile ecosystem, it is important to consider alternative proxy measurements from passive sampling devices. The predictive model developed in this study that was based on data collected using a sediment porewater passive sampling device provides a low impact, simple approach to predict PAH levels in butter clams within a factor of 2. As anthropogenic impacts on ecosystems continue to increase, the importance of accurately and noninvasively measuring contaminant accumulation in organisms will grow in importance.

Acknowledgments

This work was funded by the National Institute of Environmental Health Sciences grants P42-ES016465, P30ES000210 and T32ES007060-32. We would like to thank the Native American tribes in this study, who wish to remain anonymous, for their assistance in all aspects of this study including study design, sample location identification, sample collection, sample processing, and analysis. Additionally, we are grateful for the analytical expertise and assistance in the field provided by Glenn Wilson, Gary Points, Holly Dixon, Carey Donald, Alan Bergmann, and Jorge Padilla.

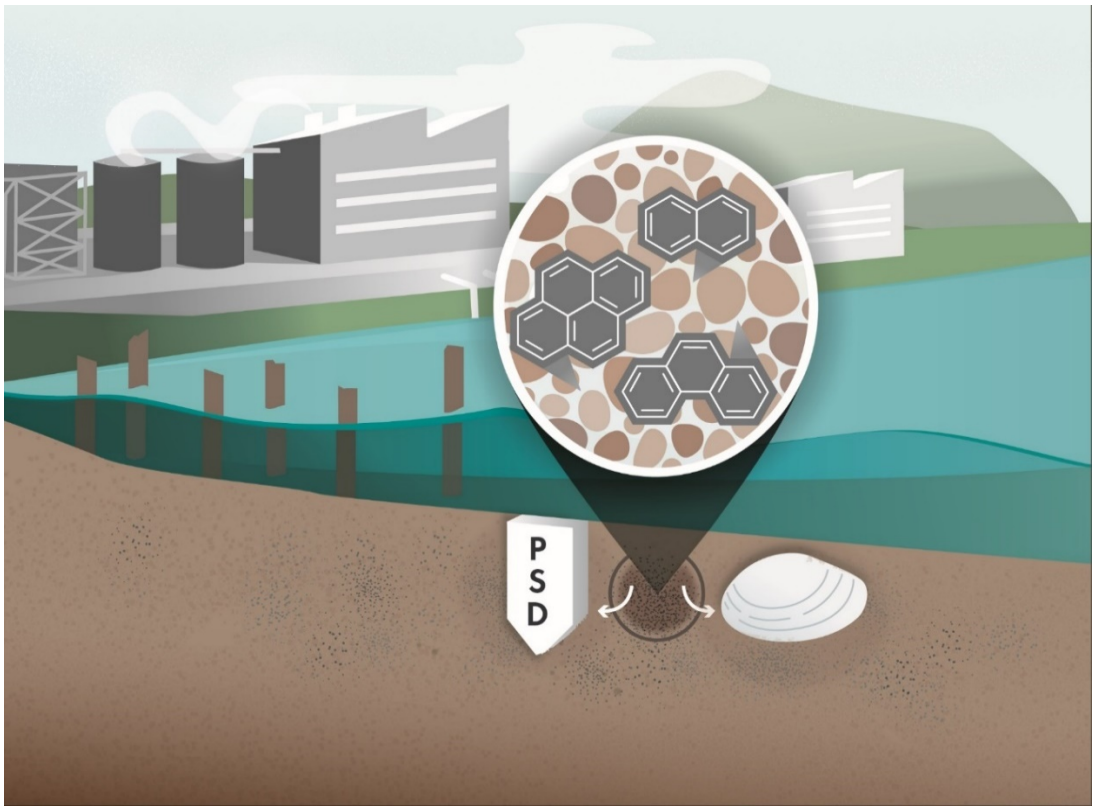

Figure 3.1. Sediment porewater passive sampling devices (PSDs) were spatially and temporally paired with collection of 5 butter clams at each of 4 locations on adjudicated usual and accustomed tribal fishing grounds in the Salish Sea Region of the Pacific Northwest. Both sediment porewater and clams were analyzed for 62 individual PAHs.

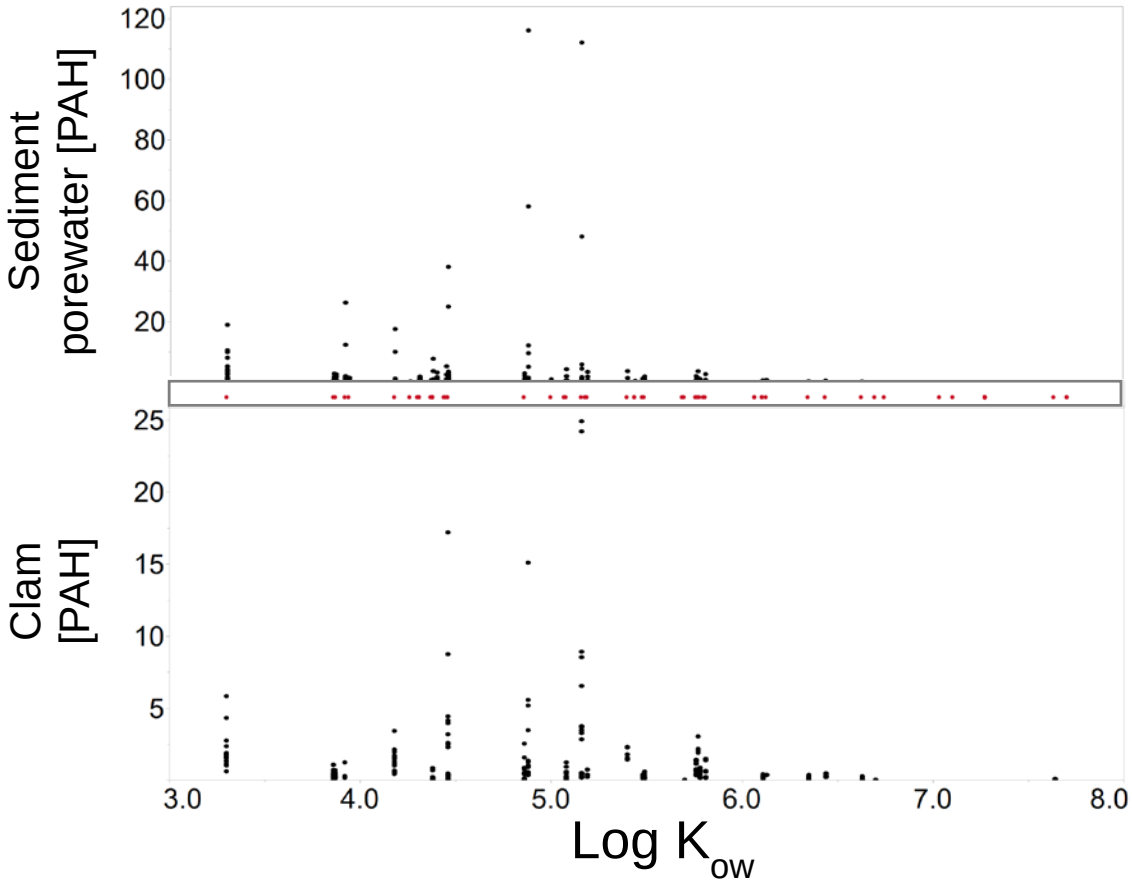

Figure 3.2. Individual PAH concentrations in clams (ng/g) and in sediment porewater (ng/L) versus log K_{ow}. Red points represent the 62 individual PAHs in the analytical method for both clams and sediment porewater. 42 individual PAHs were detected in either the clam or the sediment porewater. Of the 24 PAHs in the method with a log K_{ow} of 6 or greater only 7 of these were detected in either the sediment porewater or clams. .

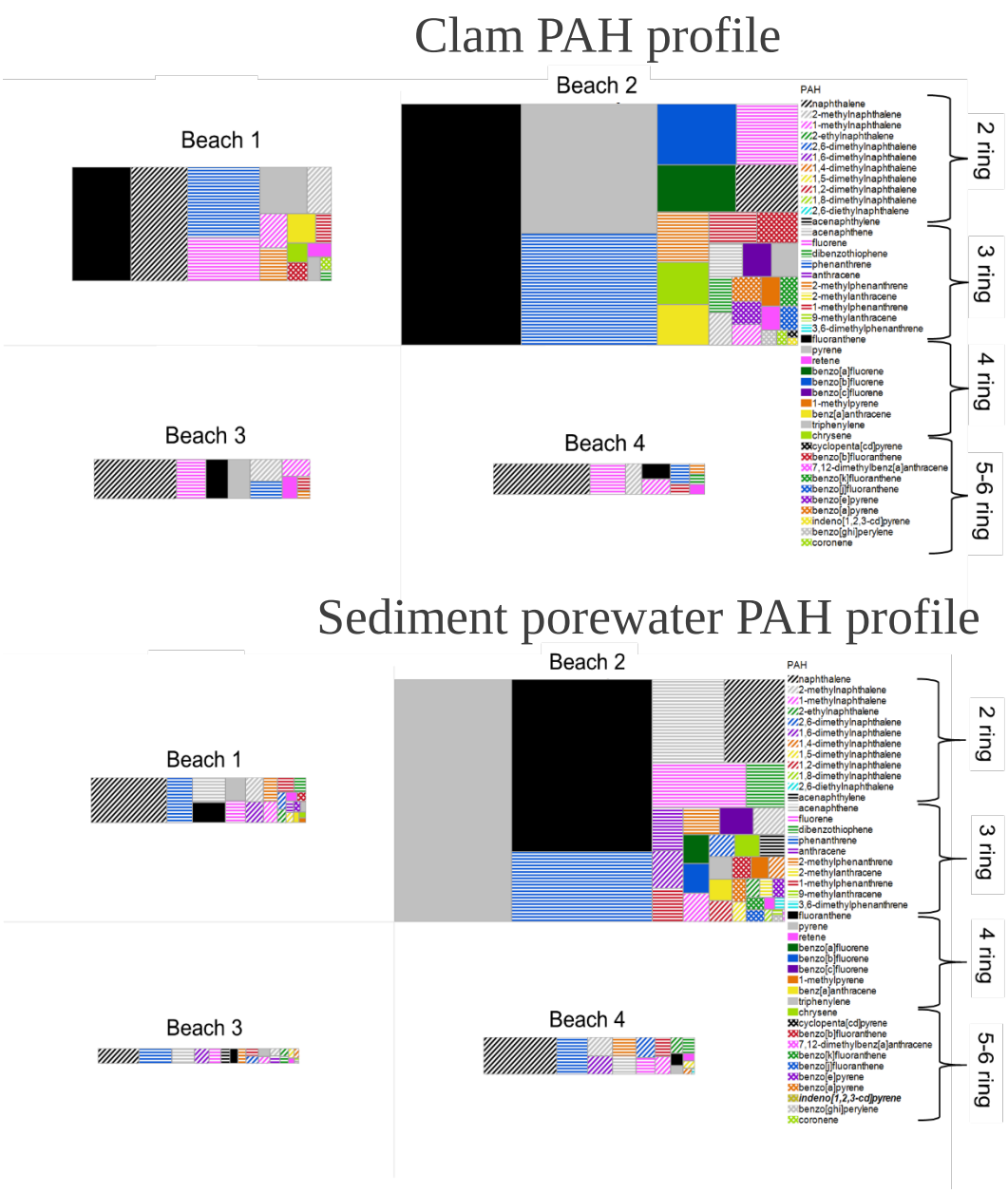

Figure 3.3 PAH profiles in clams and sediment porewater. The entire size of the 4 rectangles indicates the relative ∑62 PAH concentration at each of the locations. The size of the individual colored rectangles indicates the relative individual PAH concentration as a fraction of the ∑62 PAH concentration for each beach location. The sizes of the rectangles are directly comparable between beaches for each matrix. .

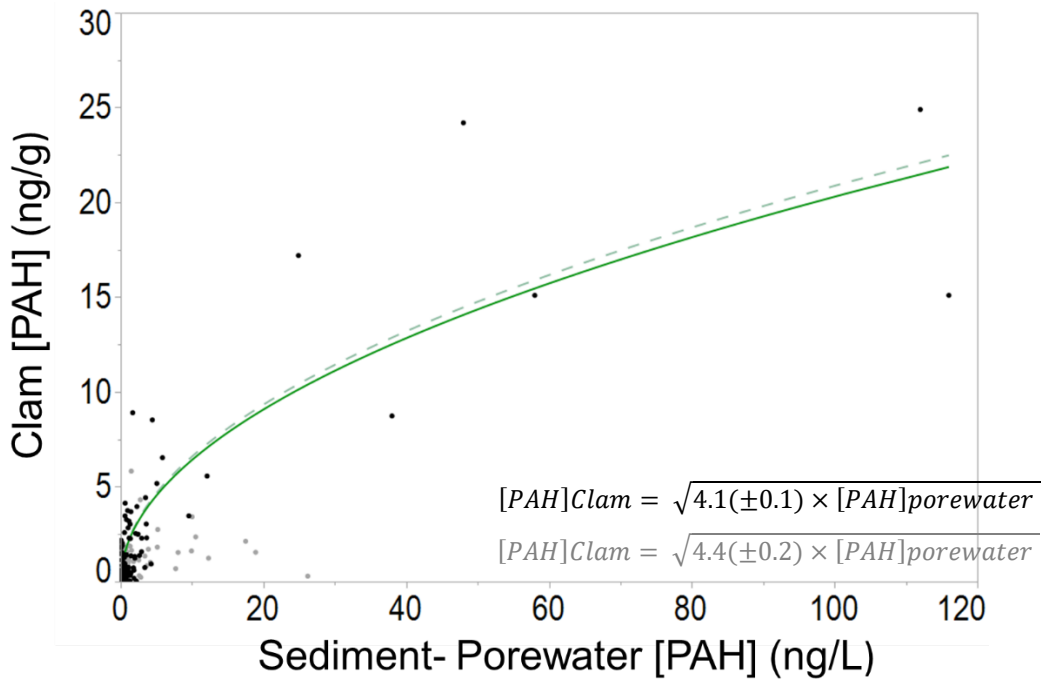

Figure 3.4. Regression of 42 PAHs detected in spatially paired sediment porewater passive samples (ng/L) and in clams (ng/g). Gray points indicate PAHs with less than 3-full -rings. Excluding these points, a second regression was constructed (dashed line, gray font). The intercept was set to 0 (slope ± standard error). .

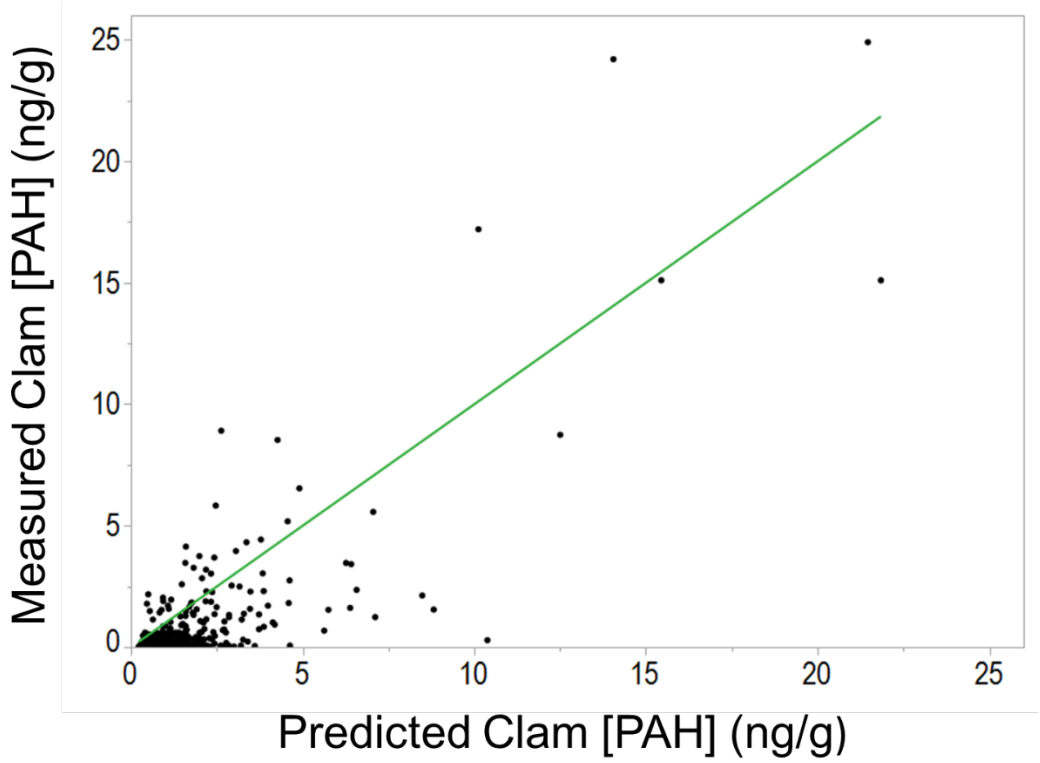

Figure 3.5 PAH concentration measured in clam tissue (ng/g) vs. PAH concentration predicted in clam tissue (ng/g) from freely dissolved concentrations of PAH in sediment porewater. Predicted PAH concentrations were derived from *Equation 1* from the linear regression model displayed in Figure 3.4. The reference line indicates where predicted/measured values = 1. On average, the predicted concentrations by the model were within a factor of 1.9 ± 0.2 of the measured values when considering only predicted and measured values greater than 1 ng/g. .

Table 3.1. Range of concentrations for ∑62 PAH in sediment porewater (ng/L) and the edible fraction of clam (ng/g) at beaches 1-4. Using the EPA RPF approach, the benzo[a]pyrene equivalence (ng/g) and corresponding excess lifetime cancer risk (ELCR) was calculated for both subsistence consumers (100g/d) and consumers in the general population (4.6g/d). .

	Beach 1	Beach 2	Beach 3	Beach 4
∑62[PAH] Sediment porewater (ng/L)	5.0 - 19	12 - 390	1.2 – 5.5	5.5 - 15
∑62[PAH] Clam (ng/g)	12 - 18	25 - 81	4.1 – 4.7	2.7 – 4.4
BaP_{eq} Clam (ng/g)	0.45 – 0.59	5.7 - 18	0.032 – 0.041	0.014 – 0.021
ELCR Clam (*subsistence*)	4.7 – 6.1	59 - 186	0.33 – 0.43	0.15 – 0.22
ELCR Clam (*general*)	0.22 – 0.24	2.7 – 8.6	0.015 – 0.020	0.0068 – 0.056

CHAPTER 4 – SYSTEMATIC DEVELOPMENTAL NEUROTOXICITY ASSESSMENT OF A REPRESENTATIVE PAH SUPERFUND MIXTURE IN ZEBRAFISH

‡Mitra C. Geier and ‡D. James Minick, Lisa Truong, Susan Tilton, Kim A. Anderson, Robert L. Tanguay

Department of Environmental and Molecular Toxicology, Oregon State University, ALS 1007, Corvallis, OR, 97331

‡ These co-authors contributed equally to this manuscript.

Submitted: Toxicology and Applied Pharmacology

Abstract

Superfund sites often consist of complex mixtures of polycyclic aromatic hydrocarbons (PAHs). It is widely recognized that PAHs pose risks to human health, but the risks posed by exposure to PAH mixtures is unclear. We developed and constructed an environmentally relevant PAH mixture with the top 10 most prevalent PAHs (Supermix 10) from a Superfund site using environmental passive sampling data. Using the zebrafish model, we evaluated the developmental and neurotoxicity of SM10 and the 10 individual constituents. Zebrafish embryos were exposed from 6-120 hours post fertilization to (1) the SM10 mixture, (2) a broad range individual PAHs; pyrene, fluoranthene, retene, benzo[a]anthracene, chrysene, naphthalene, acenaphthene, phenanthrene, fluorene, and 2-methylnaphthalene. We identified that SM10 and only 3 of the individual PAHs were toxic. Subsequently, we constructed and exposed developing zebrafish to two sub-mixtures: SM3 (comprised of 3 of the developmentally toxicity PAHs) and SM7 (7 non-toxic PAHs) and found that the SM3 toxicity profile was similar to SM10. To determine if exposures activated the AHR pathway, the spatial tissue expression of CYP1A was evaluated in the 10 individual PAHs and the 3 mixtures. The results demonstrated that the developmental toxicity observed in SM10 and general concentration addition models can explain SM3, and that this mixture activates the AHR. Adults developmentally exposed to SM10 also exhibited decreased learning and responses to startle stimulus indicating that developmental SM10 exposures affect neurobehavior. Collectively, these results exemplify the utility of zebrafish as a surrogate to investigate the developmental and neurotoxicity of complex mixtures.

Introduction

Polycyclic aromatic hydrocarbons (PAHs) are ubiquitous environmental contaminants formed from both anthropogenic and non-anthropogenic sources [91, 99]. There is growing recognition of the human hazard potential of various classes of PAHs, and the limited data regarding their toxicity, specifically on the nervous system. Prenatal PAH exposures have been associated with neurobehavioral effects [22, 100-102]. These studies have correlated developmental PAH exposure to decreased cognitive development and childhood IQ [17, 22, 101, 103-105], and increased rates of ADHD [18]. These findings are supported by vertebrate models demonstrating short and long term neurodevelopmental effects of developmental PAH exposure [19, 20, 106-113]

PAHs are typically classified as human hazards due to their carcinogenicity and/or mutagenicity, but the concern regarding the developmental toxicity of PAHs has increased in recent years. PAHs cross the placenta during pregnancy [114, 115] in mammalian models, developmental PAH exposures cause oxidative stress and cardiovascular toxicity [106, 116-119]. Some of the observed PAH toxicity is AHR dependent in mice [120] and AHR2 in zebrafish [20, 121, 122].

The majority of these laboratory toxicity tests and risk assessments have focused on individual chemical rather than chemical mixtures [33, 34]. In the environment, organisms are generally exposed to complex chemical mixtures, rather than to individual chemicals [123, 124]. Though knowledge of individual chemical toxicities is critically important, mixtures of chemicals may exhibit significantly different toxicities than their individual components for a variety of reasons, including competition for receptors, metabolic modulation, and altered bioavailability [33, 125, 126]. Attempts to balance real-world complex chemical mixture exposures with available experimental methods have resulted in three main approaches (1) component based, (2) whole mixture, and (3) ‘sufficiently similar’ [34, 35].

Component based approaches utilize individual chemical toxicities to predict the toxicity of mixtures. This approach is only appropriate for groups of chemicals in which the mechanisms of toxicity are well established as either similar or independent, and are therefore limited in scope and considered the least comprehensive by the United States EPA [35, 123]. In the case of PAHs, toxic equivalency factors (TEFs) have been developed for carcinogenicity, but applying this same technique to developmental effects is not appropriate and does not adequately address the reality of multiple mechanisms leading to these effects [127].

The most comprehensive approach to understanding complex chemical mixture toxicity is to directly assess the toxicity of whole chemical mixtures. Whole mixture approaches are

financially and practically onerous and the seemingly infinite number of potential mixtures in the environment makes these approaches often unfeasible [124]. Perhaps most importantly, the identification of specific toxicants contributing to whole mixture toxicity and their mechanisms of action can be immensely challenging [128].

To combat these practicality issues, the US EPA conceptualized the third approach—representative, or "sufficiently similar" mixtures, defined as: "A mixture [where]…its components are not very different and are contained in about the same proportions as the mixture of concern." This approach produces a simplified and well-defined mixture that allows for the direct comparison of concentration-response curves of the mixture with individual components [35]. The foundation of this approach is a fixed ratio design which assumes that the relative ratios of chemicals from common sources are similar, and that the ratios are vital to understanding the effects in the mixture[34]. The sufficiently similar mixture approach may represent a compromise between the whole mixture and component based approaches.

In the environment, PAHs exist primarily as complex mixtures with ratios reflective of their sources [90, 91, 113].The Portland Harbor Superfund Site (PHSS) is a prime example of a location with multiple PAH sources resulting in exposure of humans and other organisms to complex PAH mixtures through contact with contaminated water and sediment [129] The PHSS is located on the Willamette River upstream of its confluence with the Columbia River in Portland, Oregon [130]. Legacy sources (e.g. manufacturing and creosote operations), and modern (e.g. vehicle emissions and urban runoff contribute) to PAH load in the PHSS [131].

In order to assess the developmental toxicity of a PAH mixture, a sufficiently similar PHSS mixture consisting of the 10 most abundant PAHs from surface water (SM10) was constructed based on environmental passive sampling data from 2010 and 2015 [131, 132]. We used the zebrafish model to investigate the toxicity of the individual PAHs compared to the SM10 mixture and to evaluate the long-term effects in adult animals. Previous work has demonstrated that developmental exposure to benzo[a]pyrene resulted in persistent long-term deficits as adults, such as learning and memory during an active avoidance test [20, 133-135]. Here, we exposed embryonic zebrafish to both the individual 10 PAHs, and SM10 from 6-120 hour post fertilization (hpf) and evaluated morphological and behavioral changes at 120 hpf. We quantitatively compared the developmental toxicity effect levels for individual PAHs and mixtures to determine if the effects followed general concentration addition. To investigate the role of AHR in mediating these effects, we evaluated the expression of CYP1A in animals with AHR transiently

knocked down. Finally, to assess if developmental exposure to a PAH mixture (SM10) leads to life-long behavioral effects; we exposed animals during development and raised them in chemical-free water into adulthood, and tested the behavioral deficits. Together this data demonstrates an approach using the zebrafish model to assess short and long-term developmental neurotoxicity of an environmentally relevant representative PAH mixture

Materials and Methods

Study area and mixture construction

The Portland Harbor Superfund site (PHSS) is located on the Willamette River from river mile 1.8 to 11.2 as measured upstream of its confluence with the Columbia River in Portland, Oregon (Figure A1). The PHSS was added to the Superfund National Priorities List in 2000 due to high levels of PAHs, PCBs, dioxins, and metals in the sediment and overlying water. In two previously reported studies, low density polyethylene PSDs were deployed in the surface water in 2010 and 2015 at a total of 7 different sites making up a total of 18 individual samples. Environmental concentrations are provided in Appendix C (Table C1 and Table C2) and detailed study descriptions are provided in the previously published studies [131, 132]. The surrogate mixture SM10 was constructed with relative ratios of PAHs, which fall within the range of ratios of the 10 PAHs with the highest average concentrations as measured in 2010 and 2015 (Table 4.1). These 10 PAHs from highest concentration to lowest are: pyrene, fluoranthene, retene, benzo[a]anthracene, chrysene, naphthalene, acenaphthene, phenanthrene, fluorene, and 2-methylnaphthalene. Supermix3 (SM3) was constructed with the three PAHs which caused morphological effects individually as determined in this study: pyrene, retene, and benz[a]anthracene. The remaining 7 PAHs were combined to make Supermix7 (SM7).

Zebrafish husbandy

Wildtype Tropical 5D zebrafish were maintained at the Sinnhuber Aquatic Research Laboratory (SARL), at Oregon State University (Corvallis, OR, USA) under a 14:10 hour light/dark cycle. Fish were raised in densities of ~500 fish/50-gallon tank at 28°C in recirculating filtered water supplemented with Instant Ocean salts. Care for the adult zebrafish followed protocols previously published [136]. Spawning funnels were placed in tanks the night prior, and the following morning

embryos were collected, staged and maintained in plastic petri dishes in an incubator at 28°C in embryo media (EM) [137]. Embryo media consisted of 15 mM NaCl, 0.5 mM KCl, 1 mM $MgSO_4$, 0.15 mM KH_2PO_4, 0.05 mM Na_2HPO_4 and 0.7mM $NaHCO_3$ [138].

Exposures

To remove potential chemical barrier effects and to simply endpoint assessments, the chorions of 4 hpf embryos were enzymatically removed using a custom automated dechorionator, and at 6 hpf embryos were placed one per well in round bottom 96-well plates prefilled with 100 µL EM, using automated embryo placement systems [139]. A Hewlett Packard D300e chemical dispenser was used to dispense 100% DMSO stock into 4 replicate exposure plates. Final DMSO concentrations were normalized to 1% (vol/vol), a percentage previously demonstrated to not induce adverse morphological phenotypes [118] and plates were gently shaken during dispensing. Plates were sealed to minimize evaporation, wrapped in aluminum foil to block external light, and shaken overnight on an orbital shaker at 235 rpm at 28°C to enhance solution uniformity [140]. Embryos were statically exposed until 120 hpf, and kept in a 28°C incubator for the duration of the exposure.

Initial exposure concentrations were increased by approximately six orders of magnitude compared to environmental concentrations to ensure detection of bioactivity. For the morphology screening experiments, the initial range finding studies consist of nominal exposure concentrations to identify a maximum tolerable dose to allow for a more precise estimate of effect levels. For the individual PAHs, 5 concentrations were tested (50, 35.6, 11.2, 5, and 1.00 µM), while for the mixtures (SM10, SM7, and SM3) exposures were a percentage of the prepared stock: 1.0, 0.91, 0.81, 0.72, 0.63, 0.53, 0.44, 0.34, 0.25, 0.16, and 0.063%. For SM10, a follow up study comprised of a percentage range of 1.0, 0.81, 0.63, 0.44, 0.33, 0.28, 0.23, 0.19, 0.14, 0.094, and 0.047% was performed. In the case of SM7, an additional exposure occurred at the following concentrations: 2.00, 1.82, 1.62, 1.44, 1.26, 1.06, 0.88, 0.68, 0.5, 0.32 and 0.126%. Exposure concentrations for EC_{50} determinations were the same as the morphology screening for SM10 and SM3. Although 3 PAHs caused adverse effects, only 2 (pyrene and retene) of the 10 individual PAHs developmental toxicity results yield data where an EC_{50} value could be determined. The exposure concentrations for these experiments are as follows: retene, 22, 20, 18, 16, 14, 12, 10, 8, 6, 4, and 2 µM; pyrene, 50, 47, 44, 41, 38, 35, 32, 29, 26, 23, and 20 µM. EC_{50} values for SM7

and the remaining PAHs were not determined due to an inability to cause 50% effect within the concentrations tested.

Developmental toxicity screening

All exposure plates followed protocols described in Truong et al [141]. Briefly, at 24 hpf embryos were visually assessed for mortality, developmental progression, notochord formation, and spontaneous motion. At 120 hpf, larvae were further assessed for 18 developmental endpoints: mortality, yolk sac edema, pericardial edema, body axis, trunk length, caudal fin, pectoral fin, pigmentation, somite, eye, snout, jaw, otolith, brain, notochord and circulatory malformations, swim bladder presence and inflation, and touch response [142]. Responses were recorded as a binary absence or presence of an abnormal morphology for each endpoint for each fish. Lowest effect levels (LELs) were calculated for each endpoint using a binomial test to estimate significance thresholds as previously described ($p<0.05$) [140].

Embryonic photomotor response

Embryonic photomotor response (EPR) was evaluated in 24 hpf embryos using a custom built photomotor response assay tool (PRAT)[143]. After exposures, embryos were not exposed to light until administration of the EPR test. The test consisted of: 30 s of darkness (Background); first pulse of intense light; 9 s darkness (Excitation); second pulse of intense light (1000 LUX); 10 s darkness (Refractory). Pixel changes between video frames were recorded to quantify total movement for each embryo across the test. Before analysis, wells with adverse effects (including mortality) observed at 24 hpf were removed. Statistical significance was assessed separately for each interval (Background, Excitation, and Refractory), using a Kolmogerov-Smirnov (KS) test (Bonferroni-corrected p value threshold = 0.05) against the vehicle control animals [144].

Larval photomotor response

Larval photomotor response (LPR) was evaluated with a light-dark cycle in 120 hpf larvae using the ViewPoint Zebrabox system and video tracking software (ViewPoint Life Sciences, Lyon, France)[145]. Fish with any observed morphology endpoints were excluded from behavioral

analysis. There were a total of 4 light cycles, each light cycle consisting of 3 minutes in the light (525 LUX), and 3 minutes in the dark. Before analysis, wells with mortality or morbidity were removed. Statistical significance was quantified using a KS test ($p<0.05$) on measured Area Under the Curve, dividing the dark and light cycles into separate bins, and was further constrained by a 50% threshold of significance for hyper or hypoactivity [20].

Adult exposures

For adult studies, 288 embryos were statically exposed to 0.1% SM10 in 0.1% DMSO and a 0.1% DMSO vehicle control from 6 - 120 hpf in individual wells on 96 well plates as described above. The final DMSO concentration was 0.1% in the exposure wells. The concentration of 0.1% SM10 was chosen due to the lack of overt morphological effects at 120 hpf. At 120 hpf, exposed animals were rinsed with clean water and raised on the lab system as described in zebrafish husbandry. At 30 days, juvenile fish were split into a 9L with a density of ~45 fish per tank. At approximately 6 months, a subset of ~60 animals were randomly chosen for behavior, respiration, and learning assessments.

Habituation to an audio startle stimulus was tested in adult fish using the zebrafish visual imaging system (zVIS) as previously described [20, 109]. Briefly, 48 adult fish (24 male, 24 female) per treatment group were individually placed into an array of 8 tanks (12cm x 12cm) filled with 750 mL of fish water. Taps were generated by an electric solenoid below each tank. Following a 10-minute acclimation period, a total of ten taps were delivered, with 20s following each tap, after which the distance moved was quantified for both SM10 and vehicle controls.

An active avoidance conditioning test was used to assess learning and performance differences in SM10 developmentally exposed zebrafish compared to controls. Custom built shuttleboxes, previously described [141], were used with a modified protocol to test for learning deficiencies. Briefly, zebrafish were conditioned to leave a darkened side (conditioned stimulus), by using a shock pulse on this “incorrect side”, and swim to the non-shock blue-lighted, “correct side” compartment within an 8 sec “seek period” to avoid the mild shock. The shuttlebox test consisted of a 10-minute acclimation period in the dark, followed by 30 consecutive trials. Each trial consisted of an 8 sec. seek period, initiated by the conditioned stimulus (CS), a blue LED light. If the fish did not swim to the correct side before the end of the seek period, or after the seek period

was over crossed back to the incorrect side after it had occupied the correct side, the unconditioned stimulus (US), a mild shock (2.8V, 500ms duration, at a 1sec interval, for a maximum 16 sec duration), was administered until the fish returned to the correct side. After each 24 sec trial, there was a 60 sec inter-trial interval where both sides of the shuttlebox were lighted blue, before the next trial began. If the zebrafish did not leave the incorrect side for the entire 24 sec trial, for 8 trials in a row, the fish would "fail out" and the test would stop. Conversely, if the fish left the incorrect side before the end of the seek period and did not cross back to the incorrect side for the entire 24 sec trial, the fish received no shock.

Immunohistochemistry

Immunohistochemistry (IHC) of cytochrome P450, family 1, subfamily A (CYP1A) protein localization was performed as previously described[146]. Briefly, wildtype embryos were exposed from 6 to 120 hpf to 0.43% for the mixtures, and the highest soluble concentration tested that did not cause significant mortality for the individuals. Two replicates of 8 larvae each were euthanized with tricaine at 120 hpf, and fixed overnight in 4% paraformaldehyde at 4°C. Fixed embryos were permeablized 10 minutes on ice in 0.005% trypsin, rinsed with PBS+Tween 20 (PBST) and post-fixed in 4% paraformaldehyde for 10 minutes. Larvae were blocked with 10% normal goat serum (NGS) in PBS+0.5% Triton X-100 (PBSTx) for 1 hour at RT, and incubated overnight in the primary antibody mouse α fish CYP1A monoclonal antibody (BiosenseLaboratories, Bergen, Norway) (1:500) in 1% NGS. Larvae were washed in PBST and incubated for 2 hours in secondary antibody (Fluor 594 goat anti-mouse, IgG). Eight embryos per treatment group were assessed by epi-fluorescence microscopy using a Keyance BZ-X700 microscope with 10× and 20× objectives and assessed for tissue-specific CYP1A expression patterns.

Morpholino injections

Embryos were injected at the single cell stage with a fluorescein-tagged translation-blocking morpholino targeting AHR2 (AHR2-MO, 5'TGTACCGATACCCGCCGACATGGTT3'), splice-blocking morpholinos targeting AHR1A (AhR1a-MO, 5'CTTTTGAAGTGACTTTTGGCCCGCA3'), or AHR1B (AHR1B-MO, 5'ACACAGTCGTCCATGATTACTTTGC3'), or a standard nonsense control (c-MO,

5’CCTCTTACCTCAGTTACAATTTATA3’) purchased from Gene Tools (Philomath, Oregon) at a concentration of 0.6 mM. Injection volume was ~2 nl. Fertilized, normally developing embryos were screened for morpholino incorporation at 4 hpf by fluorescence microscopy. Embryos with evenly incorporated morpholino were then dechorionated. Following dechorionation, embryos were exposed to SM10 or individual PAHs using the same methods as in the developmental toxicity screening as described above.

Statistics

The statistical software JMP Pro version 13.0.0 was used to calculate EC_{50} values for SM10, SM3, pyrene, and retene. Each concentration response curve consisted of 11 concentrations with n=32 fish at each concentration and were constructed with a binomial distribution and logistic regression. Confidence intervals for EC_{50} values were calculated based on n=4 and n=3 individual concentration response curves for SM10 and SM3 respectively. Confidence intervals were not calculated for individual PAH concentration response curves. Concentration response curves can be found in the supplemental data (Figure C1 and C2). Significance of adult startle response assay was assessed using a Single Factor Repeated Measure Analysis of Variance (ANOVA) and a Treatment by Subject ANOVA, with a Tukey Post Hoc Test, where significance was determined to be $p<0.05$.

Results and Discussion

Evaluating developmental toxicity of a chemical mixture

Laboratory experiments typically evaluate the toxicity of one chemical in isolation, which is unrealistic compared to what occurs in the environment. A sufficiently similar PAH mixture was constructed and assessed in the developmental zebrafish model to assess the short and long term developmental neurotoxicty of an environmentally relevant representative PAH mixture.

Construction of mixture

Supermix10 (SM10) was constructed from the top 10 most abundant PAHs in the freely dissolved phase of the water column in the Portland Harbor Superfund site, as measured by passive sampling devices during the summer of 2010 and 2015 [131, 132]. These 10 PAHs accounted for 87%, by mass, of ∑33 PAH in 2010 and 76%, by mass, of ∑62 PAH in 2015. The environmental

representativeness of SM10 over time is demonstrated by the fact that in both 2010 and 2015, the top 10 most abundant PAHs were the same. Despite the representativeness of this mixture, it is important to note that several known bioactive PAHs were detected in one or both years and are not included in SM10 including: benzo[a]pyrene, benzo[c]fluorene, benzo[k]fluoranthene, and benzo[j]fluoranthene [19, 88].

The constructed SM10 used in this study consisted of concentrations with approximately 6 orders of magnitude higher than environmental levels. This ensured bioactivity was detectable, and allowed more detailed interrogation of pathways of toxicity involved in the mixture (Table 4.1).

Developmental toxicity of individual PAHs

To assess the potential roles of the 10 components of SM10 in its developmental toxicity, we defined the developmental toxicity profile for each of the individual compounds, including morphological and behavioral effects, and the specific tissue expression of CYP1A. All compounds except 2-methylnaphthalene were bioactive in at least one assay (Figure 4.1). The remaining 9 compounds had effects in at least one phase of the LPR. Retene and benzo[a]anthracene had effects in the excitation phase of EPR, and retene also had significant effects during the baseline phase. Abnormalities in either phase have been demonstrated to be highly predictive of morphological effects at 5 dpf [144]. Accordingly, only pyrene, retene and benzo[a]anthracene had morphological effects. Several other studies have shown these compounds to cause developmental toxicity in zebrafish ([19, 113, 147, 148]. The developmental toxicity profiles shared several common endpoints between these three compounds, including yolk sac, pericardial edema, axial and pectoral fin malformations. Pyrene additionally caused an abnormal touch response, while retene and benzo[a]anthracene produced craniofacial malformations. Retene was the most toxic of the 10 compounds, with lower LELs than the other compounds and significant mortality at 24 and 120hpf. Because retene is primarily derived from the combustion of wood, this indicates that sources of PAHs outside of the Superfund site may be important contributors to developmental toxicity within the Superfund site [149].

CYP1A expression is a biomarker for activation of the AhR pathway. Of the ten PAHs, five induced CYP1A expression in the tissue. All the compounds that expressed CYP1A had

expression in the vasculature, which is associated with AhR2 mediated toxicity [150]. Fluoranthene additionally had CYP1A expression in the yolk, which has been previously observed, but the mechanism for this expression pattern remains unknown [151].

Developmental toxicity of constructed mixtures

Zebrafish embryos developmentally exposed to SM10 elicited both morphological and neurobehavioral endpoints (Figure 4.1). Ten of the 18 morphological endpoints were adversely affected, and at 120 hpf, the larval exhibited abnormal swimming behavior in both the light and dark phase. The comparison of the toxicity profile for SM10 and the individual PAHs revealed 3 PAHs that were likely driving the mixture toxicity. To test this hypothesis, we constructed two mixtures: (1) SM3, which consisted of the 3 constituents (pyrene, retene and benzo[a]anthracene) in the same ratios as in SM10 and (2) SM7 which consisted of the same ratios for the 7 non-bioactive PAHs.

Overall, the morphological endpoints affected by SM10 and SM3 were very similar to each other and to the endpoints of the individual components. The components of SM7 did not cause morphological effects and the range of exposure concentrations for SM7 did not exceed the individual exposure concentrations. Therefore, morphological effects were not expected following SM7 exposure. However, developmental exposure of SM7 caused both yolk sac edema and mortality at five days suggesting alternate affected pathways and/or synergistic effects. Significant LPR effects were observed even at the lowest concentrations tested for all three mixtures, as might be expected, due to LPR being the most common endpoint across the individual components. Significant effects were also observed in the excitation period of the EPR for all three mixtures. While this was expected for SM10 and SM3, because individual constituents of these mixtures had EPR effects, these effects would not have been expected in SM7. These results indicate the most robust endpoint for detecting individual bioactivity and predicting mixture activity in the zebrafish assay is the LPR (in only morphologically normal animals).

SM10 and SM3 morphology effects correlated well with effects observed in the individual compounds, with pectoral fin, pericardial and yolk sac edema, and craniofacial malformations

dominating morphological effects at the lower concentrations. However, despite the fact that the higher mixture concentrations did not exceed those of the individual PAH exposures, there were several endpoints at these higher concentrations that only appeared in the mixture exposures, including: caudal fin, swim bladder, trunk, somites and notochord. While individually SM7's components did not have morphology effects (except for the cumulative measure "any effect" for phenanthrene), the mixture resulted in 120 hpf mortality and yolk sac edema.

This underlines the need to consider mixtures effects in environmental exposures. These results are similar to previous findings, which showed that a complex PAH mixture can produce effects on neurodifferentiation that differ in magnitude and direction from a single PAH [152]. Interestingly, when compared to SM10, SM3 generally had morphology effects at higher concentrations, but a higher proportion of the cumulative effects endpoints were attributable to mortality. This suggests that the seven additional compounds may play some role in tempering the lethality of SM10, but not the overall prevalence of the any effect endpoint.

Assessment of Assumption of Additivity

Risk assessment practices for PAHs are based upon individual PAH toxicities, developed for carcinogenicity, with the assumption that PAHs have similar mechanisms of action and therefore behave in an additive manner as mixtures [123]. However, it has been well demonstrated that PAHs have dissimilar mechanisms of action in both their developmental toxicity and genotoxicity [113, 127, 153]. In order to simplify the data and enable evaluation of the usefulness of an additivity model with PAHs with disparate modes of action, morphological effects of SM10 and SM3 in zebrafish were tested with the additivity model using the "any effect" endpoint, which is a summation of all individual morphological endpoints. The cumulative EC_{50} value of the "any effect" endpoint in SM10 was 0.24% with a confidence range of 0.13% to 0.29%. The cumulative EC_{50} value of SM3 was higher (0.39%) ranging from 0.28% to 0.60%. The mixture of all 10 constituents is more potent than the mixture of the 3 bioactive constituents (0.24% vs 0.39%), but not statistically different due to the large 95% confidence intervals, 0.098-0.36% and 0.15-0.61% for SM10 and SM3 respectively. However, the data demonstrates the remaining 7 PAH constituents were more toxic in the SM7 mixture, then when evaluated individually (Figure 4.1), thus

suggesting possible interactions when combined in a mixture of more PAHs. This interaction may result in the lower EC_{50} observed in the SM10.

The assumption of additivity for both SM10 and SM3 was tested using Equation 1:

$$\sum_{i=1}^{n} \frac{c_i}{ECx_i} = 1 \quad (1)$$

In this equation, *c* is the concentration of the individual component in the EC_x of the mixture (x=50 in this case), *EC* is the EC_x of the individual compound, and *i* is the *i*th component in an *n*-compound mixture. If mixture toxicity was purely additive, a value of 1 would be expected. Here, the average value was 0.82 for SM10 with a 95% confidence interval of 0.34 to 1.3. For SM3, the average value was 1.3 with a 95% confidence interval of 0.52 to 2.1. Both of the confidence intervals overlap with 1 and therefore we cannot reject the premise of additivity for these mixtures.

Previous work has demonstrated that concentration addition can yield an accurate prediction of combination effects with mixtures of PAHs that operate diverse modes of action [34, 154]. Here, despite the known diverse modes of action for PAH developmental toxicity and the disparate individual PAH toxicity profiles presented in this study, we cannot reject the use of the concentration addition model for assessing the developmental toxicity of this Superfund PAH mixture when considering the any effect endpoint. However, the assumption of additivity may not be appropriate for all PAH mixtures, and warrants further investigation with other mixtures. Additionally, the any effect endpoint doesn't represent the full resolution of the zebrafish model, and might not be adequate to fully distinguish the developmental hazard posed by environmental mixtures.

AHR-mediated toxicity observed in 3 mixtures

In SM10 and SM3, CYP1A expression was primarily in the vasculature, while in SM7, there was no appreciable CYP1A tissue expression observed. Knockdown of AHR2 eliminated vasculature expression and produced liver expression in SM3, but in SM10 vasculature expression persisted along with liver expression (Figure 4.3). When the different isoforms of AHR was transiently knocked down using morpholinos, then exposed to SM3, CYP1A tissue expression was obliterated, while those exposed to SM10 still had some CYP1A expression. Liver expression has

previously been associated with AHR1A dependent PAH toxicity [150], but has not been previously observed following AHR2 knockdown. Although the reason for this change in tissue expression is not completely clear, there are potential explanations. First, it is possible that in the absence of AHR2, AHR1A may become the primary receptor for some ligands[150]. Additionally, PAH metabolism maybe altered in the absence of AHR2 and produces a ligand with a higher affinity for AHR1A. It is suspected that AHR1A, though unable to bind may large parent PAHs, may be able to bind smaller PAH metabolites [155]. Finally, altered PAH metabolism may modulate oxidative stress response which modulates the expression of CYP1A directly [156]. These hypotheses should be pursued in future work.

Although individually knocking down AHR1A and AHR1B did not have an appreciable effect on the vasculature expression of CYP1A in SM3 and SM10, knockdown of all three isoforms eliminated CYP1A expression in SM3. However, in SM10, while it reduced the intensity of expression patterns overall, knockdown of all three AHR isoforms did not completely eliminate CYP1A expression. It is possible that combined, the five AHR active PAHs present in SM10 overpowered the incomplete knockdown of the receptors.

Developmental exposure results in long term neurobehavioral effects

To assess if developmental exposure to the SM10 leads to life-long behavioral effects, we exposed animals during development and raised them in chemical-free water into adulthood, and tested the adults for learning and memory deficits. The developmentally exposed adult zebrafish were assessed for distance moved in response to successive mechanical taps (Figure 4.2). Over the course of repeated taps, control fish increasingly habituate to the stimulus and decrease their total distance moved. In SM10 exposed fish, the response to the first tap was not significantly different compared to carrier control fish ($p=0.48$). Both treatment groups significantly habituated to successive taps starting on the 3rd tap ($p<0.001$), however the rate of habituation was greater for control animals than SM10 exposed animals ($p<0.001$), and SM10 exposed animals moved significantly greater distances over the course of the test than control animals.

Fish were also assessed for learning by being conditioned to move to the dark side of a two-chamber box. Developmental SM10 exposure resulted in differences in learning in adult

zebrafish. Fish exposed to SM10 took longer to make their first move to the correct side, with a higher intercept and lower slope than the DMSO controls (Table 4.3), and a significant difference between treatment and control ($p=0.005$). Additionally, treated fish spent less time overall on the correct side than controls ($p=0.001$), and were less likely to learn over the course of the trial.

These results indicate that developmental exposure to SM10 can result in long term behavioral effects, including a decreased ability to habituate to environmental stimuli and a decreased learning capacity. This is consistent with previous epidemiological studies reporting the neurological effects of PAH exposure during development [18, 22, 101] and effects on neurodifferentiation and neurobehavior [152, 157]. While it has been previously demonstrated that developmental exposure to chlorpyrifos can significantly increase overall startle response in adult zebrafish [158], startle response effects have not been previously observed for adult zebrafish developmentally exposed to PAHs. However, startle response effects have been observed in the progeny of zebrafish developmentally exposed to benzo[a]pyrene [109]. Collectively, this demonstrates exposure to SM10 results in neurobehavioral defects as larvae and adults.

Limitations

There are several important limitations to the interpretations of the results of this study. Exposure concentrations in the present study are higher than reported environmental concentrations in the PHSS [131, 132]. Additionally, PAHs are known to sorb to the walls of 96 well polystyrene exposure plates [159] which creates uncertainty in the actual exposure concentrations of this study. This study is therefore a hazard assessment and not an assessment of the risk posed by environmentally relevant concentrations. Further work is also needed to quantify exposure and tissue burden during the course of the study. It is noteworthy that in our assays phenanthrene did not elicit cardiovascular effects previously reported in several studies [106, 160, 161]. However, this discrepancy can be explained by differences in exposure methods, because the previous studies all employed repeated exposures, rather than the static exposures used in this study.

Conclusions

At any one time, humans and other organisms are exposed to hundreds of chemicals. Therefore, understanding the toxicity of mixtures is essential. The representative mixture approach demonstrated in this study may offer a more comprehensive and practical alternative to component based and whole mixture approaches respectively. With this approach, we were able to identify the mixture components that drive toxicity, provided insight into the potential mechanisms of toxicity for these mixtures, and show that these environmentally relevant mixtures have behavioral effects in adult fish following developmental exposure. Additionally, while uncertainty exists due to a lack of exposure concentrations over time, the developmental effects caused by these PAH mixtures appear to behave in an additive manner. However, we also showed that endpoints caused by chemical mixtures may not be predictable from single chemical effects alone. Further work is needed to improve understanding of the dosimetry, pharmacokinetics, and metabolism of this mixture. This approach should also be applied using other representative chemical mixtures from various locations and matrices including other classes of chemicals. Data of this kind would allow for comparisons between representative mixtures and allow for the determination of sufficient similarity while providing needed additional insight into toxicities of chemical mixtures.

Acknowledgements

This work was supported by National Institute of Health [P42 ES016465, T32 ES07060 and P30 ES000210]. The content is solely the responsibility of the authors and does not necessarily represent the official views of any funding organization We are highly appreciative of the staff at the Sinnhuber Aquatic Research Laboratory including Carrie Barton for fish husbandry, Jane LaDu for morpholino injections, and Greg Gonnerman for screening assistance. In addition, we are thankful for environmental data collected by Sarah Allan and the analytical expertise from Richard Scott, and Gary Points. We also thank Sean Carver for his graphical design expertise.

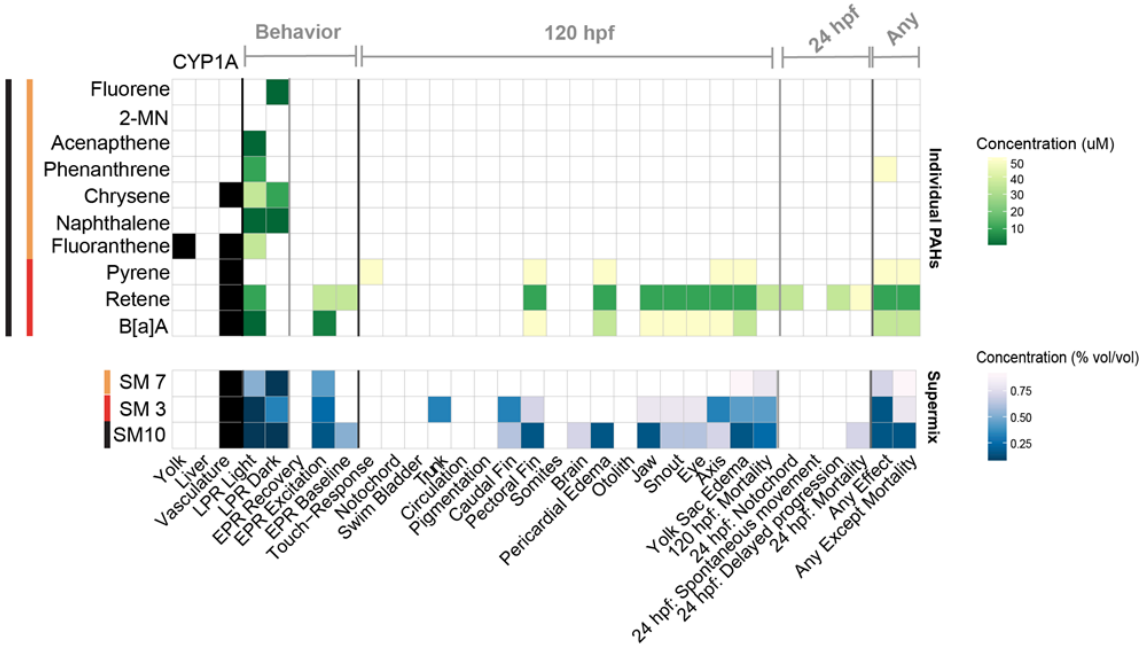

Figure 4.1 Heatmap of Lowest Effect Levels and CYP1A tissue expression for each of the individual components of SM10 in µM, compared with heatmap of Lowest Effect Concentrations and CYP1A Tissue Expression for SM10 and SM3 in percent (vol/vol). Heatmaps show 27 endpoints in 24 and 120 hpf zebrafish, and 3 tissue types where CYP1A expression was detected. Darker green or blue indicates lower concentration and higher potency. Black indicates the spatial CYP1A expression pattern. Orange bar indicates components of SM 7, red indicates components of SM3 and black indicates components of SM10.

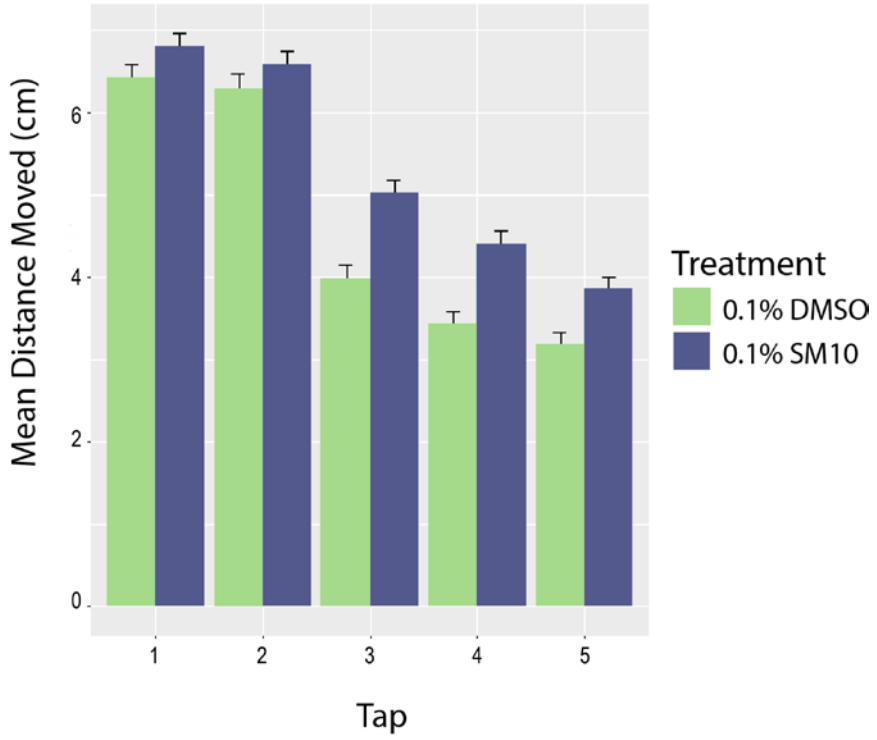

Figure 4.2. Increased distance moved after mechanical stimulus in developmentally exposed adult zebrafish. Embryos developmentally exposed to 0.1% SM10 or vehicle control (DMSO) from 6-120 hpf, and raised in chemical-free water until adulthood. Adults were evaluated for response to 5 taps using a mechanical stimulus with 20s inter-tap period. By the 3rd tap, the SM10 exposed zebrafish moved more (* denotes $p<0.05$, Single Factor Repeated Measure Analysis of Variance (ANOVA) and a Treatment by Subject ANOVA, with a Tukey Post Hoc Test).

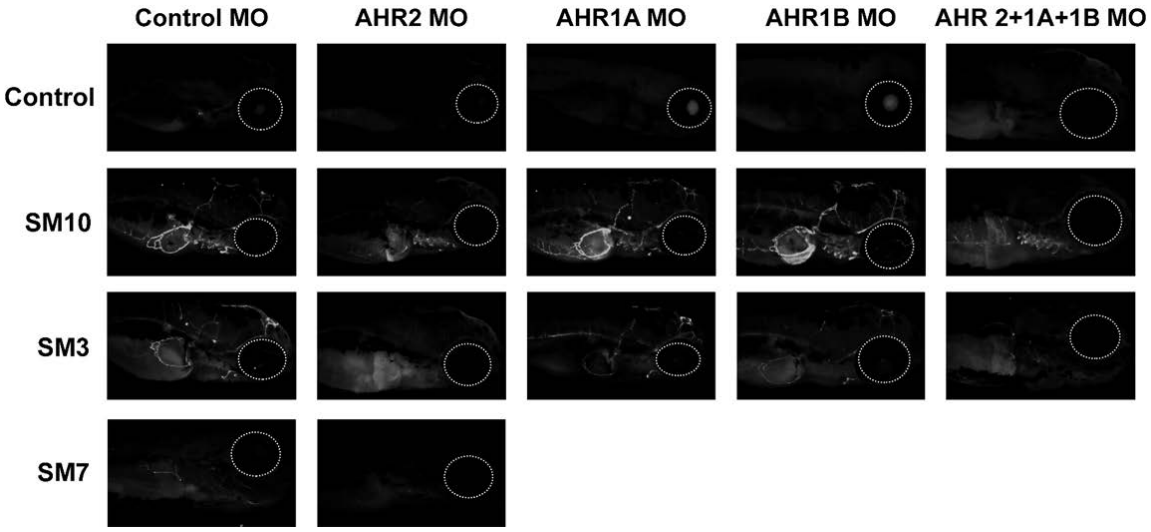

Figure 4.3. Spatial expression of AHR activation biomarker, CYP1A using immunohistochemistry. Zebrafish have 3 forms of aryl hydrocarbon receptor: AHR2, AHR1A and AHR2B. Each isoform was transiently knocked down using morpholinos (MOs) individually and in combination and the injected larvae were exposed at 6 hpf to 0.43% SM10, 0.43% SM3 or 1% DMSO. At 120 hpf, the CYP1A expression was observed in SM10 and SM3 (control MO). Exposure to SM7 did not produce CYP1A expression. The combined AhR Morpholino injected larvae had some CYP1A expression, when exposed to SM10, while those exposed to SM3 did not. Larvae were imaged from right side to better visualize liver expression. Dashed lines indicate eye position.

Table 4.1. Range of relative ratios of the 10 most abundant PAHs on average in surface waters of the Portland Harbor Superfund site based on passive sampling during 2010 and 2015. Surrogate mixtures were constructed based on the environmental ratios. The highest initial exposure concentrations (1% DMSO) are reported for Supermix10 (SM10), Supermix3 (SM3), and Supermix7(SM7). .

PAH	Environmental Ratios	Mixture Ratios	Exposure concentration (µM) SM10	SM3	SM7
Pyrene	0.50 – 1.0	1.0	24	24	-
Fluoranthene	0.45 – 1.0	1.0	24	-	48
Retene	0.083 – 1.0	0.60	13	12	-
Benzo[a]anthracene	0.053 – 0.15	0.21	4.2	4.4	-
Chrysene	0.068 – 0.26	0.20	4.4	-	8.8
Naphthalene	0.072 – 1.0	0.14	5.9	-	12
Acenaphthene	0.11 – 1.0	0.12	2.9	-	5.8
Phenanthrene	0.16 – 0.45	0.12	3.4	-	6.8
Fluorene	0.10 – 0.32	0.080	3.1	-	6.2
2-methylnaphthalene	0.049 – 0.51	0.052	1.7	-	3.4

Table 4.2. Experimentally determined EC_{50} values (µM) for individual PAHs where the EC_{50} was less than 50 µM. EC_{50} values were experimentally determined for Supermix10 (SM10) and Supermix3 (SM3) and the concentrations of the individual PAHs at the mixture EC_{50} values are reported. * *EC_{50} values greater than 50µM.* – Compound not in mixture.*

PAH	Individual EC_{50} (µM)	SM10 EC_{50} (µM)	SM3 EC_{50} (µM)
Pyrene	27	5.9	9.5
Fluoranthene	*	5.8	-
Retene	5.1	3.0	4.9
Benzo[a]anthracene	*	1.0	1.6
Chrysene	*	1.0	-
Naphthalene	*	1.4	-
Acenaphthene	*	0.81	-
Phenanthrene	*	0.70	-
Fluorene	*	0.74	-
2-methylnaphthalene	*	0.41	-

Table 4.3. Performance in the active avoidance test for 3 parameters: Total shocked time, time to accept, and total time on correct side. Animals that failed out of the test and were removed from analysis as well as those animals which successfully learned over the course of the trials are reported as percentages. The intercept and slope for the assay, and the differences between vehicle control and SM10 treated animals are reported. *p<0.05 ANOVA and Tukeys *post hoc* test.

Time Shocked

Treatment	*Failed Out*	*Learned*	*Intercept, Slope*	*Diff, p value*
Vehicle Control	0%	42.5%	1.47, -0,041	-
0.1% SM10	2.80%	40%	2.03, -0.032	0.21, 0.06

Decision Time

Treatment	*Failed Out*	*Learned*	*Intercept, Slope*	*Diff, p value*
Vehicle Control	0%	35%	4.945, -0.067	-
0.1% SM10	2.80%	22.9%	5.119, -0.013	0.44, 0.005*

Time on Correct Side

Treatment	*Failed Out*	*Learned*	*Intercept, Slope*	*Diff, p value*
Vehicle Control	0%	47.5%	18.164, 0.102	-
0.1% SM10	2.80%	29.2%	17.611, 0.063	0.55, 0.001*

CHAPTER 5 – CONCLUSION AND FUTURE DIRECTIONS

Summary

Quantifying the freely dissolved, unbound fraction of chemical (C_{free}) is essential for understanding many important contaminant processes in the environment. Passive sampling offers a direct and accurate method for measuring C_{free}. The work in the dissertation utilizes passive sampling devices to measure C_{free} in the sediment porewater, water, and air to measure and assess the diffusive flux, bioaccumulation, and toxicity of PAHs. Work was conducted at two urban Superfund sites in Portland, Oregon as well as on Native American land in the Puget Sound region of the Salish Sea.

In Chapter 2, for the first time, the diffusive flux of PAHs was measured across the sediment-water and water-air interfaces concurrently. Results from this study at the Portland Harbor Superfund site (PHSS) and the McCormick and Baxter Superfund site (MCBSS) may help remediation managers and risk assessors prioritize cleanup efforts and identify potential PAH sources which may undermine those efforts. Additionally, this study showed that PAHs may ultimately be transported from the sediment to the air resulting in exposure to PAHs for those living near the PHSS. This finding highlights the importance of considering the inhalation route of exposure for those who live near sites with sediment contamination.

In Chapter 3, a passive sampling model was constructed to predict the accumulation of 62 PAHs in butter clams, an important food source for Native American tribes of the Salish Sea region. This model built upon previous work to predict PAH bioaccumulation in clams by incorporating 59 additional PAHs and by assessing accumulation in the entire edible fraction of the clam as determined by Native American tribes. The model in this study was able to predict PAH clam concentrations from sediment porewater concentrations within a factor of 2. Importantly, this model may obviate the need to remove clams, for biomonitoring purposes, from an already fragile ecosystem. Ultimately, results from this study highlight the usefulness and applicability of this passive sampling predictive model for monitoring PAH levels in this important Native American cultural resource.

In Chapter 4, we round out assessment of PAH transport and bioaccumulation by examining the toxicity of an environmentally relevant, passive sampling derived, PAH mixture in zebrafish. Importantly, we showed that the general concentration addition model may be sufficient for assessing the summation of developmental toxicity endpoints for these PAH mixtures in zebrafish. However, when considering individual toxic endpoints, significant differences existed between the individual components and the mixtures. Additionally, developmental exposure resulted in significant neurological effects in adult fish at low concentrations. This study adds to the growing concern regarding the neurological impacts of PAHs and highlights the importance of considering the toxicity of environmental mixtures.

Ultimately, the work in this dissertation will increase our understanding of contaminant processes in the environment and ultimately serve to help protect the health of humans and other organisms.

Future directions: Advective flux

In Chapter 2, the diffusive flux of PAHs was reported across the sediment-water interface in the Portland Harbor and across the sediment cap at the MCBSS. Previous studies have also focused on diffusive flux when quantifying the transport of contaminants [24, 55]. However, contaminants may also be transported through advective flux resulting from wave pumping, tidal pumping, or groundwater flow[162, 163]. Effective management of contaminated sites requires evaluation of all contaminant transport pathways which ultimately may lead to exposure for humans and organisms [163]. Measurement of advective flux from the sediment to water is important for understanding how contaminated sediments may affect the quality of overlying water and provides necessary information to design effect sediment caps [164]. For example, previous work has shown that PAHs may break through a non-reactive cap in the presence of groundwater advection in a short period of time[163].

Measuring the advective flux of contaminants first requires measuring advective flow. Generally, the first step in measuring advective flow is to identify areas of seepage. This is because the majority of discharge can occur in a small percentage of the total area of a site[165]. After determining areas of seepage, the next step is to assess the magnitude and direction of advective flow. The traditional and most common method for assessing the advective flow of water across the sediment-water interface is through the use of a seepage meter[164]. The advective flux of

contaminants can then be measured by incorporating the advective flow measurements with measurements of contaminants in the sediment porewater and overlying water.

Preliminary work

Initial work was performed in order to quantify the advective flux of PAHs at a creosote contaminated site in St. Helens, Oregon. In order to measure advective flow, seepage meters were constructed following guidance from the USGS[166]. These seepage meters were constructed from metal, 55 gallon drums cut in half. The drums were inserted into the sediment with the closed top of the drum remaining submerged and fitted with plastic tubing connected to a sealed bag (Figure 5.1). The bag was located approximately 2m away from the drum to avoid disturbing the sediment and artificially affecting advective flow. Advective flow was measured with the volume of water collected in the bag, the area of the drum, and time. To measure advective flux, passive sampling devices were placed in the sediment and in the overlying water to measure PAH concentrations.

In an initial field trial of the seepage meters, advective flow was measured at 3 locations at the St. Helens site in September of 2017 for approximately 6 hours surrounding high tide. The seepage meters appeared to be functioning as designed and advective flow measurements were recorded. One of the sampling locations was in an area with a known groundwater seep and at this location, the flow rate was determined to be 10 L/m^2d from the sediment to the water. At the two other locations, flow measurements were lower in magnitude and in opposite directions.

Based on the success of the first trial, the seepage meters were deployed along with PSDs at the St. Helens site in October, 2017 to quantify the advective flux of PAHs. This work was coupled with a site assessment study in coordination with the Oregon Department of Environmental Quality to measure sediment porewater and water PAH concentrations. Seven locations were selected for measurement of advective flux because of previously measured seeps. Deployment of the seepage meters was planned such that flow would be measured during high and low tide cycles in order to capture the effect of tidal pumping on groundwater flow. Overall, the results from this work were inconclusive due to unexpected lowering of water levels which uncovered the seepage meters during low tide. However, the data indicated that advective flow could effectively be measured using the seepage meters. At the location near a known seep, flow was

measured at 1.73 L/m^{2}d during low tide from the sediment to the water and 1.53 L/m^{2}d during high tide from the water to the sediment. These results fit what is known about the effects of tidal pumping on groundwater flow. Despite the inability to characterize advective flow and subsequently the advective flux of PAHs at the St. Helens site, these preliminary studies will serve as a building block for future studies to measure the advective flux of contaminants. Ultimately, measuring the advective flux of contaminants will provide information necessary to design effective remediation strategies in order to limit contaminant exposure for humans and other organisms.

Figure 5.1. Deployment of half-barrel seepage meters at a creosote contaminated site in St. Helens, Oregon. When paired with passive sampling devices to measure concentrations of contaminants in the sediment porewater, the seepage meters can be used to determine the advective flux of contaminants.

Bibliography

1. Reichenberg, F.; Mayer, P., Two complementary sides of bioavailability: Accessibility and chemical activity of organic contaminants in sediments and soils. *Environmental Toxicology and Chemistry* **2006,** *25*, (5), 1239-1245.

2. Mayer, P.; Vaes, W. H. J.; Wijnker, F.; Legierse, K. C. H. M.; Kraaij, R.; Tolls, J.; Hermens, J. L. M., Sensing dissolved sediment porewater concentrations of persistent and bioaccumulative pollutants using disposable solid-phase microextraction fibers. *Environmental Science & Technology* **2000,** *34*, (24), 5177-5183.

3. Lydy, M. J.; Landrum, P. F.; Oen, A. M. P.; Allinson, M.; Smedes, F.; Harwood, A. D.; Li, H.; Maruya, K. A.; Liu, J., Passive sampling methods for contaminated sediments: State of the science for organic contaminants. *Integrated Environmental Assessment and Management* **2014,** *10*, (2), 167-178.

4. Hawthorne, S. B.; Azzolina, N. A.; Neuhauser, E. F.; Kreitinger, J. P., Predicting bioavailability of sediment polycyclic aromatic hydrocarbons to hyalella azteca using equilibrium partitioning, supercritical fluid extraction, and pore water concentrations. *Environmental Science & Technology* **2007,** *41*, (17), 6297-6304.

5. Mayer, P.; Parkerton, T. F.; Adams, R. G.; Cargill, J. G.; Gan, J.; Gouin, T.; Gschwend, P. M.; Hawthorne, S. B.; Helm, P.; Witt, G.; You, J.; Escher, B. I., Passive sampling methods for contaminated sediments: Scientific rationale supporting use of freely dissolved concentrations. *Integr Environ Assess Manag* **2014,** *10*, (2), 197-209.

6. Fernandez, L. A.; Gschwend, P. M., Predicting bioaccumulation of polycyclic aromatic hydrocarbons in soft-shelled clams (mya arenaria) using field deployments of polyethylene passive samplers. *Environmental Toxicology and Chemistry* **2015,** *34*, (5), 993-1000.

7. Muijs, B.; Jonker, M. T., Does equilibrium passive sampling reflect actual in situ bioaccumulation of pahs and petroleum hydrocarbon mixtures in aquatic worms? *Environ Sci Technol* **2012,** *46*, (2), 937-44.

8. Jahnke, A.; MacLeod, M.; Wickstrom, H.; Mayer, P., Equilibrium sampling to determine the thermodynamic potential for bioaccumulation of persistent organic pollutants from sediment. *Environ Sci Technol* **2014,** *48*, (19), 11352-9.

9. Fadaei, H.; Watson, A.; Place, A.; Connolly, J.; Ghosh, U., Effect of pcb bioavailability changes in sediments on bioaccumulation in fish. *Environmental Science & Technology* **2015,** *49*, (20), 12405-12413.

10. Heijden, S. A. v. d.; Jonker, M. T. O., Pah bioavailability in field sediments: Comparing different methods for predicting in situ bioaccumulation. *Environmental Science & Technology* **2009,** *43*, (10), 3757-3763.

11. Huckins, J. N.; Petty, J. D.; Booij, K., Monitors of the organic chemicals in the environment. In *Monitors of the organic chemicals in the environment*, Springer: New York, NY, 2006; p 223.

12. Ghosh, U.; Kane Driscoll, S.; Burgess, R. M.; Jonker, M. T.; Reible, D.; Gobas, F.; Choi, Y.; Apitz, S. E.; Maruya, K. A.; Gala, W. R.; Mortimer, M.; Beegan, C., Passive sampling methods for contaminated sediments: Practical guidance for selection, calibration, and implementation. *Integr Environ Assess Manag* **2014,** *10*, (2), 210-23.

13. Khairy, M. A.; Lohmann, R., Field validation of polyethylene passive air samplers for parent and alkylated pahs in alexandria, egypt. *Environ Sci Technol* **2012,** *46*, (7), 3990-8.

14. Burgess, R. M.; Lohmann, R.; Schubauer-Berigan, J. P.; Reitsma, P.; Perron, M. M.; Lefkovitz, L.; Cantwell, M. G., Application of passive sampling for measuring dissolved concentrations of organic contaminants in the water column at three marine superfund sites. *Environmental Toxicology and Chemistry* **2015,** *34*, (8), 1720-1733.

15. Apell, J. N.; Gschwend, P. M., Validating the use of performance reference compounds in passive samplers to assess porewater concentrations in sediment beds. *Environ Sci Technol* **2014,** *48*, (17), 10301-7.

16. Baird, W. M.; Hooven, L. A.; Mahadevan, B., Carcinogenic polycyclic aromatic hydrocarbon-DNA adducts and mechanism of action. *Environ Mol Mutagen* **2005,** *45*, (2-3), 106-14.

17. Jedrychowski, W. A.; Perera, F. P.; Majewska, R.; Mrozek-Budzyn, D.; Mroz, E.; Roen, E. L.; Sowa, A.; Jacek, R., Depressed height gain of children associated with intrauterine exposure to polycyclic aromatic hydrocarbons (pah) and heavy metals: The cohort prospective study. *Environ Res* **2015,** *136*, 141-7.

18. Perera, F. P.; Chang, H. W.; Tang, D.; Roen, E. L.; Herbstman, J.; Margolis, A.; Huang, T. J.; Miller, R. L.; Wang, S.; Rauh, V., Early-life exposure to polycyclic aromatic hydrocarbons and adhd behavior problems. *PLoS One* **2014,** *9*, (11), e111670.

19. Geier, M. C.; Chlebowski, A. C.; Truong, L.; Massey Simonich, S. L.; Anderson, K. A.; Tanguay, R. L., Comparative developmental toxicity of a comprehensive suite of polycyclic aromatic hydrocarbons. *Archives of Toxicology* **2017**.

20. Knecht, A. L.; Truong, L.; Simonich, M. T.; Tanguay, R. L., Developmental benzo[a]pyrene (b[a]p) exposure impacts larval behavior and impairs adult learning in zebrafish. *Neurotoxicol Teratol* **2017,** *59*, 27-34.

21. Perera, F. P.; Li, Z.; Whyatt, R.; Hoepner, L.; Wang, S.; Camann, D.; Rauh, V., Prenatal airborne polycyclic aromatic hydrocarbon exposure and child iq at age 5 years. *Pediatrics* **2009,** *124*, (2), e195-e202.

22. Perera, F. P.; Rauh, V.; Whyatt, R. M.; Tsai, W.-Y.; Tang, D.; Diaz, D.; Hoepner, L.; Barr, D.; Tu, Y.-H.; Camann, D.; Kinney, P., Effect of prenatal exposure to airborne polycyclic

aromatic hydrocarbons on neurodevelopment in the first 3 years of life among inner-city children. *Environmental Health Perspectives* **2006,** *114*, (8), 1287-1292.

23. Greenberg, M. S.; Chapman, P. M.; Allan, I. J.; Anderson, K. A.; Apitz, S. E.; Beegan, C.; Bridges, T. S.; Brown, S. S.; Cargill, J. G.; McCulloch, M. C.; Menzie, C. A.; Shine, J. P.; Parkerton, T. F., Passive sampling methods for contaminated sediments: Risk assessment and management. *Integrated Environmental Assessment and Management* **2014,** *10*, (2), 224-236.

24. Fernandez, L. A.; Lao, W.; Maruya, K. A.; Burgess, R. M., Calculating the diffusive flux of persistent organic pollutants between sediments and the water column on the palos verdes shelf superfund site using polymeric passive samplers. *Environmental Science & Technology* **2014,** *48*, (7), 3925-34.

25. Bamford, H. A.; Offenberg, J. H.; Larsen, R. K.; Ko, F.-C.; Baker, J. E., Diffusive exchange of polycyclic aromatic hydrocarbons across the air−water interface of the patapsco river, an urbanized subestuary of the chesapeake bay. *Environmental Science & Technology* **1999,** *33*, (13), 2138-2144.

26. Fang, M. D.; Lee, C. L.; Jiang, J. J.; Ko, F. C.; Baker, J. E., Diffusive exchange of pahs across the air-water interface of the kaohsiung harbor lagoon, taiwan. *J Environ Manage* **2012,** *110*, 179-87.

27. Eek, E.; Cornelissen, G.; Breedveld, G. D., Field measurement of diffusional mass transfer of hocs at the sediment-water interface. *Environmental Science & Technology* **2010,** *44*, (17), 6752-6759.

28. O.D.E.Q, Fourth five-year report for mccormick & baxter creosoting company superfund site. In 2016; p 10.

29. Donatuto, J. L.; Satterfield, T. A.; Gregory, R., Poisoning the body to nourish the soul: Prioritising health risks and impacts in a native american community. *Health, Risk & Society* **2011,** *13*, (2), 103-127.

30. Paulik, L. B.; Smith, B. W.; Bergmann, A. J.; Sower, G. J.; Forsberg, N. D.; Teeguarden, J. G.; Anderson, K. A., Passive samplers accurately predict pah levels in resident crayfish. *Sci Total Environ* **2015,** *544*, 782-791.

31. Arp, H. P.; Lundstedt, S.; Josefsson, S.; Cornelissen, G.; Enell, A.; Allard, A. S.; Kleja, D. B., Native oxy-pahs, n-pacs, and pahs in historically contaminated soils from sweden, belgium, and france: Their soil-porewater partitioning behavior, bioaccumulation in enchytraeus crypticus, and bioavailability. *Environ Sci Technol* **2014,** *48*, (19), 11187-95.

32. Hauck, M.; Huijbregts, M. A. J.; Koelmans, A. A.; Moermond, C. T. A.; Van den Heuvel-Greve, M. J.; Veltman, K.; Hendriks, A. J.; Vethaak, A. D., Including sorption to black carbon in modeling bioaccumulation of polycyclic aromatic hydrocarbons: Uncertainty analysis and comparison to field data. *Environmental Science & Technology* **2007,** *41*, (8), 2738-2744.

33. Carpenter, D. O.; Arcaro, K.; Spink, D. C., Understanding the human health effects of chemical mixtures. *Environ Health Perspect* **2002,** *110 Suppl 1*, 25-42.

34. Van Gestel, C. A. M.; Jonker, M. J.; Kammenga, J. E.; Laskowski, R.; Svendsen, C., *Mixture toxicity: Linking approaches from ecological and human toxicology*. CRC Press: New York, New York, 2011.

35. U.S.EPA, Supplementary guidance for conducting health risk assessment of chemical mixtures. **2000**.

36. Howsam, M.; Jones, K. C., Sources of pahs in the environment. In *Pahs and related compounds: Chemistry*, Neilson, A. H., Ed. Springer Berlin, Germany, 1998; pp 137-174.

37. Incardona, J. P.; Day, H. L.; Collier, T. K.; Scholz, N. L., Developmental toxicity of 4-ring polycyclic aromatic hydrocarbons in zebrafish is differentially dependent on ah receptor isoforms and hepatic cytochrome p4501a metabolism. *Toxicology and Applied Pharmacology* **2006,** *217*, (3), 308-321.

38. Gale, S. L.; Noth, E. M.; Mann, J.; Balmes, J.; Hammond, S. K.; Tager, I. B., Polycyclic aromatic hydrocarbon exposure and wheeze in a cohort of children with asthma in fresno, ca. *J Expos Sci Environ Epidemiol* **2012,** *22*, (4), 386-392.

39. Walker, S. E.; Dickhut, R. M.; Chisholm-Brause, C.; Sylva, S.; Reddy, C. M., Molecular and isotopic identification of pah sources in a highly industrialized urban estuary. *Organic Geochemistry* **2005,** *36*, (4), 619-632.

40. Wolfe, D. A.; Long, E. R.; Thursby, G. B., Sediment toxicity in the hudson-raritan estuary: Distribution and correlations with chemical contamination. *Estuaries* **1996,** *19*, (4), 901-912.

41. Allan, I. J.; Ruus, A.; Schaanning, M. T.; Macrae, K. J.; Naes, K., Measuring nonpolar organic contaminant partitioning in three norwegian sediments using polyethylene passive samplers. *Sci Total Environ* **2012,** *423*, 125-31.

42. Tang, L.; Tang, X.-Y.; Zhu, Y.-G.; Zheng, M.-H.; Miao, Q.-L., Contamination of polycyclic aromatic hydrocarbons (pahs) in urban soils in beijing, china. *Environment International* **2005,** *31*, (6), 822-828.

43. Van Metre, P. C.; Mahler, B. J.; Furlong, E. T., Urban sprawl leaves its pah signature. *Environmental Science & Technology* **2000,** *34*, (19), 4064-4070.

44. Lee, J. H.; Gigliotti, C. L.; Offenberg, J. H.; Eisenreich, S. J.; Turpin, B. J., Sources of polycyclic aromatic hydrocarbons to the hudson river airshed. *Atmospheric Environment* **2004,** *38*, (35), 5971-5981.

45. Schwarzenbach, R. P.; Gschwend, P. M.; Imboden, D. M., Environmental organic chemistry. In *Environmental organic chemsitry*, 2 ed.; John Wiley & Sons, Inc.: Hoboken, New Jersey, 2003.

46. Baker, J. E.; Eisenreich, S. J., Concentrations and fluxes of polycyclic aromatic hydrocarbons and polychlorinated biphenyls across the air-water interface of lake superior. *Environmental Science & Technology* **1990,** *24*, (3), 342-352.

47. Bi, X.; Sheng, G.; Peng, P. a.; Chen, Y.; Zhang, Z.; Fu, J., Distribution of particulate- and vapor-phase n-alkanes and polycyclic aromatic hydrocarbons in urban atmosphere of guangzhou, china. *Atmospheric Environment* **2003,** *37*, (2), 289-298.

48. Arp, H. P. H.; Breedveld, G. D.; Cornelissen, G., Estimating the in situ sediment−porewater distribution of pahs and chlorinated aromatic hydrocarbons in anthropogenic impacted sediments. *Environmental Science & Technology* **2009,** *43*, (15), 5576-5585.

49. Tidwell, L. G.; Allan, S. E.; O'Connell, S. G.; Hobbie, K. A.; Smith, B. W.; Anderson, K. A., Pah and opah flux during the deepwater horizon incident. *Environmental Science & Technology* **2016,** *50*, (14), 7489-7497.

50. Lohmann, R.; Dapsis, M.; Morgan, E. J.; Dekany, V.; Luey, P. J., Determining air-water exchange, spatial and temporal trends of freely dissolved pahs in an urban estuary using passive polyethylene samplers. *Environ Sci Technol* **2011,** *45*, (7), 2655-62.

51. McDonough, C. A.; Khairy, M. A.; Muir, D. C. G.; Lohmann, R., Significance of population centers as sources of gaseous and dissolved pahs in the lower great lakes. *Environmental Science & Technology* **2014,** *48*, (14), 7789-7797.

52. McDonough, C. A.; Puggioni, G.; Helm, P. A.; Muir, D.; Lohmann, R., Spatial distribution and air–water exchange of organic flame retardants in the lower great lakes. *Environmental Science & Technology* **2016**.

53. Gustafson, K. E.; Dickhut, R. M., Gaseous exchange of polycyclic aromatic hydrocarbons across the air−water interface of southern chesapeake bay. *Environmental Science & Technology* **1997,** *31*, (6), 1623-1629.

54. Koelmans, A. A.; Poot, A.; Lange, H. J. D.; Velzeboer, I.; Harmsen, J.; Noort, P. C. M. v., Estimation of in situ sediment-to-water fluxes of polycyclic aromatic hydrocarbons, polychlorobiphenyls and polybrominated diphenylethers. *Environmental Science & Technology* **2010,** *44*, (8), 3014-3020.

55. Eek, E.; Cornelissen, G.; Kibsgaard, A.; Breedveld, G. D., Diffusion of pah and pcb from contaminated sediments with and without mineral capping; measurement and modelling. *Chemosphere* **2008,** *71*, (9), 1629-38.

56. U.S.EPA, Portland harbor superfund site-proposed plan. In 2016.

57. Larsson, P., Contaminated sediments of lakes and oceans act as sources of chlorinated hydrocarbons for release to water and atmosphere. *Nature* **1985,** *317*, (6035), 347-349.

58. ATSDR, Public health assessment for portland harbor. In 2006.

59. U.S.EPA, Mccormick and baxter creosoting company-record of decision. In 1996.

60. Anderson, K. A.; Sethajintanin, D.; Sower, G.; Quarles, L., Field trial and modeling of uptake rates of in situ lipid-free polyethylene membrane passive sampler. *Environmental Science & Technology* **2008,** *42*, (12), 4486-4493.

61. Allan, S. E.; Smith, B. W.; Anderson, K. A., Impact of the deepwater horizon oil spill on bioavailable polycyclic aromatic hydrocarbons in gulf of mexico coastal waters. *Environmental Science & Technology* **2012,** *46*, (4), 2033-2039.

62. Donald, C. E.; Elie, M. R.; Smith, B. W.; Hoffman, P. D.; Anderson, K. A., Transport stability of pesticides and pahs sequestered in polyethylene passive sampling devices. *Environmental Science and Pollution Research* **2016,** *23*, (12), 12392-12399.

63. Anderson, K. A.; Szelewski, M. J.; Wilson, G.; Quimby, B. D.; Hoffman, P. D., Modified ion source triple quadrupole mass spectrometer gas chromatograph for polycyclic aromatic hydrocarbon analyses. *Journal of Chromatography A* **2015,** *1419*, 9.

64. Hayduk, W.; Laudie, H., Prediction of diffusion coefficients for nonelectrolytes in dilute aqueous solutions. *AlChE Journal* **1974,** *20*, 611-615.

65. Jorgensen, B. B.; Revsbech, N. P., Diffusive boundary layers and the oxygen uptake of sediments and detritus. *Limnology and Oceanography* **1985,** *30*, (1), 11.

66. Santchi, P. H.; Bower, P.; Nuffeler, U. P.; Azevedo, A.; Broecker, W. S., Estimates of the resistance to chemical transport posed by the deep-sea boundary layer. *Limnology and Oceanography* **1983,** *28*, (5), 13.

67. Liu, Y.; Wang, S.; McDonough, C. A.; Khairy, M.; Muir, D.; Lohmann, R., Estimation of uncertainty in air–water exchange flux and gross volatilization loss of pcbs: A case study based on passive sampling in the lower great lakes. *Environmental Science & Technology* **2016,** *50*, 10894-10902.

68. Lin, T.; Guo, Z.; Li, Y.; Nizzetto, L.; Ma, C.; Chen, Y., Air–seawater exchange of organochlorine pesticides along the sediment plume of a large contaminated river. *Environmental Science & Technology* **2015,** *49*, (9), 5354-5362.

69. U.S.EPA, Population surrounding 1,388 superfund remedial sites. In 2015.

70. Mueller, J. G.; Chapman, P. J.; Pritchard, P. H., Creosote-contaminated sites. Their potential for bioremediation. *Environmental Science & Technology* **1989,** *23*, (10), 1197-1201.

71. Sower, G., J. ; Anderson, K. A., Spatial and temporal variation of freely dissolved polycyclic aromatic hydrocarbons in an urban river undergoing superfund remediation. *Environmental Science & Technology* **2008,** *42*, 9065-9071.

72. Swinomish, Bioaccumulative toxics in subsistence-harvested shellfish- contaminant results and risk assessment. In Office of Planning and Community Development, W. R. P., Ed. 2006.

73. Coast salish gathering. www.coastsalishgathering.com

74. Donatuto, J.; Campbell, L.; Gregory, R., Developing responsive indicators of indigenous community health. *Int J Environ Res Public Health* **2016,** *13*, (9).

75. U.S.EPA, A decade of tribal environmental health research: Results and impacts from epa's extramural grants and fellowships programs. In 2014.

76. Bayen, S.; ter Laak, T. L.; Buffle, J.; Hermens, J. L. M., Dynamic exposure of organisms and passive samplers to hydrophobic chemicals. *Environmental Science & Technology* **2009,** *43*, (7), 2206-2215.

77. Arnot, J. A.; Gobas, F. A. P. C., A review of bioconcentration factor (bcf) and bioaccumulation factor (baf) assessments for organic chemicals in aquatic organisms. *Environmental Reviews* **2006,** *14*, (4), 257-297.

78. Boese, B. L.; Lee Ii, H.; Specht, D. T.; Randall, R.; Pelletier, J., Evaluation of pcb and hexachlorobenzene biota-sediment accumulation factors based on ingested sediment in a deposit-feeding clam. *Environmental Toxicology and Chemistry* **1996,** *15*, (9), 1584-1589.

79. Cornelissen, G.; Gustafsson, Ö.; Bucheli, T. D.; Jonker, M. T. O.; Koelmans, A. A.; van Noort, P. C. M., Extensive sorption of organic compounds to black carbon, coal, and kerogen in sediments and soils: Mechanisms and consequences for distribution, bioaccumulation, and biodegradation. *Environmental Science & Technology* **2005,** *39*, (18), 6881-6895.

80. Oen, A. M. P.; Schaanning, M.; Ruus, A.; Cornelissen, G.; Källqvist, T.; Breedveld, G. D., Predicting low biota to sediment accumulation factors of pahs by using infinite-sink and equilibrium extraction methods as well as bc-inclusive modeling. *Chemosphere* **2006,** *64*, (8), 1412-1420.

81. Fernandez, L. A.; Harvey, C. F.; Gschwend, P. M., Using performance reference compounds in polyethylene passive samplers to deduce sediment porewater concentrations for numerous target chemicals. *Environmental Science & Technology* **2009,** *43*, (23), 8888-8894.

82. Oen, A. M. P.; Janssen, E. M. L.; Cornelissen, G.; Breedveld, G. D.; Eek, E.; Luthy, R. G., In situ measurement of pcb pore water concentration profiles in activated carbon-amended sediment using passive samplers. *Environmental Science & Technology* **2011,** *45*, (9), 4053-4059.

83. Lu, X.; Skwarski, A.; Drake, B.; Reible, D. D., Predicting bioavailability of pahs and pcbs with porewater concentrations measured by solid-phase microextraction fibers. *Environmental Toxicology and Chemistry* **2011,** *30*, (5), 1109-1116.

84. Forsberg, N. D.; Smith, B. W.; Sower, G. J.; Anderson, K. A., Predicting polycyclic aromatic hydrocarbon concentrations in resident aquatic organisms using passive samplers and partial least-squares calibration. *Environmental Science & Technology* **2014,** *48*, (11), 6291-6299.

85. Joyce, A. S.; Pirogovsky, M. S.; Adams, R. G.; Lao, W.; Tsukada, D.; Cash, C. L.; Haw, J. F.; Maruya, K. A., Using performance reference compound-corrected polyethylene passive samplers and caged bivalves to measure hydrophobic contaminants of concern in urban coastal seawaters. *Chemosphere* **2015,** *127*, (Supplement C), 10-17.

86. Vinturella, A. E.; Burgess, R. M.; Coull, B. A.; Thompson, K. M.; Shine, J. P., Use of passive samplers to mimic uptake of polycyclic aromatic hydrocarbons by benthic polychaetes. *Environmental Science & Technology* **2004,** *38*, (4), 1154-1160.

87. Minick, D. J.; Anderson, K. A., Diffusive flux of pahs across sediment-water and water-air interfaces at urban superfund sites. *Environmental Toxicology & Chemistry* **2017,** *In Press*.

88. U.S.EPA, Development of a relative potency factor (rpf) approach for polycyclic aromatic hydrocarbon (pah) mixtures. In 2010.

89. U.S.EPA, Estimated fish consumption rates for the u.S. Population and selected subpopulations (nhanes 2003-2010). In EPA, U., Ed. 2014.

90. Tobiszewski, M.; Namiesnik, J., Pah diagnostic ratios for the identification of pollution emission sources. *Environ Pollut* **2012,** *162*, 110-9.

91. Yunker, M. B.; Macdonald, R. W.; Vingarzan, R.; Mitchell, R. H.; Goyette, D.; Sylvestre, S., Pahs in the fraser river basin: A critical appraisal of pah ratios as indicators of pah source and composition. *Organic geochemistry* **2002,** *33*, (4), 489-515.

92. Simpson, C. D.; Cullen, W. R.; He, T. Y. T.; Ikonomou, M.; Reimer, K. J., Metabolism of pyrene by two clam species, mya arenaria and protothaca staminea. *Chemosphere* **2002,** *49*, (3), 315-322.

93. Bebianno, M. J.; Barreira, L. A., Polycyclic aromatic hydrocarbons concentrations and biomarker responses in the clam ruditapes decussatus transplanted in the ria formosa lagoon. *Ecotoxicology and Environmental Safety* **2009,** *72*, (7), 1849-1860.

94. Liu, D.; Pan, L.; Li, Z.; Cai, Y.; Miao, J., Metabolites analysis, metabolic enzyme activities and bioaccumulation in the clam ruditapes philippinarum exposed to benzo[a]pyrene. *Ecotoxicology and Environmental Safety* **2014,** *107*, 251-259.

95. Goong, S. A.; Chew, K. K., Growth of butter clams, saxidomus giganteus deshayes, on selected beaches in the state of washington. *Journal of Shellfish Research* **2001,** *20*, (1), 6.

96. Boehm, P. D.; Page, D. S.; Brown, J. S.; Neff, J. M.; Edward Bence, A., Comparison of mussels and ssemi-permeable membrane devices as intertidal monitors of polycyclic aromatic hydrocarbons at oil spill sites. *Marine Pollution Bulletin* **2005,** *50*, (7), 740-750.

97. Lohmann, R.; Burgess, R. M.; Cantwell, M. G.; Ryba, S. A.; MacFarlane, J. K.; Gschwend, P. M., Dependency of polychlorinated biphenyl and polycyclic aromatic hydrocarbon bioaccumulation in mya arenaria on both water column and sediment bed chemical activities. *Environmental Toxicology and Chemistry* **2004,** *23*, (11), 2551-2562.

98. Cachada, A.; Ferreira da Silva, E.; Duarte, A. C.; Pereira, R., Risk assessment of urban soils contamination: The particular case of polycyclic aromatic hydrocarbons. *Science of The Total Environment* **2016,** *551*, (Supplement C), 271-284.

99. Khalili, N. R.; Scheff, P. A.; Holsen, T. M., Pah source fingerprints for coke ovens, diesel and, gasoline engines, highway tunnels, and wood combustion emissions. *Atmospheric environment* **1995,** *29*, (4), 533-542.

100. Perera, F. P.; Whyatt, R. M.; Jedrychowski, W.; Rauh, V.; Manchester, D.; Santella, R. M.; Ottman, R., Recent developments in molecular epidemiology: A study of the effects of environmental polycyclic aromatic hydrocarbons on birth outcomes in poland. *American Journal of Epidemiology* **1998,** *147*, (3), 309-314.

101. Perera, F. P.; Li, Z.; Whyatt, R.; Hoepner, L.; Wang, S.; Camann, D.; Rauh, V., Prenatal airborne polycyclic aromatic hydrocarbon exposure and child iq at age 5 years. *Pediatrics* **2009,** *124*, (2), e195-202.

102. Perera, F. P.; Wang, S.; Rauh, V.; Zhou, H.; Stigter, L.; Camann, D.; Jedrychowski, W.; Mroz, E.; Majewska, R., Prenatal exposure to air pollution, maternal psychological distress, and child behavior. *Pediatrics* **2013**.

103. Duarte-Salles, T.; Mendez, M. A.; Morales, E.; Bustamante, M.; Rodríguez-Vicente, A.; Kogevinas, M.; Sunyer, J., Dietary benzo (a) pyrene and fetal growth: Effect modification by vitamin c intake and glutathione s-transferase p1 polymorphism. *Environment international* **2012,** *45*, 1-8.

104. Rauh, V.; Whyatt, R.; Garfinkel, R.; Andrews, H.; Hoepner, L.; Reyes, A.; Diaz, D.; Camann, D.; Perera, F., Developmental effects of exposure to environmental tobacco smoke and material hardship among inner-city children. *Neurotoxicology and teratology* **2004,** *26*, (3), 373-385.

105. Edwards, S. C.; Jedrychowski, W.; Butscher, M.; Camann, D.; Kieltyka, A.; Mroz, E.; Flak, E.; Li, Z.; Wang, S.; Rauh, V., Prenatal exposure to airborne polycyclic aromatic hydrocarbons and children's intelligence at 5 years of age in a prospective cohort study in poland. *Environmental health perspectives* **2010,** *118*, (9), 1326.

106. Incardona, J. P.; Collier, T. K.; Scholz, N. L., Defects in cardiac function precede morphological abnormalities in fish embryos exposed to polycyclic aromatic hydrocarbons. *Toxicol Appl Pharmacol* **2004,** *196*, (2), 191-205.

107. Vignet, C.; Devier, M. H.; Le Menach, K.; Lyphout, L.; Potier, J.; Cachot, J.; Budzinski, H.; Begout, M. L.; Cousin, X., Long-term disruption of growth, reproduction, and behavior after

embryonic exposure of zebrafish to pah-spiked sediment. *Environ Sci Pollut Res Int* **2014,** *21*, (24), 13877-87.

108. Vignet, C.; Le Menach, K.; Lyphout, L.; Guionnet, T.; Frere, L.; Leguay, D.; Budzinski, H.; Cousin, X.; Begout, M. L., Chronic dietary exposure to pyrolytic and petrogenic mixtures of pahs causes physiological disruption in zebrafish--part ii: Behavior. *Environ Sci Pollut Res Int* **2014,** *21*, (24), 13818-32.

109. Knecht, A. L.; Truong, L.; Marvel, S. W.; Reif, D. M.; Garcia, A.; Lu, C.; Simonich, M. T.; Teeguarden, J. G.; Tanguay, R. L., Transgenerational inheritance of neurobehavioral and physiological deficits from developmental exposure to benzo [a] pyrene in zebrafish. *Toxicology and Applied Pharmacology* **2017**.

110. Brown, D. R.; Bailey, J. M.; Oliveri, A. N.; Levin, E. D.; Di Giulio, R. T., Developmental exposure to a complex pah mixture causes persistent behavioral effects in naive fundulus heteroclitus (killifish) but not in a population of pah-adapted killifish. *Neurotoxicol Teratol* **2016,** *53*, 55-63.

111. Peiffer, J.; Grova, N.; Hidalgo, S.; Salquèbre, G.; Rychen, G.; Bisson, J.-F.; Appenzeller, B. M.; Schroeder, H., Behavioral toxicity and physiological changes from repeated exposure to fluorene administered orally or intraperitoneally to adult male wistar rats: A dose–response study. *Neurotoxicology* **2016,** *53*, 321-333.

112. Chen, C.; Tang, Y.; Jiang, X.; Qi, Y.; Cheng, S.; Qiu, C.; Peng, B.; Tu, B., Early postnatal benzo(a)pyrene exposure in sprague-dawley rats causes persistent neurobehavioral impairments that emerge postnatally and continue into adolescence and adulthood. *Toxicological Sciences* **2012,** *125*, (1), 248-261.

113. Incardona, J. P.; Day, H. L.; Collier, T. K.; Scholz, N. L., Developmental toxicity of 4-ring polycyclic aromatic hydrocarbons in zebrafish is differentially dependent on ah receptor isoforms and hepatic cytochrome p4501a metabolism. *Toxicol Appl Pharmacol* **2006,** *217*, (3), 308-21.

114. Zhang, X.; Li, X.; Jing, Y.; Fang, X.; Zhang, X.; Lei, B.; Yu, Y., Transplacental transfer of polycyclic aromatic hydrocarbons in paired samples of maternal serum, umbilical cord serum, and placenta in shanghai, china. *Environ Pollut* **2017,** *222*, 267-275.

115. Perera, F. P.; Tang, D.; Tu, Y.-H.; Cruz, L. A.; Borjas, M.; Bernert, T.; Whyatt, R. M., Biomarkers in maternal and newborn blood indicate heightened fetal susceptibility to procarcinogenic DNA damage. *Environmental Health Perspectives* **2004,** *112*, (10), 1133-1136.

116. Burczynski, M.; Lin, H.; Penning, T., Isoform-specific induction of a human aldo-keto reductase by polycyclic aromatic hydrocarbons (pahs), electrophiles, and oxidative stress: Implications for the alternative pathway of pah activation catalyzed by human dihydrodiol dehydrogenase. *Cancer Research* **1999,** *59*, (3), 8.

117. Incardona, J. P.; Linbo, T. L.; Scholz, N. L., Cardiac toxicity of 5-ring polycyclic aromatic hydrocarbons is differentially dependent on the aryl hydrocarbon receptor 2 isoform during zebrafish development. *Toxicol Appl Pharmacol* **2011,** *257*, (2), 242-9.

118. Knecht, A. L.; Goodale, B. C.; Truong, L.; Simonich, M. T.; Swanson, A. J.; Matzke, M. M.; Anderson, K. A.; Waters, K. M.; Tanguay, R. L., Comparative developmental toxicity of environmentally relevant oxygenated pahs. *Toxicol Appl Pharmacol* **2013,** *271*, (2), 266-75.

119. Brown, D. R.; Thompson, J.; Chernick, M.; Hinton, D. E.; Di Giulio, R. T., Later life swimming performance and persistent heart damage following subteratogenic pah mixture exposure in the atlantic killifish (fundulus heteroclitus). *Environmental Toxicology and Chemistry* **2016**.

120. Kerley-Hamilton, J. S., Trask, Heidi W., Ridley, Christian J. A., DuFour, Eric, Lesseur, Corina, Ringelberg, Carol S., Moodie, Karen L., Shipman, Samantha L, Korc, Murray, Gui, Jiang, Shworak, Nicholas W., Tominson, Craig R., Inherent and benzo[a]pyrene-induced differential aryl hydrocarbon receptor signaling greatly affects life span, atherosclerosis, cardiac gene expression, and body and heart growth in mice. *Toxicological Sciences* **2012,** *126*, (2), 391-404.

121. Incardona, J. P.; Collier, T. K.; Scholz, N. L., Oil spills and fish health: Exposing the heart of the matter. *Journal of exposure science & environmental epidemiology* **2011,** *21*, (1), 3-4.

122. Van Tiem, L. A.; Di Giulio, R. T., Ahr2 knockdown prevents pah-mediated cardiac toxicity and xre- and are-associated gene induction in zebrafish (danio rerio). *Toxicol Appl Pharmacol* **2011,** *254*, (3), 280-7.

123. Altenburger, R.; Greco, W. R., Extrapolation concepts for dealing with multiple contamination in environmental risk assessment. *Integrated Environmental Assessment and Management* **2009,** *5*, (1), 62-68.

124. Beyer, J.; Petersen, K.; Song, Y.; Ruus, A.; Grung, M.; Bakke, T.; Tollefsen, K. E., Environmental risk assessment of combined effects in aquatic ecotoxicology: A discussion paper. *Marine Environmental Research* **2014,** *96*, (Supplement C), 81-91.

125. Cedergreen, N., Quantifying synergy: A systematic review of mixture toxicity studies within environmental toxicology. *PLOS ONE* **2014,** *9*, (5), e96580.

126. Altenburger, R.; Nendza, M.; Schüürmann, G., Mixture toxicity and its modeling by quantitative structure-activity relationships. *Environmental Toxicology and Chemistry* **2003,** *22*, (8), 1900-1915.

127. Billiard, S. M.; Meyer, J. N.; Wassenberg, D. M.; Hodson, P. V.; Di Giulio, R. T., Nonadditive effects of pahs on early vertebrate development: Mechanisms and implications for risk assessment. *Toxicol Sci* **2008,** *105*, (1), 5-23.

128. Bergmann, A. J.; Tanguay, R. L.; Anderson, K. A., Using passive sampling and zebrafish to identify developmental toxicants in complex mixtures. *Environmental Toxicology and Chemistry* **2017,** *36*, (9), 2290-2298.

129. ATSDR, Porland harbor: Recreational use In 2011.

130. U.S.EPA, Portland harbor superfund site: Proposed plan. **2016**.

131. Minick, D. J.; Anderson, K. A., Diffusive flux of pahs across sediment-water and water-air interfaces at urban superfund sites. *Environ Toxicol Chem* **2017**.

132. Allan, S. E.; Sower, G. J.; Anderson, K. A., Estimating risk at a superfund site using passive sampling devices as biological surrogates in human health risk models. *Chemosphere* **2011,** *85*, (6), 920-927.

133. Xu, X.; Scott-Scheiern, T.; Kempker, L.; Simons, K., Active avoidance conditioning in zebrafish (danio rerio). *Neurobiol Learn Mem* **2007,** *87*, (1), 72-7.

134. Xu, X.; Weber, D.; Carvan, M. J., 3rd; Coppens, R.; Lamb, C.; Goetz, S.; Schaefer, L. A., Comparison of neurobehavioral effects of methylmercury exposure in older and younger adult zebrafish (danio rerio). *Neurotoxicology* **2012,** *33*, (5), 1212-8.

135. Truong, L.; Mandrell, D.; Mandrell, R.; Simonich, M.; Tanguay, R. L., A rapid throughput approach identifies cognitive deficits in adult zebrafish from developmental exposure to polybrominated flame retardants. *Neurotoxicology* **2014,** *43*, 134-42.

136. Barton, C. L.; Johnson, E. W.; Tanguay, R. L., Facility design and health management program at the sinnhuber aquatic research laboratory. *Zebrafish* **2016,** *13*, (S1), S-39-S-43.

137. Kimmel, C. B.; Ballard, W. W.; Kimmel, S. R.; Ullmann, B.; Schilling, T. F., Stages of embryonic development of the zebrafish. *Dev Dyn* **1995,** *203*, (3), 253-310.

138. Westerfield, M., The zebrafish book: A guide for the laboratory use of zebrafish. *http://zfin.org/zf_info/zfbook/zfbk.html* **2000**.

139. Mandrell, D.; Truong, L.; Jephson, C.; Sarker, M. R.; Moore, A.; Lang, C.; Simonich, M. T.; Tanguay, R. L., Automated zebrafish chorion removal and single embryo placement: Optimizing throughput of zebrafish developmental toxicity screens. *J Lab Autom* **2012,** *17*, (1), 66-74.

140. Truong, L.; Bugel, S. M.; Chlebowski, A.; Usenko, C. Y.; Simonich, M. T.; Simonich, S. L.; Tanguay, R. L., Optimizing multi-dimensional high throughput screening using zebrafish. *Reprod Toxicol* **2016,** *65*, 139-147.

141. Truong, L.; Reif, D. M.; St Mary, L.; Geier, M. C.; Truong, H. D.; Tanguay, R. L., Multidimensional in vivo hazard assessment using zebrafish. *Toxicol Sci* **2014,** *137*, (1), 212-33.

142. Truong, L.; Harper, S. L.; Tanguay, R. L., Evaluation of embryotoxicity using the zebrafish model. *Drug Safety Evaluation: Methods and Protocols* **2011**, 271-279.

143. Noyes, P. D.; Haggard, D. E.; Gonnerman, G. D.; Tanguay, R. L., Advanced morphological-behavioral test platform reveals neurodevelopmental defects in embryonic zebrafish exposed to comprehensive suite of halogenated and organophosphate flame retardants. *Toxicological Sciences* **2015,** *145*, (1).

144. Reif, D. M.; Truong, L.; Mandrell, D.; Marvel, S.; Zhang, G.; Tanguay, R. L., High-throughput characterization of chemical-associated embryonic behavioral changes predicts teratogenic outcomes. *Arch Toxicol* **2016,** *90*, (6), 1459-70.

145. Saili, K. S.; Corvi, M. M.; Weber, D. N.; Patel, A. U.; Das, S. R.; Przybyla, J.; Anderson, K. A.; Tanguay, R. L., Neurodevelopmental low-dose bisphenol a exposure leads to early life-stage hyperactivity and learning deficits in adult zebrafish. *Toxicology* **2012,** *291*, (1), 83-92.

146. Mathew, L. K.; Andreasen, E. A.; Tanguay, R. L., Aryl hydrocarbon receptor activation inhibits regenerative growth. *Molecular pharmacology* **2006,** *69*, (1), 257-265.

147. Scott, J. A.; Incardona, J. P.; Pelkki, K.; Shepardson, S.; Hodson, P. V., Ahr2-mediated, cyp1a-independent cardiovascular toxicity in zebrafish (danio rerio) embryos exposed to retene. *Aquat Toxicol* **2011,** *101*, (1), 165-74.

148. Billiard, S. M.; Querbach, K.; Hodson, P. V., Toxicity of retene to early life stages of two freshwater fish species. *Environmental Toxicology and Chemistry* **1999,** *18*, (9), 2070-2077.

149. Stout, S. A.; Graan, T. P., Quantitative source apportionment of pahs in sediments of little menomonee river, wisconsin: Weathered creosote versus urban background. *Environmental Science & Technology* **2010,** *44*, (8), 2932-2939.

150. Goodale, B. C.; La Du, J. K.; Bisson, W. H.; Janszen, D. B.; Waters, K. M.; Tanguay, R. L., Ahr2 mutant reveals functional diversity of aryl hydrocarbon receptors in zebrafish. *PLoS One* **2012,** *7*, (1), e29346.

151. Goodale, B. C.; La Du, J.; Tilton, S. C.; Sullivan, C. M.; Bisson, W. H.; Waters, K. M.; Tanguay, R. L., Ligand-specific transcriptional mechanisms underlie aryl hydrocarbon receptor-mediated developmental toxicity of oxygenated pahs. *Toxicol Sci* **2015,** *147*, (2), 397-411.

152. Slotkin, T. A.; Skavicus, S.; Card, J.; Giulio, R. T. D.; Seidler, F. J., In vitro models reveal differences in the developmental neurotoxicity of an environmental polycylic aromatic hydrocarbon mixture compared to benzo[a]pyrene: Neuronotypic pc12 cells and embryonic neural stem cells. *Toxicology* **2017,** *377*, 49-56.

153. Labib, S.; Williams, A.; Kuo, B.; Yauk, C. L.; White, P. A.; Halappanavar, S., A framework for the use of single-chemical transcriptomics data in predicting the hazards associated with complex mixtures of polycyclic aromatic hydrocarbons. *Archives of Toxicology* **2016**, 1-18.

154. Gonçalves, R.; Scholze, M.; Ferreira, A. M.; Martins, M.; Correia, A. D., The joint effect of polycyclic aromatic hydrocarbons on fish behavior. *Environmental Research* **2008,** *108*, (2), 205-213.

155. Garner, L. V. T.; Brown, D. R.; Di Giulio, R. T., Knockdown of ahr1a but not ahr1b exacerbates pah and pcb-126 toxicity in zebrafish (danio rerio) embryos. *Aquatic Toxicology* **2013,** *142-143*, (Supplement C), 336-346.

156. Barouki, R.; Morel, Y., Repression of cytochrome p450 1a1 gene expression by oxidative stress: Mechanisms and biological implications. *Biochemical Pharmacology* **2001,** *61*, (5), 511-516.

157. Crepeaux, G.; Bouillaud-Kremarik, P.; Sikhayeva, N.; Rychen, G.; Soulimani, R.; Schroeder, H., Late effects of a perinatal exposure to a 16 pah mixture: Increase of anxiety-related behaviours and decrease of regional brain metabolism in adult male rats. *Toxicol Lett* **2012,** *211*, (2), 105-13.

158. Eddins, D.; Cerutti, D.; Williams, P.; Linney, E.; Levin, E. D., Zebrafish provide a sensitive model of persisting neurobehavioral effects of developmental chlorpyrifos exposure: Comparison with nicotine and pilocarpine effects and relationship to dopamine deficits. *Neurotoxicol Teratol* **2010,** *32*, (1), 99-108.

159. Chlebowski, A. C.; Tanguay, R. L.; Simonich, S. L., Quantitation and prediction of sorptive losses during toxicity testing of polycyclic aromatic hydrocarbon (pah) and nitrated pah (npah) using polystyrene 96-well plates. *Neurotoxicol Teratol* **2016,** *57*, 30-38.

160. Zhang, Y.; Huang, L.; Wang, C.; Gao, D.; Zuo, Z., Phenanthrene exposure produces cardiac defects during embryo development of zebrafish (danio rerio) through activation of mmp-9. *Chemosphere* **2013,** *93*, (6), 1168-1175.

161. Zhang, Y.; Huang, L.; Zuo, Z.; Chen, Y.; Wang, C., Phenanthrene exposure causes cardiac arrhythmia in embryonic zebrafish via perturbing calcium handling. *Aquatic toxicology* **2013,** *142*, 26-32.

162. Cho, Y.-M.; Werner, D.; Moffett, K. B.; Luthy, R. G., Assessment of advective porewater movement affecting mass transfer of hydrophobic organic contaminants in marine intertidal sediment. *Environmental Science & Technology* **2010,** *44*, (15), 5842-5848.

163. Gidley, P. T.; Kwon, S.; Yakirevich, A.; Magar, V. S.; Ghosh, U., Advection dominated transport of polycyclic aromatic hydrocarbons in amended sediment caps. *Environmental Science & Technology* **2012,** *46*, (9), 5032-5039.

164. Zhu, T.; Fu, D.; Jenkinson, B.; Jafvert, C. T., Calibration and application of an automated seepage meter for monitoring water flow across the sediment-water interface. *Environmental Monitoring and Assessment* **2015,** *187*, (4), 171.

165. Selker, J.; Selker, F.; Huff, J.; Short, R.; Edwards, D.; Nicholson, P.; Chin, A., Practical strategies for identifying groundwater discharges into sediment and surface water with fiber optic

temperature measurement. *Environmental Science: Processes & Impacts* **2014,** *16*, (7), 1772-1778.

166. Rosenberry, D. O.; LaBaugh, J. W., Field techniques for estimating water fluxes between surface water and ground water. In Interior, U. S. D. o. t.; Survey, U. S. G., Eds. 2008; pp 54-64.

167. Minar, N. Wind history http://windhistory.com/ (September 19, 2016),

168. Roux, M. a. V.; Temprado, M.; Chickos, J. S.; Nagano, Y., Critically evaluated thermochemical properties of polycyclic aromatic hydrocarbons. *Journal of Physical and Chemical Reference Data* **2008,** *37*, (4), 1855.

169. Ma, Y.-G.; Lei, Y. D.; Xiao, H.; Wania, F.; Wang, W.-H., Critical review and recommended values for the physical-chemical property data of 15 polycyclic aromatic hydrocarbons at 25c. *Journal of Chemical & Engineering Data* **2010,** *55*, 819-825.

170. Johnson, M. T., A numerical scheme to calculate temperature and salinity dependent air-water transfer velocities for any gas. *Ocean Science* **2010,** *6*, (4), 913-932.

171. Nightingale, P. D.; Malin, G.; Law, C. S.; Watson, A. J.; Liss, P. S.; Liddicoat, M. I.; Boutin, J.; Upstill-Goddard, R. C., In situ evaluation of air-sea gas exchange parameterizations using novel conservative and volatile tracers. *Global Biogeochemical Cycles* **2000,** *14*, (1), 373-387.

172. Duce, R. A.; Liss, P. S.; Merrill, J. T.; Atlas, E. L.; Buat-Menard, P.; Hicks, B. B.; Miller, J. M.; Prospero, J. M.; Arimoto, R.; Church, T. M.; Ellis, W.; Galloway, J. N.; Hansen, L.; Jickells, T. D.; Knap, A. H.; Reinhardt, K. H.; Schneider, B.; Soudine, A.; Tokos, J. J.; Tsunogai, S.; Wollast, R.; Zhou, M., The atmospheric input of trace species to the world ocean. *Global Biogeochemical Cycles* **1991,** *5*, (3), 193-259.

173. Lohmann, R., Critical review of low-density polyethylene's partitioning and diffusion coefficients for trace organic contaminants and implications for its use as a passive sampler. *Environ Sci Technol* **2012,** *46*, (2), 606-18.

174. Booij, K.; Hoedemaker, J. R.; Bakker, J. F., Dissolved pcbs, pahs, and hcb in pore waters and overlying waters of contaminated harbor sediments. *Environmental Science & Technology* **2003,** *37*, (18), 4213-4220.

175. Adams, R. G.; Lohmann, R.; Fernandez, L. A.; MacFarlane, J. K., Polyethylene devices: Passive samplers for measuring dissolved hydrophobic organic compounds in aquatic environments. *Environmental Science & Technology* **2007,** *41*, (4), 1317-1323.

APPENDICES

Appendix A: Supporting Information to Chapter 2 – Diffusive flux of PAHs across sediment-water and water-air interfaces at urban Superfund Sites

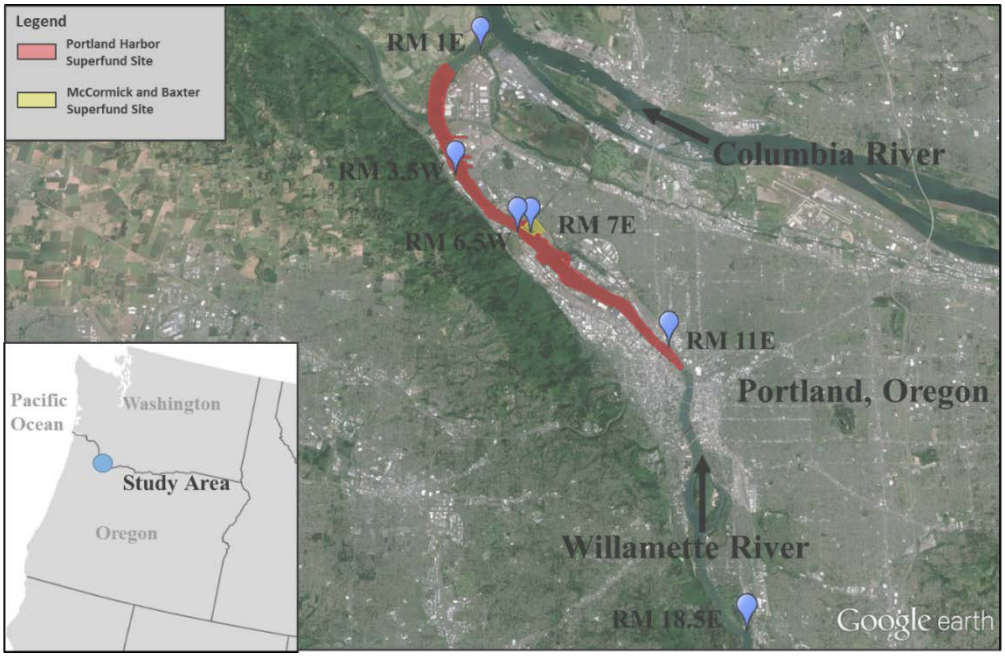

Figure A1. Portland Harbor and McCormick and Baxter Superfund sites.

Figure A2. Pictures of Portland Harbor sampling locations.

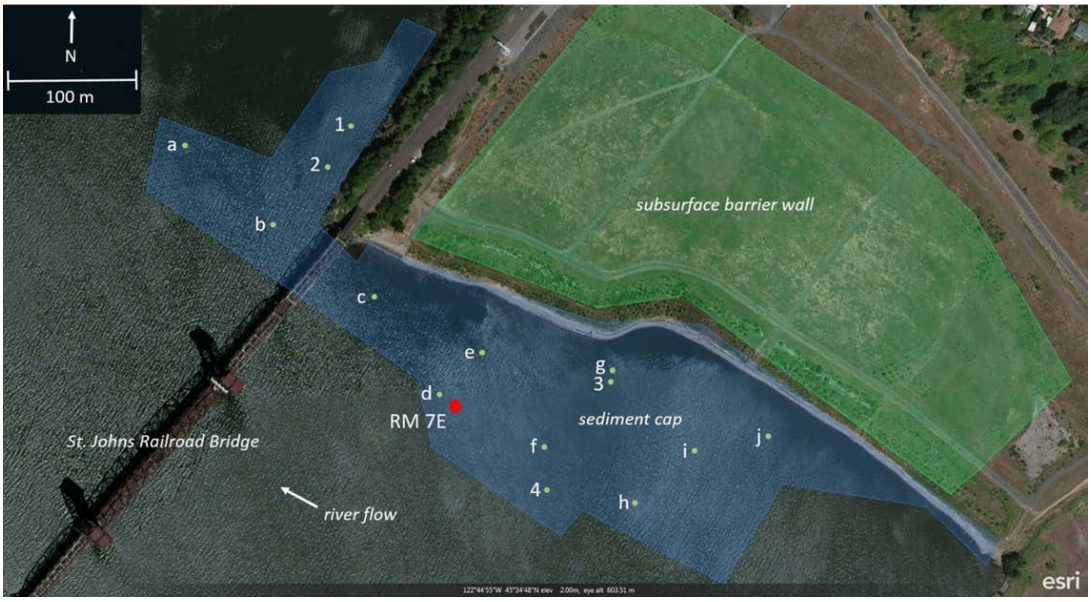

Figure A3. McCormick and Baxter Superfund Site sampling locations. Green shading and blue shading represent the approximate boundaries of an upland barrier wall and sediment cap respectively. RM7E was part of the larger PHSMS study and had paired sediment-water and water-air PSDs .

Table A1. Method quantification limits. Estimated MQLs were based on average performance reference compound derived sampling rates. Water MQLs were calculated for both 5 LDPE (25 g) and 1 LDPE (5 g).

Compound	Abbreviation	MQL(ng/L)			
		porewater	surface water -25g	surface water-5g	Air (ngm³)
Naphthalene	Nap	0.70	0.11	0.54	1.3
2-Methylnaphthalene	Nap2Me	0.18	0.016	0.087	0.19
1-Methylnaphthalene	Nap1Me	0.070	0.0063	0.034	0.075
2-Ethylnaphthalene	Nap2Et	0.15	0.0073	0.050	0.10
2,6-Dimethylnaphthalene	Nap26DMe	0.14	0.0076	0.050	0.089
1,6-Dimethylnaphthalene	Nap16DMe	0.12	0.0055	0.039	0.062
1,4-dimethylnaphthalene	Nap14DMe	0.19	0.0095	0.065	0.11
1,5 dimethylnaphthalene	Nap15DMe	0.18	0.0089	0.061	0.10
1,2-Dimethylnaphthalene	Nap12DMe	0.15	0.0081	0.053	0.094
1,8-Dimethylnaphthalene	Nap18DMe	0.14	0.0078	0.050	0.092
2,6-Diethylnaphthalene	Nap26DEt	0.094	0.0024	0.024	0.023
Acenaphthylene	ANL	0.54	0.044	0.24	0.047
Acenaphthene	AN	0.25	0.021	0.12	0.12
Fluorene	FE	0.14	0.0088	0.054	0.026
Dibenzothiophene	DBT	0.037	0.0018	0.012	0.00077
Phenanthrene	PH	0.067	0.0030	0.022	0.0024
Anthracene	AC	0.15	0.0070	0.049	0.0055
2-Methylphenanthrene	PH2Me	0.047	0.0015	0.013	0.00097
2-Methylanthracene	AC2Me	0.056	0.0016	0.015	0.00095
1-Methylphenanthrene	PH1Me	0.12	0.0034	0.032	0.0019
9-Methylanthracene	AC9Me	0.10	0.0029	0.027	0.0016
3,6-Dimethylphenanthrene	PH36DMe	0.048	0.0012	0.012	0.00046
Fluoranthene	FA	0.040	0.0011	0.010	0.00013
2,3-Dimethylanthracene	AC23DMe	0.063	0.0015	0.016	0.00060
9,10-Dimethylanthracene	AC910DMe	0.10	0.0023	0.024	0.00071
Pyrene	Pyr	0.051	0.0016	0.014	0.00020
Retene	Ret	0.13	0.0026	0.030	0.00060
Benzo(a)fluorene	BaFE	0.12	0.0028	0.029	0.00043
Benzo(b)flourene	BbFE	0.12	0.0027	0.029	0.00028
Benzo(c)fluorene	BcFE	0.035	0.0010	0.010	0.00015
1-Methylpyrene	P1ME	0.044	0.0010	0.011	0.00011
Benz(a)anthracene	BaA	0.092	0.0020	0.022	0.00018
Cyclopenta(c,d)pyrene	CPcdP	0.065	0.0014	0.015	0.000079
Triphenylene	Tphen	0.048	0.0011	0.012	0.000064
Chrysene	CH	0.062	0.0013	0.015	0.00010
6-Methylchrysene	CH6Me	0.12	0.0025	0.028	0.00017
5-Methylchrysene	CH5Me	0.14	0.0028	0.032	0.00019
Benzo(b)fluoranthene	BbF	0.046	0.0010	0.011	0.000051
7,12-Dimethylbenz(a)anthracene	AC7 12DmeBa	0.12	0.0025	0.028	0.00019
Benzo(k)fluoranthene	BkF	0.072	0.0015	0.017	0.000063
Benzo(j)fluoranthene	BjF	0.077	0.0016	0.018	0.000070
Benzo(e)pyrene	BeP	0.11	0.0023	0.026	0.000068
Benzo(a)pyrene	BaP	0.16	0.0034	0.038	0.00014
Indeno(1,2,3-c,d) pyrene	IP	0.049	0.0010	0.011	0.000023
Dibenz(a,h)anthracene	DBahA	0.19	0.0038	0.045	0.000083
Picene	Pic	0.18	0.0035	0.041	0.000060
Benzo(ghi)perylene	BghiP	0.060	0.0012	0.014	0.000030
Anthanthrene	AA	0.075	0.0015	0.017	0.000022
Naptho[1,2-b]fluoranthene	N12bF	0.090	0.0017	0.020	0.000019
Naptho[2,3-j]fluoranthene	N23jF	0.090	0.0017	0.020	0.000019
Dibenzo(a,e)fluoroanthene	DBaeF	0.13	0.0025	0.029	0.000027
Dibenzo(a,l)pyrene	DBalP	0.18	0.0034	0.041	0.000024
Naptho[2,3-k]fluoranthene	N23kF	0.090	0.0017	0.020	0.000019
Naptho[2,3-e]pyrene	N23eP	0.090	0.0017	0.020	0.000019
Dibenzo(a,e)pyrene	DBaeP	2.38	0.046	0.54	0.00031
Coronene	CO	0.24	0.0047	0.056	0.000028
Dibenzo(e,l)pyrene	DBelP	0.090	0.0017	0.020	0.000019
Naptho[2,3-a]pyrene	N23aP	0.090	0.0017	0.020	0.000019
Benzo(b)perylene	BbPery	0.090	0.0017	0.020	0.000019
Dibenzo(a,i)pyrene	DbaiP	0.38	0.0074	0.087	0.000081
Dibenzo(a,h)pyrene	DBahP	0.14	0.0027	0.032	0.000030

Table A2. Physical-Chemical parameters used in the study. Sources/Methods: [1]LeBas Method; [2]EPI Suite v. 4.11: †Hansch et al, 1995; ‡KOWWIN v. 1.10; §Vieth et al, 1979; ¶Alcorn et al, 1993; $Wang et al, 1986; ††Sangster et al, 1993; ‡‡Mackay, 1992; $$De Maagd et al, 1998; §§De Voogt et al, 1990.[3]KOAWIN v.1.10; [4]Bond Method; Ksw and Ksa calculations are detailed in section 2.5 of SI.

Target Compounds	MW (g/mol)	[1]Molar Volume	[2]logK_{ow}	[3]logK_{oa}	[4]H(atmm^{3}mol^{-1})	logK_{sw}	log $K_{sa\ (298)}$
Nap	128.17	147.6	3.30†	5.045	5.26E-04	3.29	5.22
Nap2Me	142.2	173.5	3.86†	5.534	5.80E-04	3.94	5.86
Nap1Me	142.2	173.5	3.87†	5.547	5.80E-04	3.95	5.87
Nap2Et	156.09	192	4.38†	6.038	7.71E-04	4.45	6.28
Nap26DMe	156.22	192	4.31†	5.892	6.41E-04	4.39	6.30
Nap16DMe	156.22	192	4.44†	6.022	6.41E-04	4.51	6.42
Nap14DMe	156.22	192	4.37†	6.172	6.41E-04	4.44	6.36
Nap15DMe	156.22	192	4.38†	6.224	6.41E-04	4.45	6.36
Nap12DMe	156.22	192	4.31†	5.892	6.41E-04	4.39	6.30
Nap18DMe	156.22	192	4.26†	6.224	6.41E-04	4.34	6.25
Nap26DEt	184.27	236.4	4.3‡	6.585	1.13E-3	5.12	6.85
ANL	152.19	165.7	3.94†	6.272	5.48E-05	4.02	6.99
AN	154.2	173.1	3.92†	6.044	2.82E-04	4.00	6.27
FE	166.223	187.9	4.18†	6.585	1.67E-04	4.26	6.79
DBT	184.26	191.3	4.38†	7.240	2.79E-05	4.45	7.79
PH	178.23	199.2	4.46†	7.222	5.13E-05	4.52	7.59
AC	178.23	199.2	4.45†	7.093	5.13E-05	4.51	7.58
PH2Me	192.25	221.4	4.86§	7.495	5.67E-05	4.85	7.90
AC2Me	192.25	221.4	5.0¶	6.586	5.67E-05	4.95	8.00
PH1Me	192.25	221.4	5.08$	7.776	5.67E-05	5.01	8.06
AC9Me	192.25	221.4	5.07††	7.870	5.67E-05	5.00	8.05
PH36DMe	206.28	243.6	5.44‡	8.033	6.25E-05	5.23	8.27
FA	202.26	217.3	5.16†	8.601	8.30E-06	5.06	8.97
AC23DMe	206.28	243.6	5.44‡	8.033	6.25E-05	5.23	8.27
AC910DMe	206.28	243.6	5.69††	8.283	6.25E-05	5.36	8.40
Pyr	202.25	213.8	5.18‡‡	8.193	8.30E-06	4.86	8.78
Ret	234.33	288	6.35‡	8.697	1.10E-04	5.60	8.47
BaFE	216.227	239.5	5.40††	8.364	1.63E-05	5.21	8.86
BbFE	216.227	239.5	5.77$	9.566	1.63E-05	5.40	9.05
BcFE	216.227	239.5	5.19‡	8.366	1.63E-05	5.08	8.73
P1ME	216.28	236	5.48‡	8.907	9.16E-06	5.25	9.16
BaA	228.2879	250.8	5.76$	9.069	5.01E-06	5.39	9.59
CPcdP	226.27	231.9	5.70‡	10.151	8.65E-07	5.36	10.32
Tphen	228.29	250.8	5.49$	10.691	5.01E-06	5.26	9.45
CH	228.28	250.8	5.81$$	9.480	5.01E-06	5.41	9.61
CH6Me	242.31	273	6.07‡	9.716	5.53E-06	5.52	9.71
CH5Me	242.31	273	6.07‡	9.716	5.53E-06	5.52	9.71
BbF	252.3	268.9	5.78$	10.351	8.10E-07	5.40	10.45
AC7 12DmeBa	256.34	295.2	5.8†	9.613	6.10E-06	5.41	9.59
BkF	252.3	268.9	6.11$$	10.732	8.10E-07	5.53	10.58
BjF	252.3	268.9	6.11‡	10.590	8.10E-07	5.53	10.58
BeP	252.3	265.4	6.44§§	11.351	8.10E-07	5.63	10.67
BaP	252.3	280.2	6.13$$	10.859	8.10E-07	5.54	10.58
IP	276.33	283.5	6.7‡	11.547	1.31E-07	5.68	11.57
DBahA	278.3466	302.4	6.75††	11.779	4.89E-07	5.68	11.01
Pic	278.354	302.4	7.11§§	11.809	4.89E-07	5.71	11.04
BghiP	276.33	280	6.63†	11.499	1.31E-07	5.67	11.56
AA	276.33	280	7.04§§	12.311	1.31E-07	5.71	11.61
N12bF	302.36	320.5	7.28‡	12.770	7.91E-08	5.71	11.89
N23jF	302.36	320.5	7.28‡	12.770	7.91E-08	5.71	11.89
DBaeF	302.37	320.5	7.28‡	12.771	7.91E-08	5.71	11.89
DBalP	203.27	317	7.71§§	13.20	7.91E-08	5.67	11.60
N23kF	302.37	320.5	7.28‡	12.770	7.91E-08	5.71	11.89
N23eP	302.37	317	7.28‡	12.770	7.91E-08	5.71	11.89
DBaeP	302.37	317	7.71§§	13.20	7.91E-08	5.67	11.85
CO	300.35	294.6	7.64§§	13.702	2.12E-08	5.68	12.43
DBelP	302.36	317	7.28‡	12.770	7.91E-08	5.71	11.89
N23aP	302.36	317	7.28‡	12.770	7.91E-08	5.71	11.89
BbPery	302.36	317	7.28‡	12.770	7.91E-08	5.71	11.89
DbaiP	302.37	317	7.28‡	12.770	7.91E-08	5.71	11.89
DBahP	302.37	317	7.28‡	12.770	7.91E-08	5.71	11.89

GC Program

60°C for 1 minute (min), 40°C min^{-1} to 180°C then 3° C min^{-1} to 230°C then 1.5 ° C min^{-1} to 235°C then 15° C min^{-1} to 280°C for 10 min then 6°C/min to 298 °C for then 16° C min^{-1} to 350°C until the

completion of the sample run. Helium was employed as a carrier gas at a rate of 2.25mL x min^{-1} and nitrogen was used as a collision gas at a flow rate of 1.5mL min^{-1}.

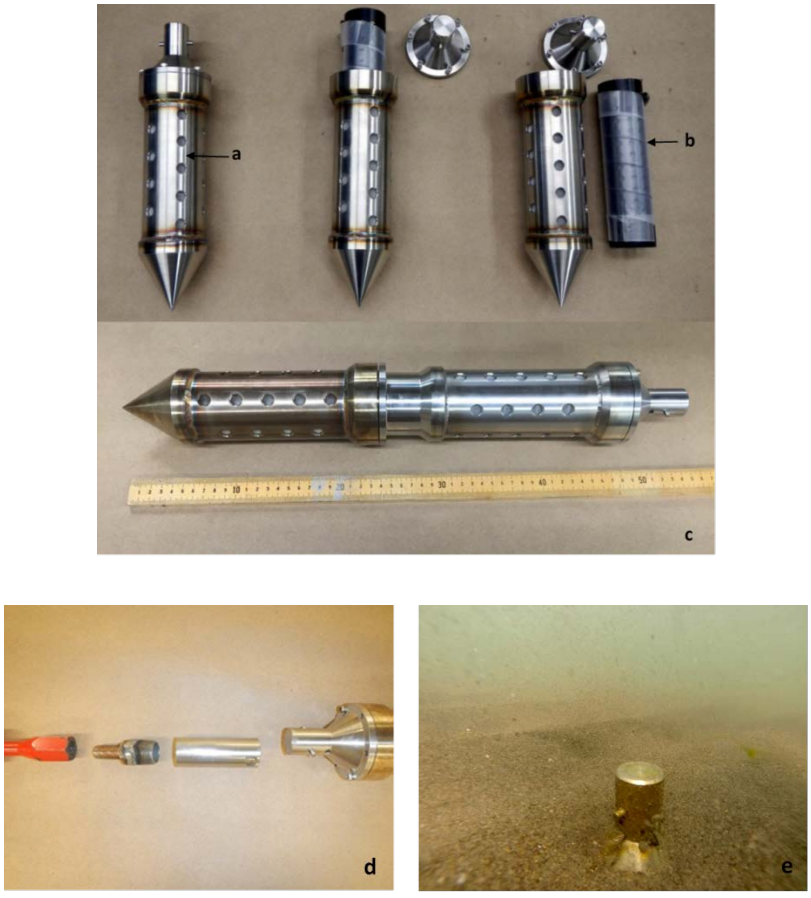

Figure A4: Sediment probe with stainless steel mesh windows (a), and LDPE wrapped around aluminum insert (b). Probes can be stacked (c) for porewater measurements at different depths. A stainless steel probe to slide hammer adapter was constructed and is seen below (d). Probe is deployed so that the top is flush with sediment surface (e). .

Table A3. MS Parameters. Two or more qualifying ions were identified for each compound and quantification was by absolute peak area based on a 1/x linear least-squares fit. Source: AS = AccuStandard (New Haven, CT), CIL = Cambridge Isotope Laboratories, Inc. (Andover, MA), CDN = C/D/N Isotope Inc. (Quebec, Canada), FI = Fisher

(Hampton, NH), CS = ChemService (West Chester, PA), SA = Sigma-Aldrich (St. Louis, MO), CH = Chiron AS (Trondheim,Norway),TRC = Toronto Research Chemical (Ontario, Canada), PSCI = Penn State Cancer Inst. (Hershey, PA), Surrogate used for quantitation: †Naphthalene-D8, ‡Acenaphthylene-D8, §Phenanthrene-D10, ¶Fluoranthene-D10, $Chrysene-D12, ††Benzo(a)pyrene-D12

	Retent	Quantifier		Collision	Qualifier		Collision	Detection		
Name	Time	Precursor	Product	Energy	Precursor	Product	Energy (V)	LOD (pg/uL)	CF R^2	CAS #
Nap-d8 SS*	4.11	136	108	20	136	84	25	0.33	na	1146-65-2
Nap†	4.12	128	102	20	128	78	20	1.04	0.9999	91-20-3
Nap2Me†	4.57	142	141	15	142	115.1	20	0.70	0.9998	91-57-6
Nap1Me†	4.69	142	141	15	142	115.1	20	0.28	0.9998	90-12-0
Nap2Et†	5.00	141	115	15	156	141	15	0.97	0.9997	939-27-5
Nap26DMe†	5.07	156	141	15	141	115	15	0.89	0.9999	28804-88-8
Nap16Dme†	5.22	156	141	15	141	115	15	0.81	0.9998	575-43-9
Nap14Dme†	5.37	156	141	15	141	115	15	1.24	0.9994	571-58-4
Nap15Dme†	5.40	156	141	15	141	115	15	1.19	0.9999	571-61-9
Nap12Dme†	5.49	156	141	15	141	115	15	0.94	0.9996	573-98-8
ANL-d8 SS*	5.66	160	158	30	158	156	30	0.33	na	93951-97-4
ANL‡	5.69	152	126	30	152	102	30	2.33	0.9995	208-96-8
Nap18Dme‡	5.72	156	141	15	141	115	15	0.83	0.9998	569-41-5
AN‡	5.86	153	127	30	153	77	45	1.07	0.9995	83-32-9
Nap26DEt‡	6.22	169	154	20	169	153	30	0.81	0.9999	59919-41-4
FE-d10 PRC	6.67	176	174	15	174	172	20	0.33	0.9992	81103-79-9
FE‡	6.73	166	165	15	165	164	20	0.79	0.9970	86-73-7
DBT‡	9.24	184	152	25	184	139	30	0.24	0.9965	132-65-0
PH-d10 SS*	9.60	188	160	20	188	186	15	1.67	na	1517-22-2
PH§	9.71	178	152	25	176	150	25	0.46	0.9999	85-01-8
AC§	9.86	178	152	25	176	150	25	1.05	0.9998	120-12-7
PH2Me§	11.61	192	191	20	192	189	40	0.39	0.9990	2531-84-2
AC2Me§	11.75	192	191	20	192	189	40	0.47	0.9990	613-12-7
PH1Me§	12.23	192	191	20	192	189	40	1.06	0.9995	832-69-9
AC9Me§	13.24	192	191	20	192	189	40	0.87	0.9988	779-02-2
PH36DMe¶	13.24	206	191	16	206	205	16	0.42	0.9982	1576-67-6
AC23DMe¶	15.14	206	191	16	206	205	16	0.34	0.9979	613-06-9
FA-d10 SS*	15.53	212	208	35	210	208	15	1.67	na	93951-69-0
FA¶	15.66	202	200	35	201	200	15	0.54	0.9984	206-44-0
p,p' DDE-d8 PRC*	16.26	254	184	30	326	254	15	1.67	0.9997	93952-19-3
AC910DMe¶	17.20	206	191	16	206	205	16	0.85	0.9991	781-43-1
Pyr d10-PRC	17.20	212	208	35	210	208	15		0.9600	1718-52-1
Pyr§	17.20	202	200	35	201	200	15	0.42	0.9983	129-00-0
Ret§	17.38	219	204	20	219	203	20	0.84	0.9977	483-65-8
BaFE§	19.35	216	215	25	215	189	25	1.67	0.9999	238-84-6
BbFE§	19.73	216	215	25	215	189	25	1.67	0.9999	243-17-4
BcFE§	19.83	216	215	25	215	189	25	0.30	0.9939	205-12-9
P1ME§	20.89	216	215	25	215	189	25	0.38	0.9987	2381-21-7
BaA§	25.75	228	226	30	113	112	10	0.75	0.9989	56-55-3
CPcdP§	25.95	226	225	30	226	224	40	0.53	0.9982	27208-37-3
CH-d12 SS*	25.95	240	236	35	240	212	30	1.67	na	1719-03-5
Tphen§	26.04	228	226	30	113	112	10	0.41	0.9988	217-59-4
CH§	26.10	228	226	30	113	112	10	0.50	0.9999	218-01-9
CH6Me§	27.67	242	241	20	241	239	30	0.89	0.9978	1705-85-7
CH5Me§	27.74	242	241	20	241	239	30	1.67	0.9998	3697-24-3
BbF-d12-PRC*	30.25	264	260	35	264	236	30	1.67	0.9991	205-99-2
BbF††	30.35	252	250	30	126	113	10	0.37	0.9997	205-99-2
AC712DmeBa††	30.43	256	241	15	241	239	25	0.94	1.0000	57-97-6
BkF††	30.48	252	250	30	126	113	10	0.53	0.9989	207-08-9
BjF††	30.56	252	250	30	126	113	10	0.56	0.9997	205-82-3
BeP††	32.25	252	250	30	126	113	10	0.71	0.9998	192-97-2
BaP-d12 SS*	32.41	264	260	35	264	236	30	1.67	na	63466-71-7
BaP††	32.58	252	250	30	126	113	10	1.18	0.9997	50-32-8
Perylene-D12	33.14	264	260	35	264	236	30		na	1520-96-3
IP‡‡	40.34	276	274	45	138	137	15	0.26	0.9974	193-39-5
DBAhA‡‡	40.41	278	276	35	125	124	10	1.02	0.9981	53-70-3
Pic‡‡	41.29	278	276	35	125	124	10	0.74	0.9984	213-46-7
BghiP-d12 SS*	41.60	288	284	40	144	142	20	1.67	na	93951-66-7
BghiP‡‡	41.71	276	274	45	138	137	15	0.34	0.9988	191-24-2
AA‡‡	42.20	276	274	45	138	137	15	0.33	0.9969	191-26-4
N12bF‡‡	44.20	302	300	40	302	301	20	1.67	0.9992	5385-22-8
N23iF‡‡	44.28	302	300	40	302	301	20	1.67	0.9985	205-83-4
DBaeF‡‡	44.43	302	300	40	302	301	20	0.47	0.9984	5385-75-1
DBalP‡‡	44.59	302	300	40	302	301	20	0.48	0.9980	191-30-0
N23kF‡‡	44.84	302	300	40	302	301	20	1.67	0.9977	207-18-1
N23eP‡‡	45.18	302	300	40	302	301	20	1.67	0.9989	193-09-9
DBaeP‡‡	45.50	302	300	40	302	301	20	6.44	0.9987	192-65-4
CO‡‡	45.69	300	298	50	300	299	35	0.70	0.9984	191-07-1
DBelP‡‡	45.72	302	300	40	302	301	20	1.67	0.9987	192-51-8
N23aP‡‡	45.86	302	300	40	302	301	20	1.67	0.9676	196-42-9
BbPer‡‡	45.93	302	300	40	302	301	20	1.67	0.9965	197-70-6
DbaiP‡‡	46.03	302	300	40	302	301	20	1.42	0.9963	189-55-9
DBahP‡‡	46.83	302	300	40	302	301	20	0.52	0.9950	189-64-0

Table A4. Sampling Parameters.

Location	Matrix	Start date	End date	Deployment time (days)	Average Temp (°C)	Approximate water depth (m)
RM18.5E	sediment (0-0.25m)	9/14/2015	10/19/2015	35	NA	1
	water ($0.3m_{bottom}$)	9/14/2015	10/19/2015	35	NA	1
	water ($1m_{surface}$)	9/14/2015	10/19/2015	35	NA	9
	air	9/14/2015	10/19/2015	35	NA	9
RM11E	sediment (0-0.25m)	9/14/2015	10/19/2015	35	NA	1
	water ($0.3m_{bottom}$)	9/14/2015	10/19/2015	35	NA	1
	water ($1m_{surface}$)	9/14/2015	10/19/2015	35	NA	6
	air	9/14/2015	10/19/2015	35	NA	6
RM7E	sediment (0-0.25m)	9/15/2015	10/6/2015	21	NA	12
	water ($0.3m_{bottom}$)	9/15/2015	10/6/2015	21	NA	12
	water ($1m_{surface}$)	9/15/2015	10/6/2015	21	NA	12
	air	9/15/2015	10/6/2015	21	NA	12
RM6.5W	sediment (0-0.25m)*	9/14/2015	10/19/2015	35	18.7	1
	water ($0.3m_{bottom}$)	9/14/2015	10/19/2015	35	18.3	2
	water ($1m_{surface}$)*	9/14/2015	10/19/2015	35	18.5	8
	air*	9/14/2015	10/19/2015	35	16.9	8
RM3.5W	sediment (0-0.25m)	9/14/2015	10/19/2015	35	NA	1
	water ($0.3m_{bottom}$)	9/14/2015	10/19/2015	35	NA	1
	water ($1m_{surface}$)	9/14/2015	10/19/2015	35	NA	7
	air	9/14/2015	10/19/2015	35	NA	7
RM1E	sediment (0-0.25m)	9/14/2015	10/19/2015	35	NA	1
	water ($0.3m_{bottom}$)	9/14/2015	10/19/2015	35	NA	1
	water ($1m_{surface}$)	9/14/2015	10/19/2015	35	NA	4
	air	9/14/2015	10/19/2015	35	NA	4
a	sediment (0-0.25m)	9/15/2015	10/6/2015	21	19.0	8
	water ($0.3m_{bottom}$)	9/15/2015	10/6/2015	21	NA	8
b	sediment (0-0.25m)	9/15/2015	10/6/2015	21	19.1	5
	water ($0.3m_{bottom}$)	9/15/2015	10/6/2015	21	19.0	5
c	sediment (0-0.25m)	9/15/2015	10/6/2015	21	19.1	3
	water ($0.3m_{bottom}$)	9/15/2015	10/6/2015	21	18.9	3
d	sediment (0-0.25m)	9/15/2015	10/6/2015	21	19.1	12
	water ($0.3m_{bottom}$)	9/15/2015	10/6/2015	21	18.9	12
e	sediment (0-0.25m)	9/15/2015	10/6/2015	21	19.2	1
	water ($0.3m_{bottom}$)	9/15/2015	10/6/2015	21	18.9	1
f	sediment (0-0.25m)	9/15/2015	10/6/2015	21	18.9	6
	water ($0.3m_{bottom}$)	9/15/2015	10/6/2015	21	NA	6
g	sediment (0-0.25m)	9/16/2015	10/6/2015	20	18.8	2
	water ($0.3m_{bottom}$)	9/16/2015	10/6/2015	20	NA	2
h	sediment (0-0.25m)	9/15/2015	10/6/2015	21	18.7	6
	water ($0.3m_{bottom}$)	9/15/2015	10/6/2015	21	18.9	6
i	sediment (0-0.25m)	9/16/2015	10/6/2015	20	19.2	1
	water ($0.3m_{bottom}$)	9/16/2015	10/6/2015	20	NA	1
j	sediment (0-0.25m)	9/15/2015	10/6/2015	21	19.1	1
	water ($0.3m_{bottom}$)	9/15/2015	10/6/2015	21	NA	1
	sediment (0-0.25m)	9/15/2015	10/6/2015	21	19.1	1
1	sediment (0.25-0.5m)	9/15/2015	10/6/2015	21	19.1	1
	water ($0.3m_{bottom}$)	9/15/2015	10/6/2015	21	18.9	1
2	sediment (0-0.25m)	9/15/2015	10/6/2015	21	NA	1
	sediment (0.25-0.5m)	9/15/2015	10/6/2015	21	NA	1
	water ($0.3m_{bottom}$)	9/15/2015	10/6/2015	21	19.1	1
3	sediment (0-0.25m)	9/15/2015	10/6/2015	21	19.1	1
	sediment (0.25-0.5m)	9/15/2015	10/6/2015	21	NA	1
	water ($0.3m_{bottom}$)	9/15/2015	10/6/2015	21	NA	1
4	sediment (0-0.25m)	9/16/2015	10/6/2015	20	NA	11
	sediment (0.25-0.5m)	9/16/2015	10/6/2015	20	NA	11
	water ($0.3m_{bottom}$)	9/16/2015	10/6/2015	20	NA	11

Deployment conditions

Average water temperatures shown above in Figure S3 during the three-week deployment (September 15/16- October 5) at the McCormick and Baxter Superfund Site for all locations and matrices ranged from

18.69-19.25°C with an average of 18.99°C as measured by Onset TidbiT v2 Water Temperature Data Logger. For the five-week deployment in the PHSMS (September 14- October 19) temperatures measured in the sediment PSD, both water PSDs, and air PSDs at RM 6.5W were used as a surrogate for their respective matrices at all other locations. The average water temperature for these four PSDS was 18.48°C with a range of 18.34-18.69°C. The average air temperature for the five-week deployment was determined to be 16.85°C and this was used for all water-air flux calculations.

Water velocity and discharge data for the Willamette River in Portland was obtained from USGS station #14211720 which is located in downtown Portland at approximately RM13. During the course of deployment, the flow velocity ranged from -57 cms^{-1} to 30.1 cms^{-1} for this tidally influenced river. The average net flow velocity was 6.5 cms^{-1}, and 6.3 cms^{-1} for the three and five week deployments respectively. Boundary layer thickness is dependent on absolute flow, independent of direction, and this was 14.5 cms^{-1} and 14.1 cms^{-1} for the three and five-week deployments. Average river discharge was 222 and 216 m^3s^{-1} for the three and five week deployments respectively.

Wind speed and precipitation data were obtained from the National Climate Data Center (NCDC) as measured at the Portland International Airport at 5.8 meters above the ground. The average wind speed was 2.43 ms^{-1} during the first three weeks and 2.27 ms^{-1} during the entire five weeks. For calculation of air flux, 2.43 ms^{-1} was used for RM 7E and 2.27 ms^{-1} was used for the other locations. The prevailing wind direction in September and October is from the northwest as seen below.

Figure A5. Prevailing wind direction. Average prevailing wind direction in the Portland area in September and October of 2006-2010, provided by Wind History[167]. Bars point in the direction from which the winds originate.

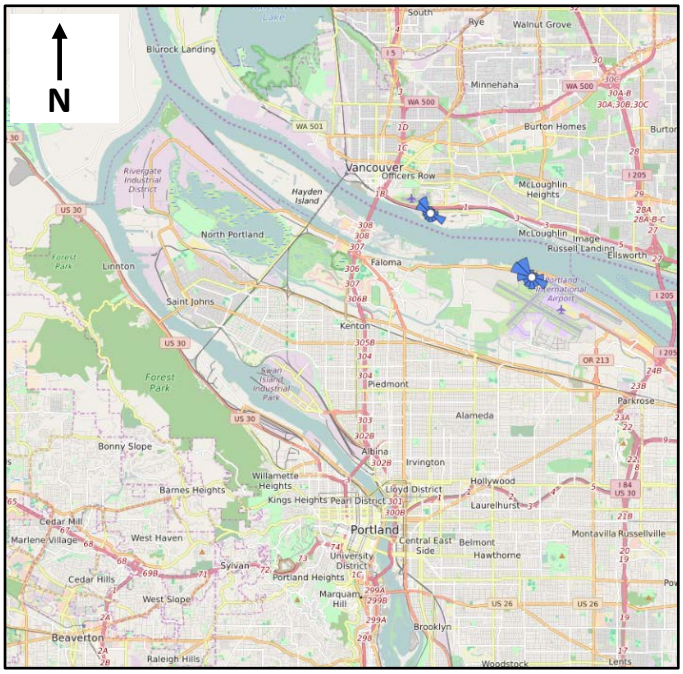

Quality Control

Instrument blanks and reagent blanks were below levels of detection for all analytes. Instrument precision and accuracy were assessed by running a duplicate and over spike sample resulting in a relative standard deviation of 1.89% and 17.8% (99.3% accuracy) respectively across all analytes. Continuing calibration verifications samples were run every 12 samples or less and all met data quality objectives as having >80% of target analytes quantifying within 20% of known value. Analysis of instrument variation was based a known concentration of internal standard (perylene-d12) and this variation across samples is seen below in *figure S5* with an overall relative standard deviation of 8.1%. Average field blank and cleaning blank levels for the Portland Harbor and McCormick and Baxter deployments are seen below in *figure S5*. For each set of samples, the average field blank and cleaning blank concentrations were summed and this value was subtracted from each sample prior to back calculating to environmental conditions.

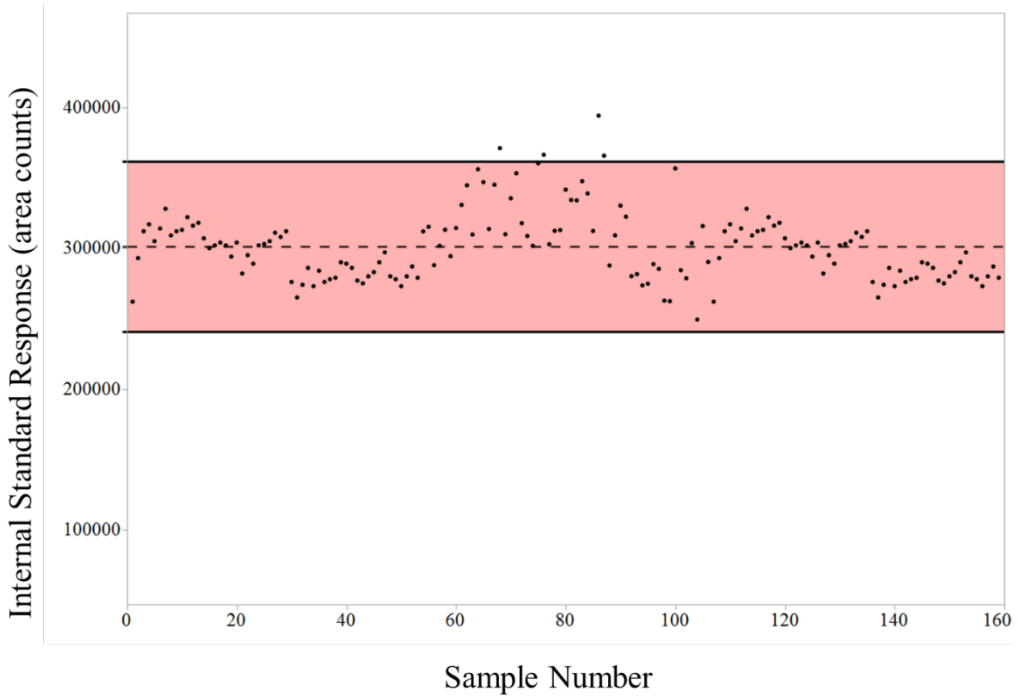

Figure A6. Internal Standard Response. Perylene-d12 response shown to assess instrument variability over duration of sample analysis. Red shaded region represents ±20% of mean. .

Table A5: Blank Analysis. Average field/cleaning blanks concentrations (ng/ml) in LDPE extract, instrument quantification limit (ng/ml), and percent of average analyte in sample for Portland Harbor (PH) and McCormick and Baxter (MCB) deployments. IQL is defined as instrument quantification limit.

	Field Blank (ng/ml)		Cleaning Blank (ng/ml)		IQL (ng/ml)	Average % of Sample	
	PH	MCB	PH	MCB		PH	MCB
Naphthalene	15.2	15.2	21.8	21.7	5.2	28.6	32.6
2-Methylnaphthalene	14.0	9.7	10.6	11.4	3.5	13.5	22.4
1-Methylnaphthalene	8.4	5.7	7.5	7.4	1.4	11.5	1.9
2-Ethylnaphthalene	1.9	BLOD	5.2	6.2	4.8	9.2	4.1
2,6-Dimethylnaphthalene	7.1	BLOD	5.3	6.5	4.4	6.9	0.7
1,6-Dimethylnaphthalene	7.3	BLOD	6.5	8.2	4.1	6.2	0.6
Acenaphthene	BLOD	BLOD	BLOD	15.9	5.4	NA	0.1
Fluorene	BLOD	BLOD	BLOD	5.9	3.9	NA	0.1
Phenanthrene	5.3	6.4	3.3	BLOD	2.3	0.2	NA

Table A6: Replicate Analysis. Relative Standard Deviation (%) for porewater, water, and air based on n=3 at RM 6.5. Porewater measurements are 'approximates' due to high sediment heterogeneity. Dashes indicate the calculations were not possible due to lack of detects. .

Target Compounds	Porewater	Water	Air
Nap	-	6.0	1.3
Nap2Me	-	6.6	2.7
Nap1Me	-	4.7	2.8
Nap2Et	-	2.2	5.4
Nap26DMe	-	3.6	4.5
Nap16DMe	-	3.1	4.7
Nap14DMe	-	2.7	8.3
Nap15DMe	-	3.0	3.6
Nap12DMe	-	3.8	4.0
Nap18DMe	-	-	-
Nap26DEt	-	-	-
ANL	82	3.5	9.6
AN	133	2.0	3.8
FE	73	2.2	4.1
DBT	51	3.1	3.4
PH	50	2.4	2.7
AC	40	2.4	-
PH2Me	46	0.19	9.1
AC2Me	40	1.0	15.6
PH1Me	45	1.6	11.7
AC9Me	-	3.0	-
PH36DMe	41	0.88	17.5
FA	42	1.9	43.1
AC23DMe	39	0.8	-
AC910DMe	-	-	-
Pyr	37	1.2	43.2
Ret	31	1.4	21.9
BaFE	39	1.8	45.4
BbFE	39	2.7	-
BcFE	40	2.4	39.1
P1ME	35	0.1	51.4
BaA	35	1.6	58.1
CPcdP	38	3.0	56.6
Tphen	31	3.4	49.2
CH	35	2.5	57.8
CH6Me	35	12	-
CH5Me	-	-	-
BbF	33	4.7	62.5
AC7 12DmeBa	-	2.9	-
BkF	35	4.5	59.5
BjF	38	6.5	58.5
BeP	31	5.4	-
BaP	34	8.1	0.0
IP	43	23	58.4
DBahA	-	-	-
Pic	51	21	-
BghiP	36	18	-
AA	42	21	-
N12bF	-	-	-
N23jF	-	-	-
DBaeF	-	-	-
DBalP	-	-	-
N23kF	-	-	-
N23eP	-	-	-
DBaeP	-	-	-
CO	-	34	-
DBelP	-	-	-
N23aP	-	-	-
BbPery	-	-	-
DbaiP	-	-	-
DBahP	-	-	-

Table A7: Portland Harbor PAH. Porewater and water PAH concentrations (ng/L) and PAH air concentrations (ng/m3) at Portland Harbor sampling sites. Values at RM6.5 represent the average of n=3 replicates for air and water, and n=3'approximates' for porewater.

	RM 18.5E				RM 11E				RM 7E			
	porewater (0-0.25m)	Water ($0.3m_{bottom}$)	Water ($1m_{surface}$)	air	porewater (0-0.25m)	Water ($0.3m_{bottom}$)	Water ($1m_{surface}$)	air	porewater (0-0.25m)	Water ($0.3m_{bottom}$)	water ($1m_{surface}$)	air
Nap	BLOQ	4.5E-01	4.9E-01	4.5E+01	BLOQ	5.4E-01	5.1E-01	4.6E+01	BLOQ	1.0E+00	6.6E-01	9.3E+01
Nap2Me	BLOQ	5.0E-01	3.5E-01	1.7E+01	8.7E-01	4.5E-01	5.8E-01	2.2E+01	1.1E+00	3.1E-01	2.9E-01	5.3E+01
Nap1Me	BLOQ	3.2E-01	2.2E-01	1.1E+01	9.3E-01	3.0E-01	4.0E-01	1.4E+01	7.2E-01	2.6E-01	2.7E-01	3.1E+01
Nap2Et	7.0E-02	6.0E-02	4.4E-02	1.4E+00	5.7E-01	6.6E-02	8.1E-02	2.3E+00	3.5E-01	6.1E-02	4.3E-02	4.6E+00
Nap26DMe	BLOQ	2.1E-01	1.5E-01	4.4E+00	2.3E+00	2.1E-01	2.4E-01	7.5E+00	6.3E-01	2.2E-01	1.8E-01	1.3E+01
Nap16DMe	BLOQ	2.1E-01	1.5E-01	4.6E+00	2.1E+00	2.1E-01	2.3E-01	7.4E+00	5.1E-01	2.3E-01	1.8E-01	1.1E+01
Nap14DMe	BLOQ	3.2E-02	2.2E-02	6.0E-01	1.2E+00	3.3E-02	3.8E-02	1.1E+00	BLOQ	5.5E-02	3.8E-02	1.5E+00
Nap15DMe	BLOQ	3.0E-02	2.1E-02	8.0E-01	1.2E+00	3.6E-02	4.3E-02	1.3E+00	BLOQ	6.2E-02	4.3E-02	1.7E+00
Nap12DMe	BLOQ	4.3E-02	3.1E-02	1.2E+00	1.1E+00	4.3E-02	5.3E-02	1.8E+00	1.7E-01	6.1E-02	4.8E-02	2.5E+00
Nap18DMe	BLOQ	BLOQ	BLOQ	BLOQ	BLOQ	BLOQ	BLOQ	BLOQ	BLOQ	BLOQ	BLOQ	BLOQ
Nap26DEt	BLOQ	BLOQ	BLOQ	BLOQ	BLOQ	BLOQ	BLOQ	BLOQ	BLOQ	BLOQ	BLOQ	BLOQ
ANL	BLOQ	5.6E-02	4.3E-02	1.9E-01	BLOQ	7.9E-02	1.1E-01	1.9E-01	BLOQ	1.3E-01	1.5E-01	2.6E-01
AN	BLOQ	2.0E-01	1.3E-01	5.3E+00	3.1E+01	3.4E-01	4.4E-01	1.7E+01	7.7E+00	1.6E+00	1.2E+00	4.7E+01
FE	5.6E-01	1.8E-01	1.2E-01	3.5E+00	2.3E+01	2.7E-01	3.1E-01	1.1E+01	2.2E+00	7.7E-01	5.8E-01	2.1E+01
DBT	4.7E-01	1.1E-02	6.1E-03	4.7E-02	2.9E+00	1.8E-02	1.9E-02	1.6E-01	2.6E-01	5.0E-02	3.4E-02	3.0E-01
PH	4.7E+00	2.5E-01	1.6E-01	2.2E+00	6.3E+01	3.5E-01	3.9E-01	6.9E+00	2.4E+00	6.5E-01	4.8E-01	1.2E+01
AC	1.1E-01	7.2E-02	5.9E-02	1.0E-01	3.3E+00	9.9E-02	1.1E-01	3.4E-01	6.5E-01	2.2E-01	1.7E-01	4.8E-01
PH2Me	1.3E+00	1.2E-01	8.8E-02	1.9E-01	3.3E+00	1.7E-01	1.7E-01	4.7E-01	4.5E-01	1.5E-01	1.5E-01	4.2E-01
AC2Me	BLOQ	3.1E-02	2.9E-02	1.2E-02	3.3E-01	5.0E-02	5.8E-02	2.1E-02	9.8E-02	6.3E-02	6.1E-02	1.8E-02
PH1Me	8.7E-01	8.1E-02	5.9E-02	7.8E-02	2.0E+00	1.0E-01	1.1E-01	1.4E-01	3.7E-01	1.3E-01	1.0E-01	1.2E-01
AC9Me	BLOQ	3.3E-02	3.0E-02	BLOQ	BLOQ	3.0E-02	2.7E-02	BLOQ	BLOQ	4.2E-02	3.0E-02	BLOQ
PH36DMe	BLOQ	6.0E-02	6.3E-02	1.3E-02	3.4E-01	9.5E-02	1.0E-01	3.5E-02	1.3E-01	1.0E-01	1.0E-01	1.9E-02
FA	3.4E-01	7.0E-01	6.1E-01	4.2E-02	2.0E+01	1.3E+00	1.1E+00	1.6E-01	3.0E+00	2.4E+00	2.1E+00	2.6E-01
AC23DMe	BLOQ	2.0E-02	2.2E-02	4.7E-03	1.4E-01	3.7E-02	4.4E-02	9.5E-03	BLOQ	3.7E-02	3.9E-02	5.0E-03
AC910DMe	BLOQ	BLOQ	BLOQ	BLOQ	BLOQ	BLOQ	BLOQ	BLOQ	BLOQ	BLOQ	BLOQ	BLOQ

Table A7 (Cont.)

	RM 18.5E				RM 11E				RM 7E			
	porewater (0-0.25m)	water ($0.3m_{bottom}$)	water ($1m_{surface}$)	air	porewater (0-0.25m)	water ($0.3m_{bottom}$)	water ($1m_{surface}$)	air	porewater (0-0.25m)	water ($0.3m_{bottom}$)	water ($1m_{surface}$)	air
Pyr	2.2E-01	5.0E-01	5.3E-01	2.4E-02	1.1E+01	1.1E+00	1.1E+00	7.5E-02	2.2E+00	1.7E+00	1.6E+00	1.1E-01
Ret	1.3E+00	7.8E-01	5.7E-01	1.0E-01	1.8E+00	2.2E+00	5.9E-01	4.2E-02	2.4E+00	9.3E-01	8.0E-01	2.3E-02
BaFE	BLOQ	5.9E-02	6.5E-02	1.3E-03	9.0E-01	1.1E-01	1.2E-01	2.5E-03	3.4E-01	1.8E-01	1.9E-01	3.0E-03
BbFE	BLOQ	4.6E-02	4.8E-02	8.3E-04	9.3E-01	8.9E-02	9.2E-02	1.5E-03	3.3E-01	1.5E-01	1.4E-01	2.0E-03
BcFE	BLOQ	2.3E-02	2.4E-02	7.9E-04	4.1E-01	4.2E-02	4.5E-02	1.4E-03	1.2E-01	6.6E-02	6.6E-02	1.7E-03
P1ME	BLOQ	2.9E-02	3.1E-02	7.7E-04	2.5E-01	6.7E-02	8.3E-02	2.4E-03	1.3E-01	7.9E-02	7.0E-02	1.2E-03
BaA	BLOQ	5.3E-02	5.4E-02	8.0E-04	4.3E-01	1.2E-01	1.3E-01	1.2E-03	3.4E-01	2.3E-01	2.0E-01	1.1E-03
CPcdP	BLOQ	3.3E-02	4.1E-02	1.7E-04	BLOQ	4.1E-02	4.3E-02	2.9E-04	BLOQ	3.2E-02	3.3E-02	1.5E-04
Tphen	BLOQ	5.6E-02	5.6E-02	3.1E-04	2.5E-01	1.0E-01	1.0E-01	5.6E-04	2.0E-01	1.3E-01	1.3E-01	4.4E-04
CH	BLOQ	8.5E-02	8.0E-02	9.9E-04	5.8E-01	1.5E-01	1.6E-01	1.7E-03	4.7E-01	2.8E-01	2.3E-01	1.5E-03
CH6Me	BLOQ	1.4E-02	1.1E-02	BLOQ	BLOQ	1.4E-02	2.1E-02	BLOQ	BLOQ	3.4E-02	1.6E-02	BLOQ
CH5Me	BLOQ	BLOQ	BLOQ	BLOQ	BLOQ	BLOQ	BLOQ	BLOQ	BLOQ	BLOQ	BLOQ	BLOQ
BbF	BLOQ	2.6E-02	2.4E-02	2.6E-04	2.3E-01	6.3E-02	6.0E-02	3.6E-04	2.3E-01	9.6E-02	6.5E-02	2.2E-04
AC712DmeBa	BLOQ	5.4E-03	4.4E-03	BLOQ	BLOQ	1.4E-02	1.3E-02	BLOQ	BLOQ	9.7E-03	6.6E-03	BLOQ
BkF	BLOQ	1.1E-02	9.3E-03	1.2E-04	1.1E-01	2.6E-02	2.5E-02	1.6E-04	1.3E-01	4.2E-02	2.8E-02	1.0E-04
BjF	BLOQ	1.2E-02	1.0E-02	1.9E-04	1.4E-01	2.9E-02	2.7E-02	2.3E-04	BLOQ	4.5E-02	2.8E-02	1.3E-04
BeP	BLOQ	2.9E-02	2.7E-02	9.0E-05	2.1E-01	6.5E-02	6.3E-02	1.3E-04	2.0E-01	8.8E-02	5.8E-02	BLOQ
BaP	BLOQ	9.0E-03	8.6E-03	1.5E-04	BLOQ	2.6E-02	2.8E-02	1.8E-04	BLOQ	4.5E-02	2.2E-02	BLOQ
IP	BLOQ	7.0E-03	5.7E-03	1.2E-04	1.1E-01	1.4E-02	1.2E-02	1.2E-04	BLOQ	1.8E-02	8.5E-03	7.1E-05
DBahA	BLOQ	BLOQ	BLOQ	BLOQ	BLOQ	BLOQ	BLOQ	BLOQ	BLOQ	BLOQ	BLOQ	BLOQ
Pic	BLOQ	BLOQ	BLOQ	BLOQ	BLOQ	7.1E-03	5.9E-03	BLOQ	BLOQ	BLOQ	BLOQ	BLOQ
BghiP	BLOQ	1.5E-02	1.4E-02	1.3E-04	1.2E-01	2.4E-02	2.1E-02	1.7E-04	1.6E-01	2.9E-02	1.4E-02	7.8E-05
AA	BLOQ	BLOQ	BLOQ	2.8E-05	BLOQ	2.9E-03	2.5E-03	3.5E-05	BLOQ	5.1E-03	1.8E-03	BLOQ
CO	BLOQ	BLOQ	BLOQ	BLOQ	BLOQ	BLOQ	BLOQ	BLOQ	BLOQ	BLOQ	BLOQ	BLOQ

Table A7 (Cont.)

	RM 6.5W				RM 3.5W				RM 1E			
	porewater (0-0.25m)	water ($0.3m_{bottom}$)	Water ($1m_{surface}$)	air	porewater (0-0.25m)	water ($0.3m_{bottom}$)	water ($1m_{surface}$)	air	porewater (0-0.25m)	water ($0.3m_{bottom}$)	Water ($1m_{surface}$)	air
Nap	BLOQ	3.4E+00	2.5E+00	3.2E+01	1.3E+00	4.1E-01	8.2E-01	2.2E+01	BLOQ	BLOQ	1.0E+00	2.7E+01
Nap2Me	BLOQ	5.4E-01	4.9E-01	1.4E+01	BLOQ	2.8E-01	3.3E-01	9.3E+00	BLOQ	BLOQ	2.9E-01	9.5E+00
Nap1Me	9.0E-01	6.4E-01	5.2E-01	9.1E+00	1.9E-01	3.4E-01	3.6E-01	6.1E+00	BLOQ	2.5E-02	2.9E-01	6.5E+00
Nap2Et	1.9E-01	9.6E-02	8.3E-02	1.6E+00	2.2E-01	5.9E-02	5.9E-02	1.1E+00	BLOQ	3.4E-02	3.8E-02	1.1E+00
Nap26DMe	7.2E-01	3.8E-01	3.1E-01	5.1E+00	4.4E-01	2.4E-01	2.3E-01	3.7E+00	BLOQ	7.7E-02	1.4E-01	2.9E+00
Nap16DMe	1.0E+00	3.6E-01	3.1E-01	5.2E+00	4.4E-01	2.6E-01	2.5E-01	4.2E+00	BLOQ	9.0E-02	1.5E-01	3.2E+00
Nap14DMe	1.6E+00	1.2E-01	6.7E-02	7.5E-01	3.4E-01	5.7E-02	5.6E-02	6.0E-01	BLOQ	2.1E-02	2.9E-02	4.4E-01
Nap15DMe	8.4E-01	9.6E-02	7.0E-02	9.7E-01	4.0E-01	6.5E-02	6.2E-02	7.8E-01	BLOQ	2.4E-02	2.9E-02	5.6E-01
Nap12DMe	8.2E-01	1.2E-01	8.0E-02	1.3E+00	4.7E-01	7.0E-02	6.8E-02	1.0E+00	BLOQ	1.8E-02	3.6E-02	7.4E-01
Nap18DMe	2.7E-01	BLOQ	BLOQ	BLOQ	BLOQ	BLOQ	BLOQ	BLOQ	BLOQ	BLOQ	BLOQ	BLOQ
Nap26DEt	BLOQ	BLOQ	BLOQ	BLOQ	BLOQ	BLOQ	BLOQ	BLOQ	BLOQ	BLOQ	BLOQ	BLOQ
ANL	1.9E+00	7.6E-01	4.8E-01	1.1E-01	BLOQ	4.0E-01	4.3E-01	1.0E-01	BLOQ	2.0E-01	2.7E-01	1.2E-01
AN	2.8E+01	3.8E+00	1.8E+00	1.3E+01	6.8E+00	1.3E+00	1.3E+00	1.3E+01	3.8E-01	5.2E-01	6.0E-01	4.1E+00
FE	2.7E+00	1.5E+00	9.8E-01	8.5E+00	8.8E+00	8.7E-01	8.3E-01	1.1E+01	3.4E-01	3.6E-01	4.3E-01	3.1E+00
DBT	8.6E-01	2.9E-01	1.5E-01	1.9E-01	1.2E+00	1.0E-01	9.1E-02	2.2E-01	2.4E-01	2.0E-02	3.1E-02	4.4E-02
PH	3.4E+00	3.0E+00	1.8E+00	7.1E+00	1.7E+01	1.5E+00	1.2E+00	1.1E+01	2.3E+00	5.1E-01	5.2E-01	1.9E+00
AC	1.6E+00	9.1E-01	5.6E-01	3.7E-01	6.4E-01	4.3E-01	4.3E-01	3.7E-01	BLOQ	1.5E-01	1.7E-01	6.5E-02
PH2Me	1.4E+00	1.0E+00	4.9E-01	5.0E-01	1.6E+00	3.7E-01	3.4E-01	5.6E-01	6.7E-01	1.6E-01	1.7E-01	1.5E-01
AC2Me	3.8E-01	3.0E-01	1.6E-01	3.5E-02	9.0E-02	1.3E-01	1.3E-01	2.3E-02	BLOQ	5.0E-02	5.4E-02	9.6E-03
PH1Me	1.3E+00	5.0E-01	2.5E-01	1.6E-01	1.1E+00	2.5E-01	2.3E-01	1.8E-01	4.3E-01	1.0E-01	1.0E-01	6.2E-02
AC9Me	BLOQ	4.0E-02	3.2E-02	BLOQ	BLOQ	3.0E-02	3.3E-02	BLOQ	BLOQ	1.1E-02	1.3E-02	BLOQ
PH36DMe	4.8E-01	3.2E-01	1.8E-01	3.3E-02	2.0E-01	1.6E-01	1.7E-01	2.7E-02	8.7E-02	8.4E-02	9.6E-02	1.1E-02
FA	9.8E+00	8.6E+00	5.0E+00	2.3E-01	3.6E+00	5.3E+00	5.0E+00	3.9E-01	1.0E+00	1.8E+00	1.9E+00	4.9E-02
AC23DMe	2.6E-01	1.5E-01	8.8E-02	9.9E-03	7.8E-02	7.6E-02	8.1E-02	6.9E-03	BLOQ	3.6E-02	4.3E-02	3.8E-03
AC910DMe	BLOQ	BLOQ	BLOQ	BLOQ	BLOQ	BLOQ	BLOQ	BLOQ	BLOQ	BLOQ	BLOQ	BLOQ

Table A7 (Cont.)

	RM 6.5W				RM 3.5W				RM 1E			
	porewater (0-0.25m)	Water ($0.3m_{bottom}$)	Water ($1m_{surface}$)	air	porewater (0-0.25m)	Water ($0.3m_{bottom}$)	Water ($1m_{surface}$)	air	porewater (0-0.25m)	Water ($0.3m_{bottom}$)	Water ($1m_{surface}$)	air
Pyr	1.2E+01	1.1E+01	5.8E+00	1.2E-01	2.8E+00	5.6E+00	5.5E+00	1.6E-01	9.1E-01	1.8E+00	1.9E+00	2.4E-02
Ret	4.5E-01	9.2E-01	9.8E-01	4.5E-02	3.7E+00	1.4E+00	1.3E+00	4.0E-02	2.8E-01	5.2E-01	5.8E-01	5.1E-02
BaFE	8.6E-01	7.1E-01	4.5E-01	3.9E-03	2.7E-01	4.3E-01	4.3E-01	4.2E-03	BLOQ	1.4E-01	1.6E-01	1.6E-03
BbFE	7.4E-01	5.7E-01	3.4E-01	2.6E-03	2.2E-01	3.3E-01	3.2E-01	2.8E-03	BLOQ	1.1E-01	1.1E-01	9.0E-04
BcFE	2.8E-01	2.6E-01	1.6E-01	2.1E-03	8.1E-02	1.5E-01	1.4E-01	2.1E-03	BLOQ	5.1E-02	5.5E-02	8.4E-04
P1ME	8.3E-01	5.3E-01	2.4E-01	2.5E-03	1.1E-01	2.1E-01	2.2E-01	1.9E-03	6.8E-02	8.1E-02	9.2E-02	1.0E-03
BaA	2.2E+00	1.6E+00	8.2E-01	2.1E-03	3.2E-01	7.0E-01	7.1E-01	2.0E-03	1.5E-01	2.0E-01	2.4E-01	8.6E-04
CPcdP	1.9E-01	1.8E-01	8.3E-02	1.9E-04	BLOQ	5.3E-02	5.8E-02	2.3E-04	BLOQ	3.0E-02	3.7E-02	9.5E-05
Tphen	7.7E-01	5.5E-01	2.9E-01	7.0E-04	1.4E-01	3.0E-01	2.7E-01	7.5E-04	9.8E-02	1.4E-01	1.6E-01	5.3E-04
CH	2.9E+00	1.8E+00	8.8E-01	2.6E-03	4.5E-01	7.9E-01	8.0E-01	2.9E-03	1.8E-01	2.8E-01	3.1E-01	1.4E-03
CH6Me	1.6E-01	5.8E-02	3.5E-02	BLOQ	BLOQ	3.1E-02	3.1E-02	BLOQ	BLOQ	1.8E-02	1.7E-02	BLOQ
CH5Me	BLOQ	BLOQ	BLOQ	BLOQ	BLOQ	BLOQ	BLOQ	BLOQ	BLOQ	BLOQ	BLOQ	BLOQ
BbF	1.3E+00	5.8E-01	2.6E-01	4.1E-04	2.1E-01	2.4E-01	2.2E-01	4.5E-04	1.2E-01	1.0E-01	1.1E-01	2.9E-04
AC7 12DmeBa	BLOQ	1.9E-02	1.2E-02	BLOQ	BLOQ	1.1E-02	1.0E-02	BLOQ	BLOQ	9.4E-03	9.0E-03	BLOQ
BkF	7.2E-01	2.8E-01	1.2E-01	1.8E-04	1.2E-01	1.1E-01	1.0E-01	2.0E-04	BLOQ	4.3E-02	4.7E-02	1.2E-04
BjF	9.0E-01	3.3E-01	1.4E-01	2.4E-04	1.3E-01	1.3E-01	1.1E-01	2.7E-04	BLOQ	5.2E-02	5.4E-02	1.8E-04
BeP	1.3E+00	5.5E-01	2.2E-01	1.3E-04	1.9E-01	2.1E-01	1.9E-01	1.4E-04	BLOQ	9.5E-02	1.0E-01	9.6E-05
BaP	1.5E+00	4.7E-01	1.7E-01	2.8E-04	BLOQ	1.3E-01	1.3E-01	BLOQ	BLOQ	4.5E-02	4.9E-02	BLOQ
IP	7.6E-01	1.1E-01	3.6E-02	1.1E-04	1.8E-01	3.7E-02	3.1E-02	1.6E-04	1.4E-01	1.9E-02	1.8E-02	9.7E-05
DBahA	BLOQ	BLOQ	BLOQ	BLOQ	BLOQ	BLOQ	BLOQ	BLOQ	BLOQ	BLOQ	BLOQ	BLOQ
Pic	1.8E-01	2.3E-02	8.9E-03	BLOQ	BLOQ	1.0E-02	8.1E-03	BLOQ	BLOQ	BLOQ	6.0E-03	BLOQ
BghiP	8.1E-01	1.5E-01	5.2E-02	1.4E-04	1.6E-01	5.2E-02	4.5E-02	1.8E-04	1.2E-01	3.0E-02	2.7E-02	9.3E-05
AA	2.0E-01	2.0E-02	7.2E-03	BLOQ	BLOQ	7.7E-03	7.0E-03	BLOQ	BLOQ	3.9E-03	2.6E-03	2.4E-05
CO	BLOQ	BLOQ	BLOQ	BLOQ	BLOQ	BLOQ	BLOQ	BLOQ	BLOQ	BLOQ	BLOQ	BLOQ

Table A8: McCormick and Baxter PAH. Porewater and water PAH concentrations (ng/L) at McCormick and Baxter Superfund Site. At locations b and d, duplicates were taken in sediment and water respectively, and the numbers in the table represent their averages. *PRC depletion in porewater at MCB-3 was <10% and therefore this data may have higher uncertainty.

	a		b		c		d		e	
	porewater (0-0.25m)	water ($0.3m_{bottom}$)	porewater (0-0.25m)	water ($0.3m_{bottom}$)	porewater (0-0.25m)	Water ($0.3m_{bottom}$)	porewater (0-0.25m)	Water ($0.3m_{bottom}$)	porewater (0-0.25m)	Water ($0.3m_{bottom}$)
Nap	BLOQ	6.2E-01	BLOQ	7.5E-01	BLOQ	5.0E-01	BLOQ	BLOQ	BLOQ	2.3E-01
Nap2Me	BLOQ	2.8E-01	BLOQ	2.1E-01	4.3E-02	1.7E-01	4.4E-01	BLOQ	BLOQ	3.6E-01
Nap1Me	BLOQ	2.0E-01	BLOQ	1.9E-01	5.9E-01	2.0E-01	3.9E-01	BLOQ	7.5E-02	3.3E-01
Nap2Et	BLOQ	BLOQ	BLOQ	BLOQ	BLOQ	BLOQ	BLOQ	BLOQ	9.8E-02	3.4E-02
Nap26DMe	1.9E-01	1.7E-01	1.4E-01	1.9E-01	7.8E+00	2.3E-01	6.4E-01	1.2E-01	4.4E-01	3.4E-01
Nap16DMe	1.2E-01	1.6E-01	8.1E-02	1.9E-01	1.3E+01	2.6E-01	6.1E-01	1.1E-01	3.7E-01	3.7E-01
Nap14DMe	BLOQ	BLOQ	BLOQ	BLOQ	4.6E+00	BLOQ	BLOQ	BLOQ	BLOQ	1.1E-01
Nap15DMe	BLOQ	BLOQ	BLOQ	BLOQ	1.3E+01	BLOQ	BLOQ	BLOQ	BLOQ	1.4E-01
Nap12DMe	BLOQ	BLOQ	BLOQ	BLOQ	1.3E+01	BLOQ	BLOQ	BLOQ	2.0E-01	1.2E-01
Nap18DMe	BLOQ	BLOQ	BLOQ	BLOQ	7.5E-01	BLOQ	BLOQ	BLOQ	BLOQ	BLOQ
Nap26DEt	BLOQ	BLOQ	BLOQ	BLOQ	5.2E-01	BLOQ	BLOQ	BLOQ	BLOQ	4.8E-02
ANL	BLOQ	BLOQ	BLOQ	BLOQ	1.1E+00	BLOQ	BLOQ	BLOQ	BLOQ	BLOQ
AN	5.1E-01	9.9E-01	4.3E-01	2.3E+00	5.6E+02	2.9E+00	8.2E+00	9.2E-01	8.5E+00	4.1E+00
FE	5.0E-01	5.1E-01	4.3E-01	8.4E-01	8.6E+00	9.6E-01	3.1E+00	4.5E-01	1.4E+00	1.4E+00
DBT	9.4E-02	4.2E-02	7.1E-02	4.2E-02	1.5E-01	5.9E-02	3.0E-01	4.0E-02	2.2E-01	1.1E-01
PH	7.1E-01	5.3E-01	6.2E-01	5.1E-01	1.2E+00	7.0E-01	3.1E+00	4.9E-01	2.2E+00	1.1E+00
AC	BLOQ	1.9E-01	BLOQ	1.8E-01	1.2E+00	2.1E-01	7.1E-01	2.1E-01	3.0E-01	3.1E-01
PH2Me	2.5E-01	1.4E-01	2.2E-01	1.5E-01	2.3E-01	1.7E-01	6.0E-01	1.3E-01	5.4E-01	2.4E-01
AC2Me	BLOQ	6.2E-02	BLOQ	6.3E-02	9.5E-02	6.8E-02	BLOQ	5.2E-02	BLOQ	8.6E-02
PH1Me	BLOQ	1.3E-01	BLOQ	1.3E-01	6.1E-01	1.5E-01	4.8E-01	1.2E-01	3.9E-01	2.3E-01
AC9Me	BLOQ	BLOQ	BLOQ	BLOQ	BLOQ	BLOQ	BLOQ	BLOQ	BLOQ	4.9E-02
PH36DMe	BLOQ	8.2E-02	BLOQ	8.9E-02	1.7E-01	9.7E-02	BLOQ	7.3E-02	BLOQ	1.3E-01
FA	7.1E-01	2.0E+00	6.9E-01	2.0E+00	6.6E+00	2.3E+00	3.9E+00	1.8E+00	1.1E+00	3.7E+00
AC23DMe	BLOQ	BLOQ	BLOQ	BLOQ	BLOQ	BLOQ	BLOQ	BLOQ	BLOQ	BLOQ
AC910DMe	BLOQ	BLOQ	BLOQ	BLOQ	BLOQ	BLOQ	BLOQ	BLOQ	BLOQ	BLOQ

Table A8 (Cont.)

	a		b		c		d		E	
	porewater (0-0.25m)	water ($0.3m_{bottom}$)	porewater (0-0.25m)	water ($0.3m_{bottom}$)	porewater (0-0.25m)	Water ($0.3m_{bottom}$)	porewater (0-0.25m)	Water ($0.3m_{bottom}$)	porewater (0-0.25m)	Water ($0.3m_{bottom}$)
Pyr	5.3E-01	1.5E+00	5.1E-01	1.5E+00	2.7E+00	1.7E+00	2.8E+00	1.3E+00	8.8E-01	2.8E+00
Ret	2.6E-01	6.8E-01	BLOQ	7.2E-01	2.6E-01	8.5E-01	2.4E+00	6.6E-01	8.3E-01	1.7E+00
BaFE	BLOQ	1.7E-01	BLOQ	1.7E-01	BLOQ	2.0E-01	4.1E-01	1.4E-01	BLOQ	2.8E-01
BbFE	BLOQ	9.3E-02	BLOQ	9.1E-02	BLOQ	1.1E-01	BLOQ	8.3E-02	BLOQ	1.5E-01
BcFE	BLOQ	7.8E-02	BLOQ	7.9E-02	BLOQ	8.8E-02	1.8E-01	7.3E-02	BLOQ	1.3E-01
P1ME	BLOQ	6.5E-02	BLOQ	6.4E-02	BLOQ	7.2E-02	1.5E-01	6.0E-02	BLOQ	1.1E-01
BaA	BLOQ	1.9E-01	BLOQ	1.8E-01	BLOQ	2.1E-01	3.9E-01	1.7E-01	BLOQ	3.2E-01
CPcdP	BLOQ	3.2E-02	BLOQ	3.3E-02	BLOQ	3.6E-02	BLOQ	2.8E-02	BLOQ	4.7E-02
Tphen	BLOQ	1.1E-01	BLOQ	1.1E-01	BLOQ	1.3E-01	2.1E-01	1.0E-01	BLOQ	2.0E-01
CH	BLOQ	2.1E-01	BLOQ	2.1E-01	BLOQ	2.4E-01	4.7E-01	1.9E-01	1.2E-01	3.8E-01
CH6Me	BLOQ	BLOQ	BLOQ	BLOQ	BLOQ	BLOQ	BLOQ	BLOQ	BLOQ	4.4E-02
CH5Me	BLOQ	BLOQ	BLOQ	BLOQ	BLOQ	BLOQ	BLOQ	BLOQ	BLOQ	4.3E-02
BbF	BLOQ	7.3E-02	BLOQ	7.0E-02	BLOQ	8.5E-02	2.4E-01	7.4E-02	9.3E-02	1.3E-01
AC712DmeBa	BLOQ	BLOQ	BLOQ	BLOQ	BLOQ	BLOQ	BLOQ	BLOQ	BLOQ	BLOQ
BkF	BLOQ	3.8E-02	BLOQ	3.6E-02	BLOQ	4.4E-02	BLOQ	3.7E-02	BLOQ	6.2E-02
BjF	BLOQ	BLOQ	BLOQ	3.0E-02	BLOQ	BLOQ	BLOQ	3.3E-02	BLOQ	5.8E-02
BeP	BLOQ	6.6E-02	BLOQ	6.3E-02	BLOQ	7.5E-02	BLOQ	6.5E-02	BLOQ	1.1E-01
BaP	BLOQ	BLOQ	BLOQ	BLOQ	BLOQ	BLOQ	BLOQ	BLOQ	BLOQ	6.6E-02
IP	BLOQ	2.7E-02	BLOQ	2.2E-02	BLOQ	3.1E-02	1.5E-01	2.5E-02	BLOQ	3.6E-02
DBahA	BLOQ	BLOQ	BLOQ	BLOQ	BLOQ	BLOQ	BLOQ	BLOQ	BLOQ	BLOQ
Pic	BLOQ	BLOQ	BLOQ	BLOQ	BLOQ	BLOQ	BLOQ	BLOQ	BLOQ	BLOQ
BghiP	BLOQ	3.6E-02	BLOQ	3.1E-02	BLOQ	4.1E-02	1.8E-01	3.5E-02	BLOQ	5.2E-02
AA	BLOQ	BLOQ	BLOQ	BLOQ	BLOQ	BLOQ	BLOQ	BLOQ	BLOQ	BLOQ
CO	BLOQ	BLOQ	BLOQ	BLOQ	BLOQ	BLOQ	BLOQ	BLOQ	BLOQ	BLOQ

Table A8 (Cont.)

	f		g		h		i		j	
	porewater (0-0.25m)	Water ($0.3m_{bottom}$)	porewater (0-0.25m)	water ($0.3m_{bottom}$)	porewater (0-0.25m)	Water ($0.3m_{bottom}$)	porewater (0-0.25m)	water ($0.3m_{bottom}$)	porewater (0-0.25m)	water ($0.3m_{bottom}$)
Nap	BLOQ	1.6E-01	9.9E+00	9.1E+01	BLOQ	BLOQ	BLOQ	5.3E+00	3.8E+00	6.4E-01
Nap2Me	BLOQ	1.3E-02	1.6E+00	1.6E+01	BLOQ	BLOQ	BLOQ	1.9E+00	3.3E+00	7.2E-01
Nap1Me	BLOQ	1.2E-01	1.6E+00	1.4E+01	BLOQ	1.1E-01	BLOQ	1.9E+00	1.8E+01	2.2E+00
Nap2Et	BLOQ	3.9E-02	1.2E-01	7.3E-01	1.2E-01	2.3E-02	BLOQ	9.3E-02	1.0E+00	1.1E-01
Nap26DMe	4.1E-02	2.5E-01	5.5E-01	3.7E+00	7.3E-01	2.2E-01	2.4E-01	5.9E-01	4.1E+02	3.7E+00
Nap16DMe	1.7E-02	2.5E-01	5.7E-01	3.6E+00	4.4E-01	2.1E-01	2.6E-01	6.2E-01	4.7E+02	5.1E+00
Nap14DMe	BLOQ	BLOQ	1.5E-01	9.3E-01	BLOQ	BLOQ	BLOQ	1.9E-01	1.2E+02	2.0E+00
Nap15DMe	BLOQ	7.8E-02	1.6E-01	9.7E-01	BLOQ	BLOQ	BLOQ	2.0E-01	1.3E+02	2.1E+00
Nap12DMe	BLOQ	5.2E-02	1.7E-01	1.0E+00	BLOQ	5.8E-02	BLOQ	2.0E-01	1.8E+02	2.4E+00
Nap18DMe	BLOQ	BLOQ	BLOQ	5.9E-02	BLOQ	BLOQ	BLOQ	BLOQ	7.0E+00	1.3E-01
Nap26DEt	BLOQ	5.6E-02	BLOQ	5.7E-02	BLOQ	5.1E-02	BLOQ	3.9E-02	2.9E+00	1.2E-01
ANL	BLOQ	BLOQ	BLOQ	5.2E-01	BLOQ	BLOQ	BLOQ	BLOQ	1.6E+01	1.0E+00
AN	BLOQ	1.3E+00	9.1E+00	4.6E+01	5.5E+00	1.4E+00	2.3E-01	7.8E+00	7.8E+03	1.1E+02
FE	1.3E-01	8.3E-01	3.3E+00	1.8E+01	1.1E+00	7.0E-01	7.7E-01	3.2E+00	3.0E+03	4.4E+01
DBT	2.5E-02	6.8E-02	9.8E-02	4.8E-01	1.8E-01	6.3E-02	1.6E-01	1.4E-01	1.6E+02	1.3E+00
PH	1.1E-01	9.3E-01	9.3E-01	4.2E+00	9.9E-01	8.8E-01	1.0E+00	1.8E+00	1.1E+03	4.4E+00
AC	BLOQ	3.1E-01	8.6E-02	8.2E-01	3.5E-01	2.7E-01	6.5E-01	3.8E-01	1.0E+02	1.4E+00
PH2Me	4.7E-02	2.8E-01	1.4E-01	2.7E-01	2.3E-01	2.5E-01	3.5E-01	2.5E-01	1.7E+01	3.3E-01
AC2Me	BLOQ	1.3E-01	BLOQ	7.9E-02	BLOQ	1.0E-01	BLOQ	8.1E-02	2.6E+00	1.3E-01
PH1Me	BLOQ	2.5E-01	1.0E-01	2.2E-01	BLOQ	2.2E-01	3.0E-01	2.2E-01	1.0E+01	3.6E-01
AC9Me	BLOQ	6.2E-02	BLOQ	4.4E-02	BLOQ	5.0E-02	BLOQ	5.0E-02	2.7E-01	4.3E-02
PH36DMe	BLOQ	1.9E-01	BLOQ	1.1E-01	BLOQ	1.6E-01	5.6E-02	1.4E-01	8.4E-01	1.4E-01
FA	2.3E-01	3.9E+00	1.9E-01	3.6E+00	1.1E+00	3.3E+00	1.4E+00	3.5E+00	6.4E+01	4.8E+00
AC23DMe	BLOQ	BLOQ	BLOQ	BLOQ	BLOQ	BLOQ	BLOQ	BLOQ	BLOQ	BLOQ
AC910DMe	BLOQ	BLOQ	BLOQ	BLOQ	BLOQ	BLOQ	BLOQ	BLOQ	BLOQ	BLOQ

Table A8 (Cont.)

	f		g		h		i		j	
	Porewater (0-0.25m)	**Water ($0.3m_{bottom}$)**	**porewater (0-0.25m)**	**Water ($0.3m_{bottom}$)**	**porewater (0-0.25m)**	**water ($0.3m_{bottom}$)**	**porewater (0-0.25m)**	**water ($0.3m_{bottom}$)**	**porewater (0-0.25m)**	**water ($0.3m_{bottom}$)**
Pyr	1.5E-01	2.7E+00	1.3E-01	2.5E+00	8.2E-01	2.3E+00	3.9E+00	2.2E+00	2.2E+01	3.2E+00
Ret	6.6E-02	1.5E+00	5.3E-02	8.0E-01	2.7E-01	1.2E+00	2.6E-01	1.1E+00	2.4E-01	8.2E-01
BaFE	BLOQ	3.3E-01	BLOQ	2.3E-01	BLOQ	2.7E-01	1.7E-01	2.6E-01	4.7E-01	2.6E-01
BbFE	BLOQ	1.7E-01	BLOQ	1.3E-01	BLOQ	1.4E-01	1.6E-01	1.4E-01	5.8E-01	1.5E-01
BcFE	BLOQ	1.4E-01	BLOQ	9.4E-02	BLOQ	1.2E-01	1.5E-01	1.1E-01	1.4E-01	1.2E-01
P1ME	BLOQ	1.2E-01	BLOQ	8.0E-02	BLOQ	9.7E-02	1.2E-01	9.0E-02	1.3E-01	9.6E-02
BaA	BLOQ	3.7E-01	BLOQ	2.4E-01	BLOQ	2.8E-01	2.0E-01	2.9E-01	2.7E-01	2.6E-01
CPcdP	BLOQ	5.4E-02	BLOQ	2.0E-02	BLOQ	4.3E-02	BLOQ	3.2E-02	BLOQ	2.4E-02
Tphen	BLOQ	2.1E-01	BLOQ	1.7E-01	BLOQ	1.7E-01	2.4E-01	1.8E-01	2.4E-01	2.0E-01
CH	BLOQ	3.8E-01	BLOQ	2.9E-01	BLOQ	3.1E-01	1.5E-01	3.5E-01	3.4E-01	3.2E-01
CH6Me	BLOQ	4.8E-02	BLOQ	3.5E-02	BLOQ	BLOQ	BLOQ	4.1E-02	BLOQ	4.0E-02
CH5Me	BLOQ	6.8E-02	BLOQ	BLOQ	BLOQ	5.8E-02	BLOQ	6.0E-02	BLOQ	3.3E-02
BbF	BLOQ	1.3E-01	BLOQ	1.2E-01	BLOQ	1.0E-01	1.4E-01	1.3E-01	1.7E-01	1.5E-01
AC712DmeBa	BLOQ	BLOQ	BLOQ	BLOQ	BLOQ	BLOQ	BLOQ	BLOQ	BLOQ	BLOQ
BkF	BLOQ	6.1E-02	BLOQ	5.4E-02	BLOQ	4.8E-02	BLOQ	5.8E-02	7.3E-02	6.4E-02
BjF	BLOQ	6.3E-02	BLOQ	5.4E-02	BLOQ	4.5E-02	BLOQ	6.1E-02	7.9E-02	6.7E-02
BeP	BLOQ	1.1E-01	BLOQ	9.3E-02	BLOQ	9.0E-02	BLOQ	1.1E-01	1.5E-01	1.2E-01
BaP	BLOQ	5.5E-02	BLOQ	BLOQ	BLOQ	BLOQ	BLOQ	5.2E-02	BLOQ	4.5E-02
IP	BLOQ	3.3E-02	BLOQ	2.7E-02	BLOQ	2.6E-02	BLOQ	3.1E-02	BLOQ	2.9E-02
DBahA	BLOQ	BLOQ	BLOQ	BLOQ	BLOQ	BLOQ	BLOQ	BLOQ	BLOQ	BLOQ
Pic	BLOQ	BLOQ	BLOQ	BLOQ	BLOQ	BLOQ	BLOQ	BLOQ	BLOQ	BLOQ
BghiP	BLOQ	5.0E-02	BLOQ	3.9E-02	BLOQ	4.0E-02	BLOQ	4.4E-02	4.2E-02	4.0E-02
AA	BLOQ	BLOQ	BLOQ	BLOQ	BLOQ	BLOQ	BLOQ	BLOQ	BLOQ	BLOQ
CO	BLOQ	BLOQ	BLOQ	BLOQ	BLOQ	BLOQ	BLOQ	BLOQ	BLOQ	BLOQ

Table A8 (Cont.)

	1			2			3			4		
	porewater (0.25-0.5m)	porewater (0-0.25m)	water ($0.3m_{bottom}$)	porewater (0.25-0.5m)	porewater (0-0.25m)	Water ($0.3m_{bottom}$)	porewater* (0.25-0.5m)	porewater* (0-0.25m)	water ($0.3m_{bottom}$)	porewater (0.25-0.5m)	porewater (0-0.25m)	water ($0.3m_{bottom}$)
Nap	BLOQ	BLOQ	1.1E+00	5.8E+01	3.0E+01	7.0E-01	5.2E+00	2.9E+00	3.3E+01	0.0E+00	BLOQ	5.2E+00
Nap2Me	BLOQ	2.1E-02	6.7E-02	6.6E+00	5.5E+00	BLOQ	4.4E+00	2.1E+00	1.4E+01	5.6E-01	BLOQ	4.4E+00
Nap1Me	6.0E-01	4.6E-01	3.8E-01	8.6E+02	6.3E+02	1.3E+00	1.9E+01	4.0E+00	1.4E+01	3.9E+00	1.3E-01	1.9E+01
Nap2Et	9.7E-02	1.7E-01	5.7E-02	5.1E+01	3.9E+01	4.7E-01	1.9E+00	4.2E-01	7.7E-01	2.2E-01	1.1E-02	1.9E+00
Nap26DMe	7.9E-01	9.2E-01	3.8E-01	1.5E+02	2.2E+02	4.4E+00	7.1E+01	2.0E+00	4.2E+00	2.1E+01	2.5E-01	7.1E+01
Nap16DMe	8.8E-01	1.1E+00	6.2E-01	3.7E+02	3.8E+02	6.3E+00	8.9E+01	1.8E+00	4.4E+00	1.2E+01	1.8E-01	8.9E+01
Nap14DMe	BLOQ	2.8E-01	2.4E-01	9.2E+01	1.4E+02	3.5E+00	5.2E+01	BLOQ	1.3E+00	2.6E+01	2.7E-01	5.2E+01
Nap15DMe	BLOQ	3.8E-01	2.7E-01	1.1E+02	1.5E+02	3.2E+00	4.4E+01	BLOQ	1.3E+00	2.6E+01	2.7E-01	4.4E+01
Nap12DMe	3.0E-01	3.6E-01	2.6E-01	1.6E+02	2.0E+02	3.5E+00	7.1E+01	7.2E-01	1.3E+00	2.2E+01	2.1E-01	7.1E+01
Nap18DMe	BLOQ	BLOQ	BLOQ	7.3E+00	9.3E+00	2.1E-01	2.9E+00	BLOQ	9.2E-02	2.0E+00	BLOQ	2.9E+00
Nap26DEt	BLOQ	BLOQ	BLOQ	9.5E-01	1.1E+00	7.9E-02	BLOQ	BLOQ	6.4E-02	BLOQ	BLOQ	BLOQ
ANL	BLOQ	BLOQ	2.4E-01	2.0E+01	2.9E+01	2.3E+00	6.4E+00	BLOQ	4.1E-01	3.7E+00	BLOQ	6.4E+00
AN	8.6E+00	1.0E+01	9.1E+00	8.7E+03	1.1E+04	1.7E+02	4.6E+03	2.0E+01	5.2E+01	1.5E+03	1.9E+01	4.6E+03
FE	3.4E+00	5.6E+00	3.5E+00	4.7E+02	1.3E+03	4.8E+01	3.2E+02	1.0E+01	2.2E+01	2.9E+02	3.3E+00	3.2E+02
DBT	1.1E+00	1.4E+00	1.1E-01	5.7E+00	9.8E+00	3.1E-01	1.7E+00	5.9E-01	6.2E-01	9.5E-01	2.5E-02	1.7E+00
PH	1.7E+01	1.8E+01	9.2E-01	3.3E+01	3.0E+01	6.3E-01	1.1E+01	3.0E+00	5.6E+00	2.4E+00	1.4E-01	1.1E+01
AC	2.4E+00	1.7E+00	2.7E-01	7.5E+00	1.3E+01	6.0E-01	3.2E+00	1.1E+00	9.7E-01	2.6E+00	BLOQ	3.2E+00
PH2Me	1.5E+00	3.3E-01	1.3E-01	4.5E+00	2.2E+00	1.9E-01	3.1E+00	7.6E-01	3.5E-01	5.4E-01	4.1E-02	3.1E+00
AC2Me	2.3E-01	4.4E-02	4.6E-02	1.2E+00	1.5E+00	1.4E-01	BLOQ	BLOQ	1.0E-01	BLOQ	BLOQ	BLOQ
PH1Me	8.7E-01	2.3E-01	1.2E-01	7.4E+00	4.9E+00	3.0E-01	2.4E+00	6.7E-01	2.8E-01	4.7E-01	BLOQ	2.4E+00
AC9Me	BLOQ	BLOQ	2.0E-02	BLOQ	1.2E-01	4.2E-02	BLOQ	BLOQ	5.4E-02	BLOQ	BLOQ	BLOQ
PH36DMe	2.2E-01	3.9E-02	6.6E-02	1.1E+00	6.5E-01	1.6E-01	4.7E-01	BLOQ	1.4E-01	BLOQ	BLOQ	4.7E-01
FA	2.8E+00	6.4E-01	1.8E+00	1.0E+01	1.3E+01	3.5E+00	7.8E+00	5.3E+00	4.6E+00	1.9E+00	2.1E-01	7.8E+00
AC23DMe	BLOQ	BLOQ	BLOQ	BLOQ	BLOQ	BLOQ	BLOQ	BLOQ	BLOQ	BLOQ	BLOQ	BLOQ
AC910DMe	BLOQ	BLOQ	BLOQ	BLOQ	BLOQ	BLOQ	BLOQ	BLOQ	BLOQ	BLOQ	BLOQ	BLOQ

Table A8 (Cont.)

	1			2			3			4		
	porewater (0.25-0.5m)	porewater (0-0.25m)	Water ($0.3m_{bottom}$)	porewater (0.25-0.5m)	porewater (0-0.25m)	Water ($0.3m_{bottom}$)	porewater* (0.25-0.5m)	porewater* (0-0.25m)	Water ($0.3m_{bottom}$)	porewater (0.25-0.5m)	porewater (0-0.25m)	Water ($0.3m_{bottom}$)
Pyr	2.2E+00	5.6E-01	1.4E+00	1.5E+01	1.4E+01	3.9E+00	6.4E+00	3.4E+00	2.9E+00	1.7E+00	1.4E-01	6.4E+00
Ret	3.3E-01	6.2E-02	4.4E-01	1.7E+01	4.1E+00	1.3E+00	4.8E+00	2.9E+00	9.9E-01	9.6E-01	7.7E-02	4.8E+00
BaFE	BLOQ	BLOQ	1.2E-01	1.5E+00	8.9E-01	2.9E-01	1.0E+00	6.5E-01	2.9E-01	BLOQ	BLOQ	1.0E+00
BbFE	BLOQ	BLOQ	6.2E-02	9.0E-01	7.1E-01	1.7E-01	BLOQ	BLOQ	1.6E-01	BLOQ	BLOQ	BLOQ
BcFE	7.8E-02	2.2E-02	5.9E-02	5.8E-01	3.0E-01	1.5E-01	4.6E-01	2.5E-01	1.2E-01	1.3E-01	BLOQ	4.6E-01
P1ME	9.6E-02	2.1E-02	4.7E-02	5.0E-01	2.8E-01	1.2E-01	4.3E-01	BLOQ	9.8E-02	1.1E-01	BLOQ	4.3E-01
BaA	BLOQ	BLOQ	1.4E-01	1.7E+00	6.3E-01	3.2E-01	9.1E-01	BLOQ	2.9E-01	BLOQ	BLOQ	9.1E-01
CPcdP	BLOQ	BLOQ	1.7E-02	BLOQ	BLOQ	4.2E-02	BLOQ	BLOQ	3.2E-02	BLOQ	BLOQ	BLOQ
Tphen	BLOQ	BLOQ	9.4E-02	6.0E-01	3.1E-01	2.2E-01	6.6E-01	3.2E-01	2.1E-01	1.9E-01	BLOQ	6.6E-01
CH	1.1E-01	3.4E-02	1.7E-01	2.1E+00	8.8E-01	4.2E-01	1.1E+00	5.6E-01	3.5E-01	2.4E-01	BLOQ	1.1E+00
CH6Me	BLOQ	BLOQ	2.0E-02	BLOQ	BLOQ	5.1E-02	BLOQ	BLOQ	BLOQ	BLOQ	BLOQ	BLOQ
CH5Me	BLOQ	BLOQ	1.9E-02	BLOQ	BLOQ	4.6E-02	BLOQ	BLOQ	7.0E-02	BLOQ	BLOQ	BLOQ
BbF	BLOQ	BLOQ	6.7E-02	8.6E-01	2.2E-01	1.6E-01	7.9E-01	3.6E-01	1.5E-01	1.9E-01	BLOQ	7.9E-01
AC712DmeBa	BLOQ	BLOQ	BLOQ	BLOQ	BLOQ	BLOQ	BLOQ	BLOQ	BLOQ	BLOQ	BLOQ	BLOQ
BkF	BLOQ	BLOQ	3.2E-02	3.8E-01	1.0E-01	7.3E-02	BLOQ	BLOQ	6.8E-02	BLOQ	BLOQ	BLOQ
BjF	BLOQ	BLOQ	3.1E-02	4.1E-01	1.1E-01	7.3E-02	BLOQ	BLOQ	6.8E-02	BLOQ	BLOQ	BLOQ
BeP	BLOQ	BLOQ	5.7E-02	6.2E-01	1.6E-01	1.4E-01	BLOQ	BLOQ	1.2E-01	BLOQ	BLOQ	BLOQ
BaP	BLOQ	BLOQ	3.0E-02	4.3E-01	BLOQ	7.1E-02	BLOQ	BLOQ	BLOQ	BLOQ	BLOQ	BLOQ
IP	BLOQ	BLOQ	1.6E-02	1.7E-01	BLOQ	3.9E-02	BLOQ	BLOQ	3.7E-02	BLOQ	BLOQ	BLOQ
DBahA	BLOQ	BLOQ	BLOQ	BLOQ	BLOQ	BLOQ	BLOQ	BLOQ	BLOQ	BLOQ	BLOQ	BLOQ
Pic	BLOQ	BLOQ	BLOQ	BLOQ	BLOQ	BLOQ	BLOQ	BLOQ	BLOQ	BLOQ	BLOQ	BLOQ
BghiP	BLOQ	BLOQ	2.2E-02	2.0E-01	5.3E-02	5.8E-02	BLOQ	BLOQ	5.7E-02	1.6E-01	BLOQ	BLOQ
AA	BLOQ	BLOQ	BLOQ	BLOQ	BLOQ	BLOQ	BLOQ	BLOQ	BLOQ	BLOQ	BLOQ	BLOQ
CO	BLOQ	BLOQ	BLOQ	BLOQ	BLOQ	BLOQ	BLOQ	BLOQ	BLOQ	BLOQ	BLOQ	BLOQ

Table A9. McCormick and Baxter sediment-water flux (ng/m^{2}d). Positive values indicate flux from sediment to water. In cases where one of either water or porewater measurement was BLOQ, the value of one-half water MQL was substituted (red numbers). NA indicates both porewater and water measurements were below MQL. *PRC depletion in porewater at MCB-3 was <10% and therefore this data may have higher uncertainty.

	a	b	c	d	e	f	g	h	i	j	1	2	3	4
Nap	-1.7E+02	-2.0E+02	-1.3E+02	NA	-5.2E+01	-3.1E+01	-2.4E+04	NA	-1.5E+03	9.4E+02	-3.0E+02	8.6E+03	-8.8E+03	NA
Nap2Me	-7.9E+01	-5.9E+01	-3.8E+01	1.3E+02	-1.0E+02	-1.5E+00	-4.2E+03	NA	-5.7E+02	7.6E+02	-1.3E+01	1.6E+03	-3.6E+03	-5.4E-01
Nap1Me	-5.7E+01	-5.6E+01	1.1E+02	1.1E+02	-7.4E+01	-3.4E+01	-3.7E+03	-3.1E+01	-5.5E+02	4.5E+03	2.2E+01	1.8E+05	-3.1E+03	-7.1E+00
Nap2Et	NA	NA	NA	NA	1.9E+01	-1.0E+01	-1.8E+02	2.7E+01	-2.6E+01	2.8E+02	3.2E+01	1.1E+04	-1.0E+02	-3.2E+00
Nap26DMe	5.9E+00	-1.5E+01	2.2E+03	1.5E+02	3.1E+01	-6.1E+01	-9.3E+02	1.5E+02	-1.0E+02	1.2E+05	1.6E+02	6.2E+04	-6.5E+02	1.5E+01
Nap16DMe	-1.1E+01	-3.1E+01	3.9E+03	1.5E+02	-1.7E+00	-6.8E+01	-9.0E+02	6.5E+01	-1.1E+02	1.4E+05	1.4E+02	1.1E+05	-7.6E+02	-9.1E+00
Nap14DMe	NA	NA	1.3E+03	NA	-3.1E+01	NA	-2.3E+02	NA	-5.4E+01	3.4E+04	1.3E+01	4.0E+04	-3.7E+02	7.9E+01
Nap15DMe	NA	NA	3.9E+03	NA	-4.0E+01	-2.1E+01	-2.4E+02	NA	-5.8E+01	3.6E+04	3.0E+01	4.4E+04	-3.7E+02	5.7E+01
Nap12DMe	NA	NA	3.9E+03	NA	2.4E+01	-1.4E+01	-2.5E+02	-1.6E+01	-5.7E+01	5.3E+04	3.0E+01	5.9E+04	-1.8E+02	4.4E+01
Nap18DMe	NA	NA	2.2E+02	NA	NA	NA	-1.6E+01	NA	NA	2.0E+03	NA	2.7E+03	-2.6E+01	NA
Nap26DEt	NA	NA	1.5E+02	NA	-1.4E+01	-1.6E+01	-1.6E+01	-1.5E+01	-1.1E+01	8.1E+02	NA	3.0E+02	-1.9E+01	NA
ANL	NA	NA	3.3E+02	NA	NA	NA	-1.5E+02	NA	NA	4.5E+03	-6.5E+01	7.8E+03	-1.2E+02	NA
AN	-1.4E+02	-5.5E+02	1.6E+05	2.1E+03	1.3E+03	-3.7E+02	-1.1E+04	1.2E+03	-2.2E+03	2.3E+06	3.8E+02	3.1E+06	-9.2E+03	5.1E+03
FE	-4.8E+00	-1.2E+02	2.2E+03	7.8E+02	-1.2E+01	-2.1E+02	-4.4E+03	1.2E+02	-7.1E+02	8.7E+05	6.2E+02	3.6E+05	-3.3E+03	7.6E+02
DBT	1.5E+01	8.6E+00	2.8E+01	7.7E+01	3.3E+01	-1.3E+01	-1.1E+02	3.5E+01	4.0E+00	4.5E+04	3.8E+02	2.8E+03	-7.9E+00	-6.8E+00
PH	5.4E+01	3.2E+01	1.4E+02	7.6E+02	3.0E+02	-2.4E+02	-9.5E+02	3.2E+01	-2.4E+02	3.1E+05	5.2E+03	8.6E+03	-7.6E+02	-1.8E+02
AC	-5.5E+01	-5.3E+01	2.8E+02	1.5E+02	-2.2E+00	-9.0E+01	-2.2E+02	2.2E+01	8.0E+01	2.9E+04	4.3E+02	3.8E+03	4.3E+01	-8.1E+01
PH2Me	3.2E+01	2.1E+01	1.9E+01	1.4E+02	8.8E+01	-6.7E+01	-3.8E+01	-5.7E+00	2.7E+01	5.0E+03	5.9E+01	5.8E+02	1.2E+02	-5.0E+01
AC2Me	-1.8E+01	-1.8E+01	8.0E+00	-1.5E+01	-2.5E+01	-3.7E+01	-2.3E+01	-3.0E+01	-2.3E+01	7.1E+02	-3.7E-01	4.0E+02	-2.9E+01	-2.9E+01
PH1Me	-3.7E+01	-3.8E+01	1.4E+02	1.1E+02	4.8E+01	-7.4E+01	-3.5E+01	-6.3E+01	2.4E+01	2.9E+03	3.1E+01	1.3E+03	1.1E+02	-5.6E+01
AC9Me	NA	NA	NA	NA	-1.4E+01	-1.8E+01	-1.3E+01	-1.4E+01	-1.4E+01	6.7E+01	-5.4E+00	2.2E+01	-1.6E+01	-1.4E+01
PH36DMe	-2.4E+01	-2.6E+01	2.0E+01	-2.1E+01	-3.9E+01	-5.5E+01	-3.2E+01	-4.6E+01	-2.4E+01	2.0E+02	-8.0E+00	1.5E+02	-4.1E+01	-4.5E+01
FA	-3.8E+02	-3.8E+02	1.3E+03	6.3E+02	-7.5E+02	-1.1E+03	-1.0E+03	-6.4E+02	-6.0E+02	1.7E+04	-3.5E+02	2.9E+03	2.1E+02	-8.4E+02
AC23DMe	NA	NA	NA	NA	NA	NA	NA	NA	NA	NA	NA	NA	NA	NA
AC910DMe	NA	NA	NA	NA	NA	NA	NA	NA	NA	NA	NA	NA	NA	NA

Table A9 (Cont.)

	a	b	c	d	e	f	g	h	i	j	1	2	3	4
Pyr	-2.8E+02	-3.0E+02	2.7E+02	4.3E+02	-5.7E+02	-7.6E+02	-6.9E+02	-4.2E+02	4.8E+02	5.6E+03	-2.4E+02	3.0E+03	1.5E+02	-5.9E+02
Ret	-1.2E+02	-2.1E+02	-1.8E+02	5.2E+02	-2.4E+02	-4.3E+02	-2.2E+02	-2.8E+02	-2.4E+02	-1.7E+02	-1.1E+02	8.1E+02	5.5E+02	-3.8E+02
BaFE	-4.9E+01	-4.9E+01	-5.7E+01	7.8E+01	-8.2E+01	-9.6E+01	-6.8E+01	-7.9E+01	-2.5E+01	6.2E+01	-3.4E+01	1.8E+02	1.0E+02	-7.2E+01
BbFE	-2.7E+01	-2.6E+01	-3.2E+01	-2.4E+01	-4.5E+01	-4.9E+01	-3.8E+01	-4.2E+01	7.5E+00	1.3E+02	-1.8E+01	1.6E+02	-4.7E+01	-4.0E+01
BcFE	-2.3E+01	-2.3E+01	-2.6E+01	3.2E+01	-3.8E+01	-4.0E+01	-2.7E+01	-3.5E+01	1.2E+01	5.7E+00	-1.1E+01	4.4E+01	3.7E+01	-3.5E+01
P1ME	-1.9E+01	-1.9E+01	-2.1E+01	2.8E+01	-3.2E+01	-3.4E+01	-2.3E+01	-2.8E+01	9.3E+00	8.8E+00	-7.4E+00	4.5E+01	-2.8E+01	-2.9E+01
BaA	-5.5E+01	-5.3E+01	-6.1E+01	6.6E+01	-9.5E+01	-1.1E+02	-7.1E+01	-8.2E+01	-2.9E+01	2.6E+00	-4.0E+01	8.9E+01	-8.3E+01	-8.1E+01
CPcdP	-9.2E+00	-9.5E+00	-1.0E+01	-8.0E+00	-1.4E+01	-1.5E+01	-5.7E+00	-1.2E+01	-9.3E+00	-6.9E+00	-4.9E+00	-1.2E+01	-9.2E+00	-1.2E+01
Tphen	-3.2E+01	-3.2E+01	-3.7E+01	3.1E+01	-5.8E+01	-6.1E+01	-5.0E+01	-5.0E+01	1.8E+01	1.1E+01	-2.7E+01	2.4E+01	3.3E+01	-4.9E+01
CH	-6.2E+01	-6.1E+01	-7.0E+01	8.3E+01	-7.6E+01	-1.1E+02	-8.6E+01	-9.0E+01	-6.0E+01	5.3E+00	-4.1E+01	1.3E+02	6.0E+01	-9.7E+01
CH6Me	NA	NA	NA	NA	-1.3E+01	-1.4E+01	-1.0E+01	NA	-1.2E+01	-1.1E+01	-5.5E+00	-1.5E+01	NA	-1.2E+01
CH5Me	NA	NA	NA	NA	-1.2E+01	-1.9E+01	NA	-1.7E+01	-1.7E+01	-9.2E+00	-5.2E+00	-1.3E+01	-2.0E+01	-1.2E+01
BbF	-2.1E+01	-2.0E+01	-2.5E+01	4.8E+01	-1.0E+01	-3.7E+01	-3.4E+01	-3.0E+01	2.6E+00	7.4E+00	-2.0E+01	1.9E+01	6.4E+01	-3.2E+01
AC712DmeBa	NA	NA	NA	NA	NA	NA	NA	NA	NA	NA	NA	NA	NA	NA
BkF	-1.1E+01	-1.0E+01	-1.3E+01	-1.1E+01	-1.8E+01	-1.8E+01	-1.6E+01	-1.4E+01	-1.7E+01	2.7E+00	-9.2E+00	8.8E+00	-2.0E+01	-1.5E+01
BjF	NA	-8.7E+00	-1.1E+01	-9.4E+00	-1.7E+01	-1.8E+01	-1.6E+01	-1.3E+01	-1.8E+01	3.6E+00	-9.0E+00	9.5E+00	-2.0E+01	-1.5E+01
BeP	-1.9E+01	-1.8E+01	-2.2E+01	-1.9E+01	-3.3E+01	-3.3E+01	-2.7E+01	-2.6E+01	-3.2E+01	9.9E+00	-1.6E+01	6.9E+00	-3.5E+01	-2.8E+01
BaP	NA	NA	NA	NA	-1.9E+01	-1.6E+01	NA	NA	-1.5E+01	-1.3E+01	-8.2E+00	-2.0E+01	NA	-1.4E+01
IP	-7.7E+00	-6.2E+00	-9.0E+00	3.5E+01	-1.0E+01	-9.5E+00	-7.7E+00	-7.5E+00	-8.8E+00	-8.3E+00	-4.7E+00	-1.1E+01	-1.1E+01	-7.2E+00
DBahA	NA	NA	NA	NA	NA	NA	NA	NA	NA	NA	NA	NA	NA	NA
Pic	NA	NA	NA	NA	NA	NA	NA	NA	NA	NA	NA	NA	NA	NA
BghiP	-1.0E+01	-8.9E+00	-1.2E+01	4.2E+01	-1.5E+01	-1.4E+01	-1.1E+01	-1.2E+01	-1.3E+01	3.8E-01	-6.2E+00	-1.6E+00	-1.6E+01	-1.2E+01
AA	NA	NA	NA	NA	NA	NA	NA	NA	NA	NA	NA	NA	NA	NA
CO	NA	NA	NA	NA	NA	NA	NA	NA	NA	NA	NA	NA	NA	NA
Σ61PAH	**-1.6E+03**	**-2.3E+03**	**1.8E+05**	**6.6E+03**	**-7.1E+02**	**-4.4E+03**	**-5.3E+04**	**-4.5E+02**	**-6.7E+03**	**3.9E+06**	**6.1E+03**	**4.0E+06**	**-3.0E+04**	**3.2E+03**

Table A10. Portland Harbor sediment-water, water-air flux (ng/m^{2}d). Positive values indicate flux from sediment to water and from water to air. Values include the use of ½ MQL if concentration in one of sediment-water or water-air not available (red values). NA indicates both sediment and water below MQL or both water and air below MQL. Values for RM6.5 are an average based on n=3.

	RM18.5E	RM11E	RM7E	RM6.5W-1	RM6.5W-2	RM6.5W-3	RM3.5W	RM1NW
Nap	-120 / -7700	-140 / -7900	-290 / -18000	-990 / -810	-990 / -670	-990 / 140	270 / -2500	NA/2900
Nap2Me	-140/ -2500	120 / -30000	230 / -10000	-160 / -1700	-160 / -1800	-160 / -1600	-79 / -1100	NA/-1200
Nap1Me	-93/ -1600	180 / -1800	130 / -5900	77 / -560	-190 / -660	-190 / -450	-44 / -360	-6.5 / -590
Nap2Et	3.0/ -150	150 / -220	84 / -820	28 / -65	-27 / -96	-27 / -60	47 / -50	-8.9 / -110
Nap26DMe	-61 / -510	610 / -900	120 / -2200	100 / -220	-110 / -320	-110 / -220	58 / -160	-22 / -220
Nap16DMe	-61 / -550	550 / -890	82 / -1900	190 / -250	-100 / -350	-100 / -240	55 / -230	-26 / -250
Nap14DMe	-8.0 / -64	350 / -120	-15 / -210	430 / 25	-33 / -0.57	-33 / 13	84 / 17	-4.7 / -18
Nap15DMe	-7.6 / -110	340 / -150	-17 / -250	220 / -20	-27 / -32	-27 / -12	100 / -3.8	-5.7 / -39
Nap12DMe	-11/ -150	320 / -230	33 / -400	210 / -64	-33 / -81	-33 / --59	120 / -41	-4.2 / -59
Nap18DMe	NA	NA	NA	78 / NA	NA	NA	78 / NA	NA
Nap26DEt	NA	NA	NA	NA / NA	NA	NA	NA	NA
ANL	-10 / -28	-17 / -16	-32 / -19	990 / 76	86 / 76	-49 / 81	-110 / 68	-53 / 33
AN	-55 / -890	9100 / -2900	1800 / -8400	22000/ -500	-390 / -750	-870 / -550	1600 / -1200	-43 / -160
FE	110 / -610	6700 / -1800	420 / -40000	1100 / -1000	170 / -1200	-250 / -1100	2300 / -1700	-4.4 / -340
DBT	130 / -8.4	860 / -30	61 / -58	240/ -25	280 / -22	-11 / -23	330 / -34	63 / -5.7
PH	1300 / -410	18000 / -1300	520 / -2400	400 / -1100	560 / -1000	-590 / -1000	4600 / -1900	510 / -280
AC	12 / -9.4	950 / -46	130 / -67	290 / 14	350 / 25	-65 / 26	63 / -1.1	-42 / 16
PH2Me	340 / -22	930 / -61	87 / -60	180/ -25	310 / -6.2	-150 / -6.7	350 / -50	150 / -0.16
AC2Me	-8.9 / 2.7	82 / 5.6	10 / 7.1	51 / 19	60 / 22	-38 / 21	-11 / 18	-14 / 7.3
PH1Me	231 / -4.9	570 / -10	69 / -6.4	310 / 6.8	430 / 14	6.0 / 13	240 / 4.5	96 / 4.9
AC9Me	-9.3 / 4.8	-8.5 / 4.4	-12 / 5.2	-11 / 5.4	-11 / 5.2	-11 / 5.0	-8.3 / 5.4	-2.8 / 2.0
PH36DMe	-18 / 8.2	71 / 11	7.3 / 14	66 / 22	110 / 25	-30 / 25	9.7 / 23	1.0 / 14
FA	-110 / 6.0	5500 / -4.5	170 / -1.7	730 / 48	1600 / 90	-1300 / 83	-500 / 42	-220 / 34
AC23DMe	-5.7 / 2.8	29 / 5.8	-11 / 6.0	49 / 13	59 / 13	-9.0 / 13	0.73 / 12	-10 / 6.7
AC910DMe	NA	NA	NA	NA	NA	NA	NA	NA
Pyr	-83 / 7.7	2800 / 11	140 / 19	1200 / 99	1200 / 120	-1600 / 120	-830 / 96	-260 / 40
Ret	140 / 120	-130 / 140	420 / 210	-120 / 240	-98 / 240	-190 / 240	670 / 320	-72 / 140
BaFE	-17 / 2.5	230 / 4.6	46 / 8.0	92 / 18	130 / 18	-94 / 18	-47 / 17	-42 / 6.4
BbFE	-13 / 1.9	250 / 3.6	50 / 6.0	92 / 14	130 / 14	-67 / 14	-31 / 13	-31 / 4.6
BcFE	-6.7 / 0.84	110 / 1.6	15 / 2.6	22 / 6.2	34 / 6.2	-40 / 6.2	-20 / 5.6	-15 / 2.1
P1ME	-8.5 / 0.58	52 / 1.5	16 / 1.5	150 / 5.0	150 / 5.5	-33 / 5.4	-27 / 4.7	-3.7 / 2.0
BaA	-15 / 0.49	90 / 1.3	32 / 2.3	300 / 9.1	340 / 9.8	-150 / 9.4	-110 / 8.0	-14 / 2.7
CPcdP	-9.6 / 0.10	-12 / 0.036	-9.2 / 0.043	24 / 0.11	9.2 / 0.16	-25 / 0.14	-15 / 0.078	-8.6 / 0.060
Tphen	-16 / 0.61	43 / 1.1	20 / 1.5	110 / 3.5	110 / 3.3	-34 / 3.4	-45 / 3.1	-13 / 1.8
CH	-25 / 0.77	120 / 1.5	56 / 2.6	500 / 9.4	530 / 11	-110 / 10	-99 / 9.1	-28 / 3.5
CH6Me	-3.8 / 0.12	-3.7 / 0.24	-9.6 / 0.20	41 / 0.36	42 / 0.47	6.9 / 0.37	-8.8 / 0.36	-5.0 / 0.19
CH5Me	NA	NA	NA	NA	NA	NA	NA	NA
BbF	-7.6 / -0.038	48 / -0.042	40 / -0.015	330 / -0.038	280 / 0.078	40 / 0.059	-10 / 0.0070	5.5 / -0.01
AC712DmeBa	-1.2 / 0.036	-3.7 / 0.14	-2.5 / 0.068	-5.3 / 0.13	-5.3 / 0.14	-5.3 / 0.13	-2.8 / 0.11	-2.37 / 0.09
BkF	-2.9 / -0.0072	26 / 0.011	26 / 0.029	200 / 0.14	170 / 0.20	26 / 0.17	1.9 / 0.13	-12.34 / 0.06
BjF	-3.3 / -0.018	34 / 0.0021	-13 / 0.024	270 / 0.14	210 / 0.23	30 / 0.20	1.5 / 0.14	-15.1 / 0.06
BeP	-8.2 / 0.030	42 / 0.081	32 / 0.097	320 / 0.31	270 / 0.38	52 / 0.34	-5.5 / 0.29	-27.53 / 0.15
BaP	-2.1 / -0.013	-7.2 / 0.013	-13 / 0.027	440 / 0.21	360 / 0.30	91 / 0.24	-39 / 0.21	-12.73 / 0.07
IP	-1.9 / -0.021	28 / -0.018	-5.1 / -0.012	300 / -0.031	200 / 0.00019	68 / -0.0066	42 / -0.021	36.56 / -0.01
DBahA	NA	NA	NA	NA	NA	NA	NA	NA
Pic	NA	-1.6 / -0.00037	NA	75 / 0.0011	-6.3 / 0.0046	20 / 0.0011	-2.5 / 0.0016	NA / -0.00026
BghiP	-4.2 / -0.020	28 / -0.030	39 / -0.012	280 / -0.036	210 / 0.0027	79 / -0.0054	33 / -0.024	25.78 / -0.01
AA	NA/-0.0051	-0.64 / -0.006	-1.3 / -0.0017	78 / -0.00055	65 / 0.00019	19 / -0.00057	-2.04 / -0.00035	-0.92 / -0.0038
CO	NA	-1.5 / 0.0024	NA	-4.2 / -0.0024	-4.2 / -0.0022	-4.2 / -0.0024	-1.3 / -0.0024	NA / -0.0024
Σ61PAH	1300/-15000	49000/-21000	4500/-55000	33000 / -5700	6300 / -6300	-6900 / -4500	8900/-8600	-130 /-5800

Table A11. Water-Air flux relative standard deviation- Portland Harbor. Numbers indicate one standard deviation based on propagation of error methods following Liu et al.[67] NA indicates not available due to lack of data.

	RM18.5E	RM11E	RM7E	RM6.5W-1	RM6.5W-2	RM6.5W-3	RM3.5W	RM1NW
Nap	0.8	0.8	0.7	2.0	2.0	2.0	1.2	1.2
Nap2Me	0.9	1.0	0.7	1.1	1.1	1.2	1.1	1.1
Nap1Me	0.9	1.0	0.7	2.0	1.8	2.0	2.0	1.4
Nap2Et	1.2	1.4	0.8	2.0	2.0	2.0	2.0	1.4
Nap26DMe	1.1	1.1	0.8	2.0	2.0	2.0	2.0	1.7
Nap16DMe	1.1	1.1	0.8	2.0	2.0	2.0	2.0	1.6
Nap14DMe	1.3	1.2	1.0	2.0	2.0	2.0	2.0	2.0
Nap15DMe	1.0	1.1	0.9	2.0	2.0	2.0	2.0	1.8
Nap12DMe	1.0	1.0	0.8	2.0	2.0	2.0	2.0	1.6
Nap18DMe	NA	NA	NA	NA	NA	NA	NA	NA
Nap26DEt	NA	NA	NA	NA	NA	NA	NA	NA
ANL	0.9	1.6	1.8	0.3	0.4	0.4	0.4	0.6
AN	0.8	0.8	0.8	2.0	2.0	2.0	1.4	2.0
FE	0.8	0.8	0.7	1.0	1.0	1.0	0.9	1.2
DBT	0.7	0.7	0.7	1.0	1.1	1.1	0.8	1.0
PH	0.7	0.7	0.7	0.9	0.9	0.9	0.8	0.9
AC	1.4	1.0	0.9	2.0	1.8	1.8	2.0	0.6
PH2Me	1.2	1.0	1.0	2.0	2.0	2.0	1.5	2.0
AC2Me	0.7	0.6	0.5	0.4	0.4	0.4	0.3	0.3
PH1Me	2.0	2.0	2.0	2.0	1.4	1.6	2.0	1.7
AC9Me	0.3	0.3	0.3	0.3	0.3	0.3	0.3	0.3
PH36DMe	0.4	0.5	0.3	0.4	0.3	0.3	0.3	0.3
FA	1.3	2.0	2.0	1.4	0.4	0.5	1.6	0.4
AC23DMe	0.4	0.4	0.3	0.3	0.3	0.3	0.3	0.3
AC910DMe	NA	NA	NA	NA	NA	NA	NA	NA
Pyr	0.6	1.2	1.0	0.5	0.3	0.3	0.4	0.3
Ret	0.3	0.3	0.3	0.3	0.3	0.3	0.3	0.3
BaFE	0.3	0.3	0.3	0.3	0.3	0.3	0.3	0.3
BbFE	0.3	0.3	0.3	0.3	0.3	0.3	0.3	0.3
BcFE	0.3	0.3	0.3	0.3	0.3	0.3	0.3	0.3
P1ME	0.4	0.4	0.3	0.3	0.3	0.3	0.3	0.3
BaA	0.4	0.3	0.3	0.3	0.3	0.3	0.3	0.3
CPcdP	0.7	1.6	0.8	0.7	0.3	0.3	0.6	0.4
Tphen	0.3	0.3	0.3	0.3	0.3	0.3	0.3	0.3
CH	0.4	0.4	0.3	0.3	0.3	0.3	0.3	0.3
CH6Me	0.3	0.3	0.3	0.3	0.3	0.3	0.3	0.3
CH5Me	NA	NA	NA	NA	NA	NA	NA	NA
BbF	1.4	1.7	2.0	2.0	0.6	0.9	2.0	2.0
AC712DmeBa	0.3	0.3	0.3	0.3	0.3	0.3	0.3	0.3
BkF	2.0	2.0	0.8	0.5	0.3	0.3	0.4	0.5
BjF	2.0	2.0	1.1	0.7	0.3	0.3	0.5	0.7
BeP	0.7	0.4	0.3	0.3	0.3	0.3	0.3	0.3
BaP	1.4	1.6	0.3	0.3	0.3	0.3	0.3	0.3
IP	1.1	1.2	1.2	1.3	2.0	2.0	1.4	1.4
DBahA	NA	NA	NA	NA	NA	NA	NA	NA
Pic	NA	0.3		0.3	0.3	0.3	0.3	0.3
BghiP	1.3	1.3	1.3	1.4	2.0	2.0	1.6	1.7
AA	0.7	0.8	0.3	0.3	0.3	0.3	0.3	0.8
CO	NA	0.3	NA	0.3	0.3	0.3	0.3	0.3

Table A12: Sediment-water flux relative standard deviation- Portland Harbor. Numbers indicate one standard deviation based on propagation of error methods following Liu et al. [67]. NA indicates not available due to lack of data.

	RM18.5E	RM11E	RM7E	RM6.5W-1	RM6.5W-2	RM6.5W-3	RM3.5W	RM1NW
Nap	0.5	0.5	0.5	0.5	0.5	0.5	0.5	0.0
Nap2Me	0.5	0.7	0.5	0.5	0.5	0.5	0.5	0.0
Nap1Me	0.4	0.5	0.6	1.2	0.4	0.4	0.9	0.5
Nap2Et	2.0	0.4	0.4	0.7	0.4	0.4	0.5	0.4
Nap26DMe	0.4	0.4	0.5	0.7	0.4	0.4	0.7	0.4
Nap16DMe	0.4	0.4	0.6	0.5	0.4	0.4	0.8	0.4
Nap14DMe	0.4	0.4	0.4	0.4	0.4	0.4	0.4	0.5
Nap15DMe	0.4	0.4	0.4	0.4	0.4	0.4	0.4	0.5
Nap12DMe	0.4	0.4	0.5	0.4	0.4	0.4	0.4	0.5
Nap18DMe	NA	NA	NA	NA	NA	NA	NA	NA
Nap26DEt	NA	NA	NA	NA	NA	NA	NA	NA
ANL	0.6	0.5	0.5	1.3	2.0	2.0	0.4	0.5
AN	0.4	1.5	1.9	1.6	2.0	0.7	1.9	2.0
FE	1.3	1.0	1.4	1.3	2.0	0.9	1.0	2.0
DBT	0.8	0.8	0.9	1.0	1.0	2.0	0.8	0.8
PH	0.8	0.7	1.0	2.0	1.8	0.6	0.8	0.9
AC	1.7	0.7	0.9	1.2	1.1	2.0	1.9	0.4
PH2Me	0.7	0.7	1.0	1.7	1.2	0.9	0.8	0.8
AC2Me	0.4	0.7	1.6	1.6	1.4	1.0	1.6	0.4
PH1Me	0.7	0.7	1.0	0.9	0.9	2.0	0.8	0.8
AC9Me	0.4	0.4	0.4	0.4	0.4	0.4	0.4	0.4
PH36DMe	0.4	0.8	2.0	1.4	1.0	1.4	2.0	2.0
FA	0.8	0.7	2.0	2.0	1.6	0.8	1.5	1.0
AC23DMe	0.4	0.8	0.4	1.0	1.0	2.0	2.0	0.4
AC910DMe	NA	NA	NA	NA	NA	NA	NA	NA
Pyr	0.7	0.7	2.0	2.0	2.0	0.8	0.8	0.8
Ret	1.2	2.0	0.8	0.8	1.0	0.5	0.7	0.7
BaFE	0.4	0.7	1.2	1.8	1.4	0.9	1.1	0.4
BbFE	0.4	0.7	1.1	1.6	1.3	1.0	1.4	0.4
BcFE	0.4	0.7	1.3	2.0	1.8	0.7	0.9	0.4
P1ME	0.4	0.7	1.3	1.1	1.1	2.0	0.8	2.0
BaA	0.4	0.7	1.6	1.3	1.2	1.2	0.7	1.9
CPcdP	0.4	0.4	0.4	1.7	2.0	0.8	0.4	0.4
Tphen	0.4	0.8	1.4	1.2	1.2	2.0	0.7	1.3
CH	0.4	0.7	1.3	1.1	1.0	2.0	0.9	1.2
CH6Me	0.4	0.4	0.4	0.7	0.7	1.7	0.4	0.4
CH5Me	NA	NA	NA	NA	NA	NA	NA	NA
BbF	0.4	0.7	0.8	0.7	0.8	2.0	2.0	2.0
AC712DmeBa	0.4	0.4	0.4	0.4	0.4	0.4	0.4	0.4
BkF	0.4	0.7	0.7	0.7	0.8	2.0	2.0	0.4
BjF	0.4	0.7	0.4	0.7	0.8	2.0	2.0	0.4
BeP	0.4	0.7	0.9	0.7	0.8	2.0	2.0	0.4
BaP	0.4	0.4	0.4	0.7	0.7	1.2	0.4	0.4
IP	0.5	0.6	0.5	0.6	0.6	0.8	0.7	0.6
DBahA	NA	NA	NA	NA	NA	NA	NA	NA
Pic	0.0	0.5	0.0	0.7	0.5	0.8	0.5	0.0
BghiP	0.5	0.6	0.6	0.6	0.6	0.8	0.7	0.7
AA	0.0	0.6	0.5	0.6	0.6	0.7	0.5	0.5
CO	NA	NA	NA	NA	NA	NA	NA	NA

Table A13: Performance reference compound recoveries. (A) % PRC retained (amount recovered (N)/ amount spiked (N_0)) and (B) amount spiked (N_0).

A

	% Retained	RM18.5E	RM11E	RM7E	RM6.5W-1	RM6.5W-2	RM6.5W-3	RM3.5W	RM1NW
Air	FE-D10	0.01	0.01	0.01	0.01	0.01	0.01	0.01	0.01
	Pyr-D10	*23*	*34*	*22*	*56*	*21*	*25*	*45*	*27*
	BbF-D12	54	67	45	94	51	57	80	62
Water	FE-D10	0.01	0.01	0.01	0.01	0.01	0.01	0.01	0.01
	Pyr-D10	*38*	*32*	*20*	*17*	*21*	*16*	*24*	*17*
	BbF-D12	103	98	73	98	98	90	99	106
Water	FE-D10	0.04	0.03	2.95		0.05	0.00	0.02	0.04
	Pyr-D10	*42*	*42*	*38*		*25*	*0.00*	*27*	*25*
	BbF-D12	100	95	68		92	0.00	99	102
Sediment	FE-D10	84	64	42	77	78	45	79	78
	Pyr-D10	89	89	67	98	103	92	93	100
	BbF-D12	97	103	76	113	118	104	106	115
		a	**b**	**c**	**d**	**e**	**f**	**g**	**h**
Water	FE-D10	0.19	0.08	0.17	1.01	0.18	0.15	0.05	0.15
	Pyr-D10	*55*	*49*	*59*	*55*	*67*	*69*	*64*	*69*
	BbF-D12	118	110	104	111	114	123	111	123
Sediment	FE-D10	*67*	*56*	*60*	*76*	*82*	*38*	*36*	*83*
	Pyr-D10	101	109	97	93	111	107	101	109
	BbF-D12	118	126	114	114	120	125	116	126
		i	**j**	**1**	**2**	**3**	**4**		
Water	FE-D10	0.22	0.02	0.13	0.01	0.17	0.51		
	Pyr-D10	*63*	*54*	*40*	*60*	*72*	*65*		
	BbF-D12	119	108	67	105	123	103		
Sediment (0-25cm)	FE-D10	*73*	*50*	*45*	*65*	*93*	*61*		
	Pyr-D10	112	86	98	84	108	66		
	BbF-D12	124	116	117	109	121	82		
Sediment	FE-D10			81	83	96	87		
	Pyr-D10			99	86	116	82		
	BbF-D12			114	107	130	106		

B

	% Retained	RM18.5E	RM11E	RM7E	RM6.5W-1	RM6.5W-2	RM6.5W-3	RM3.5W	RM1NW
Air	FE-D10	186500	186500	186500	186500	186500	186500	186500	186500
	Pyr-D10	7850	7850	7850	7850	7850	7850	7850	7850
	BbF-D12	7850	7850	7850	7850	7850	7850	7850	7850
Water	FE-D10	186500	186500	186500	186500	186500	186500	186500	186500
	Pyr-D10	7850	7850	7850	7850	7850	7850	7850	7850
	BbF-D12	7850	7850	7850	7850	7850	7850	7850	7850
Water	FE-D10	186500	186500	186500	186500	186500	186500	186500	186500
	Pyr-D10	7850	7850	7850	7850	7850	7850	7850	7850
	BbF-D12	7850	7850	7850	7850	7850	7850	7850	7850
Sediment	FE-D10	37300	37300	37300	37300	37300	37300	37300	37300
	Pyr-D10	1570	1570	1570	1570	1570	1570	1570	1570
	BbF-D12	1570	1570	1570	1570	1570	1570	1570	1570
	% Retained	a	b	c	d	e	f	g	h
Water	FE-D10	37300	37300	37300	37300	37300	37300	37300	37300
	Pyr-D10	1570	1570	1570	1570	1570	1570	1570	1570
	BbF-D12	1570	1570	1570	1570	1570	1570	1570	1570
Sediment	FE-D10	37300	37300	37300	37300	37300	37300	37300	37300
	Pyr-D10	1570	1570	1570	1570	1570	1570	1570	1570
	BbF-D12	1570	1570	1570	1570	1570	1570	1570	1570
	% Retained	i	j	1	2	3	4		
Water	FE-D10	37300	37300	37300	37300	37300	37300	37300	37300
	Pyr-D10	1570	1570	1570	1570	1570	1570	1570	1570
	BbF-D12	1570	1570	1570	1570	1570	1570	1570	1570
Sediment	FE-D10	37300	37300	37300	37300	37300	37300	37300	37300
	Pyr-D10	1570	1570	1570	1570	1570	1570	1570	1570
	BbF-D12	1570	1570	1570	1570	1570	1570	1570	1570
Sediment	FE-D10	37300	37300	37300	37300	37300	37300	37300	37300
	Pyr-D10	1570	1570	1570	1570	1570	1570	1570	1570
	BbF-D12	1570	1570	1570	1570	1570	1570	1570	1570

Table A14. McCormick and Baxter sediment bed flux (ng/m^{2}d). Diffusional flux of PAHs was determined across the boundary of the sub armoring (25-50cm) and armoring layers(0-25cm) of the sediment cap at four locations where the boundary layer is replaced by a distance (1cm) and the specific diffusivity of the chemical is adjusted by multiplication of the porosity (0.4) to the power of 4/3. {TC "A14. Sediment bed flux McCormick and Baxter " \f B\l "1" }

	1	2	3	4
Nap	-	1800	150	-
Nap2Me	-	63	140	-
Nap1Me	7.9	14000	860	220
Nap2Et	-3.8	620	83	11
Nap26DMe	-6.8	-3760	3704	1100
Nap16DMe	-12	-460	4700	620
Nap14DMe	-	-2500	-	1400
Nap15DMe	-	-2500	-	1400
Nap12DMe	-3.0	-2700	3800	1200
Nap18DMe	-	-110	-	-
Nap26DEt	-	-7	-	-
ANL	-	-546	-	-
AN	-100	-110000	260000	87000
FE	-120	-44000	17000	16000
DBT	-18	-220	60	50
PH	-80	190	420	120
AC	35	-310	110	-
PH2Me	60	120	120	25
AC2Me	9.0	-13	-	-
PH1Me	32	130	88	
AC9Me	-	-	-	-
PH36DMe	8.4	23	-	-
FA	110	-150	130	86
AC23DMe	-	-	-	-
AC910DMe	-	-	-	-
Pyr	84	41	150	77
Ret	11	530	84	38
BaFE	-	27	18	-
BbFE	-	9	-	-
BcFE	2.7	14	10	-
P1ME	3.6	11	-	-
BaA	-	50	-	-
CPcdP	-	-	-	-
Tphen	-	14	16	
CH	3.7	58	23	-
CH6Me	-	-	-	-
CH5Me	-	-	-	-
BbF		28	19	
AC712DmeBa	-		-	-
BkF	-	12	-	-
BjF	-	14	-	-
BeP	-	21	-	-
BaP	-		-	-
IP	-		-	-
DBahA	-		-	-
Pic	-		-	-
BghiP	-	6.4	-	-
AA	-	-	-	-
CO	-	-	-	-
Σ61PAH	30	-150000	300000	110000

Air/Water Concentration Calculations

Calculations to determine the vapor phase and freely dissolved concentrations of PAHs was based on the model described by *Huckins et al. [4]*. This model uses performance reference compounds (PRCs) to determine in-situ uptake rates of target compounds which takes into account variable environmental conditions such as wind speeds, temperatures, and humidity levels. Vapor phase (C_a) and freely dissolved (C_w) PAH concentrations are given by the following equations:

$$C_a = \frac{N_{analyte}}{V_s K_{sa(T)}\left(1-\exp\left(-\frac{R_s t}{V_s K_{sa}}\right)\right)} \quad \text{(Eq. A1)}$$

$$C_w = \frac{N_{analyte}}{V_s K_{sw}\left(1-\exp\left(-\frac{R_s t}{V_s K_{sw}}\right)\right)} \quad \text{(Eq. A2)}$$

where $N_{analyte}$ is the mass of the compound of interest present in the sampler (ng), V_s is the sampler volume (cm^3), t is the duration of sampling (s), and $K_{sa\,(T)}$ and K_{sw} are the sampler-air and sampler-water partition coefficients respectively and R_s is the PRC derived sampling rates. Using individual octanol-water partition coefficients (K_{ow}), values for K_{sw} were calculated according to the following empirical relationship reported by Huckins et al. [11]:

$$Log\ K_{sw} = a_0 + 2.321(logK_{ow}) - 0.1618(logK_{ow})^2 \quad \text{(Eq. A3)}$$

$$a_0 = -2.61\ for\ PAHs$$

Temperature was assumed to have minimal impact on the sampler-water partition coefficient in the temperature range of this study. Sampler-water partition coefficients were convererted to K_{sa} values at 298K ($K_{sa(298)}$) using the ideal gas constant (R), temperature ($T = 298K$) and Henry's Law Constant (H) according to the following equation:

$$K_{sa\,(298)} = \frac{K_{sw}(RT)}{H} \quad \text{(Eq. A4)}$$

A temperature corrected sampler-air partition coefficient ($K_{sa\ (T)}$) was determined using the Van't Hoff equation:

$$K_{sa\,(T)} = K_{sa\,(298)} * exp^{\frac{-\Delta H_{vap}}{R}\left(\frac{1}{T}-\frac{1}{298}\right)} \quad \text{(Eq. A5)}$$

where T is the average temperature of deployment and ΔH_{vap} is the enthalpy of vaporization which can be related to the subcooled liquid vapor pressure (P_L) following the methodology of Khairy and Lohmann [13] who present the following linear relationship:

$$\Delta \mathrm{H}_{vap} = 69.354 - 9.3891 * logP_L \quad \text{(Eq. A6)}$$

Construction of this regression are based on values for $\Delta \mathrm{H}_{vap}$ from Roux et al. [168] and values for sub-cooled liquid vapor pressure derived from Ma et al.[169] based on the following linear correlation with molecular weight (MW):

$$\log \mathrm{P}_L = 8.52 - 0.054 * MW \quad \text{(Eq. A7)}$$

Sampling rates for target analytes in water (R_{sw}) and air (R_{sa}) are calculated by first determining PRC sampling rates in water ($R_{sw,PRC}$) and air ($R_{sa,PRC}$) based upon PRC dissipation according to the following equation:

$$R_{sw,PRC} = -\frac{\ln(\frac{N}{N_0})}{t} K_{sw} V_s \quad \text{(Eq. A8)}$$

$$R_{sa,PRC} = -\frac{\ln(\frac{N}{N_0})}{t} K_{sa(T)} V_s \quad \text{(Eq. A9)}$$

where N_0 and N are the amounts of PRC at the beginning and end of sampling respectively. Target sampling rates ($\mathrm{R}_{s,analyte}$) were related to PRC sampling rates ($\mathrm{R}_{s,PRC}$) according to the following equations:

$$R_{sw,analyte} = R_{sw,PRC} * \frac{\alpha_{analyte}}{\alpha_{PRC}} \quad \text{(Eq. A10)}$$

$$R_{sa,analyte} = R_{sa,PRC} * \frac{\beta_{analyte}}{\beta_{PRC}} \quad \text{(Eq. A11)}$$

where α is a compound specific function of K_{ow} according to the following empirical relationship:

$$\log \alpha = 0.0130 \log K_{Ow}^3 - 0.3137 \log K_{OW}^2 + 2.244 \log K_{OW} \quad \text{(Eq. A12)}$$

and β is a compound specific function of K_{oA} according to the following empirical relationship:

$$\log \beta = 0.154x \; logK_{OA} - 0.8 \quad \text{(Eq. A13)}$$

LDPE were spiked with three different PRCs as described in materials and methods. For analyte sampling rate calculations, one PRC was used for each sampler with selection based on PRC dissipation between 10% and 90%.

Air-Water Flux Calculations

A Whitman two film model was used to calculate the diffusive flux of PAHs across the water-air interface ($F_{w\text{-}a}$) based on their vapor phase and freely dissolved concentrations on either side of the water air-interface according to the following equation:

$$\mathrm{F} = \mathrm{K_{ol}}\left(C_w - \frac{C_a}{H_{(T)}{}'}\right) \qquad \text{(Eq. A14)}$$

where C_w and C_a are the freely dissolved and vapor phase concentrations in the water and air respectively (ng/m^3), $H_{(T)}$' is the unitless, temperature-corrected Henry's law constant, and K_{ol} is the total mass-transfer coefficient. In this model, transport rate is limited by movement across two thin stagnant layers at the air-water interface. The water-side mass transfer coefficient (k_w) and air-side mass transfer coefficient (k_a) describe the rate of movement across these boundaries and combine to give the overall mass transfer coefficient according to the following equation*:*

$$\frac{1}{\mathrm{K_{ol}}} = \frac{1}{k_a H'_{(T)}} + \frac{1}{k_w} \qquad \text{(Eq. A15)}$$

The individual mass transfer coefficients are dependent upon empirically derived relationships which relate wind speed to compound exchange across air-water boundaries [170] and the scaling of these relationships based on Schmidt values in the case of the water-side mass transfer coefficient [171]and molecular weight in the case of the air-side mass transfer coefficient [172] seen below in equations *S12* and *S13* respectively. The water-side mass transfer coefficient is given by:

$$k_w = (0.222U^2 + 0.333U) * \left(\frac{S_{cw}}{S_{cw(CO_2)}}\right)^{-0.5} \qquad \text{(Eq. A16)}$$

Where U is the wind velocity at 10m above the surface and S_{cw} is the Schmidt value. Schmidt values were calculated from the specific diffusivity of these compounds in water (D_{iW}) based on molar volumes according to the LeBas method. The air-side mass transfer coefficient is given by:

$$k_a = \left(770 + 45MW^{\frac{1}{3}}\right) \quad \text{(Eq. A17)}$$

Further details of the calculations are described in Bamford et al. [25]. The Van't Hoff equation was modified from equation S5 to calculate the temperature corrected, unitless Henry's law constant ($H_{(T)}$') at the average temperature (T) of the deployment according to the following equation:

$$H'_{(T)} = H'_{(298)} * exp^{\frac{-\Delta H_{vap}}{R}\left(\frac{1}{T}-\frac{1}{298}\right)} \quad \text{(Eq. A18)}$$

Appendix B: Supporting Information to Chapter 3 - A passive sampling model to predict polycyclic aromatic hydrocarbons concentrations in butter clams (Saxidomus giganteus), a traditional food source for Native-American tribes of the Salish Sea Region

Table B1: Method detection and quantification limits.

Compound	Abbreviation	Method Detection Limit		Method Quantification Limit	
		porewater	c lam (ng/g)	porewater (ng/L)	clam (ng/g)
Naphthalene	Nap	0.26	0.065	1.3	0.33
2-Methylnaphthalene	Nap2Me	0.069	0.044	0.34	0.22
1-Methylnaphthalene	Nap1Me	0.027	0.018	0.14	0.09
2-Ethylnaphthalene	Nap2Et	0.059	0.061	0.29	0.30
2,6-Dimethylnaphthalene	Nap26DMe	0.057	0.056	0.28	0.28
1,6-Dimethylnaphthalene	Nap16DMe	0.047	0.051	0.24	0.25
1,4-dimethylnaphthalene	Nap14DMe	0.076	0.078	0.38	0.39
1,5 dimethylnaphthalene	Nap15DMe	0.072	0.074	0.36	0.37
1,2-Dimethylnaphthalene	Nap12DMe	0.060	0.059	0.30	0.29
1,8-Dimethylnaphthalene	Nap18DMe	0.055	0.052	0.27	0.26
2,6-Diethylnaphthalene	Nap26DEt	0.038	0.051	0.19	0.25
Acenaphthylene	ANL	0.21	0.15	1.0	0.73
Acenaphthene	AN	0.098	0.067	0.49	0.33
Fluorene	FE	0.056	0.049	0.28	0.25
Dibenzothiophene	DBT	0.015	0.015	0.07	0.08
Phenanthrene	PH	0.027	0.029	0.13	0.14
Anthracene	AC	0.061	0.066	0.30	0.33
2-Methylphenanthrene	PH2Me	0.019	0.024	0.10	0.12
2-Methylanthracene	AC2Me	0.023	0.029	0.11	0.15
1-Methylphenanthrene	PH1Me	0.050	0.066	0.25	0.33
9-Methylanthracene	AC9Me	0.041	0.054	0.21	0.27
3,6-Dimethylphenanthrene	PH36DMe	0.020	0.026	0.10	0.13
Fluoranthene	FA	0.026	0.034	0.080	0.11
2,3-Dimethylanthracene	AC23DMe	0.016	0.021	0.13	0.17
9,10-Dimethylanthracene	AC910DMe	0.042	0.053	0.21	0.26
Pyrene	Pyr	0.021	0.026	0.10	0.13
Retene	Ret	0.053	0.053	0.27	0.26
Benzo(a)fluorene	BaFE	0.079	0.10	0.24	0.31
Benzo(b)flourene	BbFE	0.085	0.10	0.25	0.31
Benzo(c)fluorene	BcFE	0.014	0.019	0.070	0.090
1-Methylpyrene	P1ME	0.018	0.024	0.092	0.12
Benz(a)anthracene	BaA	0.038	0.047	0.19	0.24
Cyclopenta(c,d)pyrene	CPcdP	0.026	0.033	0.13	0.17
Triphenylene	Tphen	0.020	0.026	0.10	0.13
Chrysene	CH	0.026	0.031	0.13	0.16
6-Methylchrysene	CH6Me	0.050	0.056	0.25	0.28
5-Methylchrysene	CH5Me	0.094	0.10	0.28	0.31
Benzo(b)fluoranthene	BbF	0.019	0.023	0.09	0.12
7,12-Dimethylbenz(a)anthracene	AC7 12DmeBa	0.048	0.059	0.24	0.29
Benzo(k)fluoranthene	BkF	0.030	0.033	0.15	0.16
Benzo(j)fluoranthene	BjF	0.032	0.035	0.16	0.17
Benzo(e)pyrene	BeP	0.047	0.044	0.24	0.22
Benzo(a)pyrene	BaP	0.068	0.074	0.34	0.37
Indeno(1,2,3-c,d) pyrene	IP	0.020	0.016	0.10	0.080
Dibenz(a,h)anthracene	DBahA	0.081	0.064	0.41	0.32
Picene	Pic	0.074	0.046	0.37	0.23
Benzo(ghi)perylene	BghiP	0.025	0.021	0.13	0.11
Anthanthrene	AA	0.031	0.021	0.16	0.10
Naptho[1,2-b]fluoranthene	N12bF	0.19	0.10	0.19	0.10
Naptho[2,3-j]fluoranthene	N23jF	0.19	0.10	0.19	0.10
Dibenzo(a,e)fluoroanthene	DBaeF	0.053	0.029	0.27	0.15
Dibenzo(a,l)pyrene	DBalP	0.074	0.030	0.37	0.15
Naptho[2,3-k]fluoranthene	N23kF	0.19	0.10	0.19	0.10
Naptho[2,3-e]pyrene	N23eP	0.19	0.10	0.19	0.10
Dibenzo(a,e)pyrene	DBaeP	1.12	0.40	4.99	2.0
Coronene	CO	0.10	0.044	0.51	0.22
Dibenzo(e,l)pyrene	DBelP	0.19	0.10	0.19	0.10
Naptho[2,3-a]pyrene	N23aP	0.19	0.10	0.19	0.10
Benzo(b)perylene	BbPery	0.19	0.10	0.19	0.10
Dibenzo(a,i)pyrene	DbaiP	0.16	0.089	0.80	0.44
Dibenzo(a,h)pyrene	DBahP	0.059	0.033	0.29	0.16

Table B2: Blank analysis. LDPE blank data represents average LDPE extract concentration (ng/ml) of PAHs in four field blanks and one cleaning blank (ng/ml). These PAHs made up on average 13% of Σ62PAHs in the sediment passive samplers. Clam blank data represents an average extract blank concentration. These PAHs made up on average 15% of Σ62PAHs in the clams. Both LDPE blank and clam blank concentrations were subtracted from sample concentrations prior to environmental back calculations.

	LDPE Blank (ng/ml)	**Clam Blank (ng/ml)**
Naphthalene	2.8	1.0
2-Methylnaphthalene	1.1	1.3
1-Methylnaphthalene	0.70	0.53
2-Ethylnaphthalene	0.10	-
2,6-Dimethylnaphthalene	0.39	-
1,6-Dimethylnaphthalene	0.17	-
Fluorene	0.15	-
Dibenzothiophene	0.030	0.0094
Phenanthrene	0.41	1.1
2-methylphenanthrene	0.10	0.64
1-methylphenanthrene	0.034	0.0024
Fluoranthene	0.031	-
Pyrene	0.023	-
Retene	0.026	0.23

Table B3. Performance reference compound data. Fraction to equilibrium is given by the final fluorene-d10 concentration in the passive sampler extract divided by the initial spike amount subtracted from one and multiplied by 100. .

Beach location	Fluorene-d10 fraction to equilibrium (%)
1	18
1	14
1	17
1	15
1	28
2	39
2	21
2	29
2	14
2	20
3	35
3	32
3	21
3	29
3	24
4	23
4	17
4	17
4	10
4	12

Table B4. Clam concentrations (ng/g). *Values indicate concentrations below limits of detection .

	Beach 1					Beach 2				
	Clam 1	**Clam 2**	**Clam 3**	**Clam 4**	**Clam 5**	**Clam 1**	**Clam 2**	**Clam 3**	**Clam 4**	**Clam 5**
Nap	1.6	1.8	2.8	4.3	5.8	1.8	1.0	0.62	1.6	2.4
Nap2Me	0.39	1.1	0.71	0.25	0.43	0.48	0.070	0.044	0.23	1.1
Nap1Me	0.47	0.52	0.53	0.35	0.50	0.29	0.17	0.11	0.31	0.70
Nap2Et	*	*	*	*	*	*	*	*	*	*
Nap26DMe	*	*	*	*	*	*	*	*	*	*
Nap16DMe	*	*	*	*	*	*	*	*	*	*
Nap14DMe	*	*	*	*	*	*	*	*	*	*
Nap15DMe	*	*	*	*	*	*	*	*	*	*
Nap12DMe	*	*	*	*	*	*	*	*	*	*
Nap18DMe	*	*	*	*	*	*	*	*	*	*
ANL	*	*	*	*	*	*	*	*	*	*
AN	*	*	*	*	*	0.17	*	*	0.29	1.2
FE	1.3	1.6	1.7	1.5	2.0	1.7	1.2	1.0	2.1	3.4
DBT	0.070	0.040	0.070	0.031	0.099	0.22	0.18	0.17	0.68	0.84
PH	2.3	2.5	3.2	2.3	2.6	4.1	4.4	4.0	8.7	17
AC	*	*	*	*	*	*	*	*	*	*
PH2Me	0.52	0.43	0.49	0.42	0.45	0.86	0.75	0.87	1.6	2.5
AC2Me	*	*	*	*	*	*	*	*	*	*
PH1Me	0.26	0.22	0.27	0.19	0.25	0.49	0.50	0.60	0.93	1.2
AC9Me	*	*	*	*	*	*	*	*	*	*
PH36DMe	*	*	*	*	*	*	*	*	*	*
FA	2.8	3.7	3.8	3.3	3.5	8.9	6.5	8.5	25	24
Pyr	0.91	1.4	1.3	0.96	1.0	5.2	3.5	5.6	15	15
Ret	0.10	0.23	0.13	0.20	0.18	0.16	0.16	0.37	0.28	0.19
BaFE	*	*	*	*	*	1.8	1.4	1.5	2.3	2.3
BbFE	*	*	*	*	*	2.2	1.9	2.0	3.0	3.0
BcFE	*	*	*	*	*	0.38	0.23	0.39	0.74	0.73
P1ME	*	*	*	*	*	0.22	0.13	0.38	0.32	0.37
BaA	*	*	*	*	*	1.1	0.67	0.77	1.3	1.4
CPcdP	*	*	*	*	*	*	*	0.040	*	*
Tphen	0.11	0.17	0.16	0.16	0.18	0.35	0.26	0.45	0.60	0.60
CH	0.21	0.20	0.21	0.16	0.23	1.5	0.59	0.65	1.4	1.4
BbF	0.16	0.21	0.20	0.18	0.21	0.88	0.42	0.73	0.62	0.60
AC7 12DmeBa	*	*	*	*	*	*	*	0.060	*	*
BkF	*	*	*	*	*	0.42	0.12	0.30	0.24	0.26
BjF	*	*	*	*	*	0.37	0.080	0.24	0.21	0.18
BeP	*	*	*	*	*	0.46	0.21	0.48	0.30	0.28
BaP	*	*	*	*	*	0.38	*	0.36	*	*
IP	*	*	*	*	*	*	*	0.040	*	*
BghiiP	*	*	*	*	*	0.18	0.040	0.28	0.040	0.028
CO	*	*	*	*	0.080	0.060	*	0.1	*	*
∑62PAH	11	14	16	14	18	34	24	30	67	81

*The following PAHs were not detected above quantification limit in any samples and are not shown in table: 2,6-diethylnaphthalene, 9-methylanthracene, 2,3-dimethylanthracne, 6-methylchrysene, 5-methylchrysene, benz[j]and[e]aceanthrylene, dibenzo[a,h]anthracene, benzo[a]chrysene, anthanthrene, naptho[1,2-b]fluoranthene, naphtho[2,3-j]fluoranthene, dibenzo(a,e)fluoranthene, dibenzo(a,l)pyrene, naphtho[2,3-k]fluoranthene , naphtho[2,3-e]pyrene , dibenzo(a,e)pyrene, benzo(e,l)pyrene, naptho[2,3-a]pyrene, benzo(b)perylene, dibenzo(a,i)pyrene, dibenzo(a,h)pyrene.

Table B4 cont.

	Beach 3					Beach 4				
	Clam 1	**Clam 2**	**Clam 3**	**Clam 4**	**Clam 5**	**Clam 1**	**Clam 2**	**Clam 3**	**Clam 4**	**Clam 5**
Nap	1.8	1.6	1.9	1.3	1.7	1.4	1.1	1.9	1.7	1.5
Nap2Me	0.35	0.32	0.33	0.54	0.26	0.35	0.16	0.35	0.22	0.20
Nap1Me	0.23	0.19	0.17	0.39	0.22	0.20	0.21	0.34	0.18	0.20
ap2Et	*	*	*	*	*	*	*	*	*	*
Nap26DMe	*	*	*	*	*	*	*	*	*	*
Nap16DMe	*	*	*	*	*	*	*	*	*	*
Nap14DMe	*	*	*	*	*	*	*	*	*	*
Nap15DMe	*	*	*	*	*	*	*	*	*	*
Nap12DMe	*	*	*	*	*	*	*	*	*	*
Nap18DMe	*	*	*	*	*	*	*	*	*	*
ANL	*	*	*	*	*	*	*	*	*	*
AN	*	*	*	*	*	*	*	*	*	*
FE	0.63	0.51	0.59	0.64	0.64	0.61	0.55	0.68	0.52	0.44
DBT	*	*	*	*	*	0.080	0.11	0.13	0.051	0.030
PH	0.11	0.27	0.33	0.38	0.37	0.18	0.33	0.47	0.029	0.029
AC	*	*	*	*	*	*	*	*	*	*
PH2Me	0.0060	0.066	0.086	0.046	0.076	0.13	0.11	0.14	0.024	0.016
AC2Me	*	*	*	*	*	*	*	*	*	*
PH1Me	0.068	0.087	0.088	0.13	*	0.097	0.097	*	*	0.068
AC9Me	*	*	*	*	*	*	*	*	*	*
PH36DMe	*	*	*	*	*	*	*	*	*	*
FA	0.40	0.45	0.50	0.51	0.41	0.27	0.18	0.24	0.23	0.22
Pyr	0.38	0.36	0.52	0.57	0.36	*	*	*	*	*
Ret	0.13	0.28	0.14	0.21	0.10	*	0.064	0.10	0.074	0.073
BaFE	*	*	*	*	*	*	*	*	*	*
BbFE	*	*	*	*	*	*	*	*	*	*
BcFE	*	*	*	*	*	*	*	*	*	*
P1ME	*	*	*	*	*	*	*	*	*	*
BaA	*	*	*	*	*	*	*	*	*	*
CPedP	*	*	*	*	*	*	*	*	*	*
Tphen	*	*	*	*	*	*	*	*	*	*
CH	*	*	*	*	*	*	*	*	*	*
BbF	*	*	*	*	*	*	*	*	*	*
AC7 12DmeBa	*	*	*	*	*	*	*	*	*	*
BkF	*	*	*	*	*	*	*	*	*	*
BjF	*	*	*	*	*	*	*	*	*	*
BeP	*	*	*	*	*	*	*	*	*	*
BaP	*	*	*	*	*	*	*	*	*	*
IP	0.021	*	*	*	*	*	*	*	*	*
BghiiP	*	*	*	*	*	*	*	*	*	*
CO	*	*	*	*	*	*	*	*	*	*
∑62PAH	4.1	4.1	4.6	4.7	4.2	3.2	3.0	4.4	3.0	2.7

*The following PAHs were not detected above quantification limit in any samples and are not shown in table: 2,6-diethylnaphthalene, 9-methylanthracene, 2,3-dimethylanthracne, 6-methylchrysene, 5-methylchrysene, benz[j]and[e]aceanthrylene, dibenzo[a,h]anthracene, benzo[a]chrysene, anthanthrene, naptho[1,2-b]fluoranthene, naphtho[2,3-j]fluoranthene, dibenzo(a,e)fluoranthene, dibenzo(a,l)pyrene, naphtho[2,3-k]fluoranthene , naphtho[2,3-e]pyrene , dibenzo(a,e)pyrene, benzo(e,l)pyrene, naptho[2,3-a]pyrene, benzo(b)perylene, dibenzo(a,i)pyrene, dibenzo(a,h)pyrene.

Table B5. Sediment porewater concentrations (ng/L). *Values indicate concentrations below limits of detection..

	Beach 1					Beach 2				
	1	**2**	**3**	**4**	**5**	**1**	**2**	**3**	**4**	**5**
Nap	9.9	5.1	5.2	2.8	1.5	0.75	4.2	1.4	19	11
Nap2Me	0.88	0.99	0.64	0.50	*	0.030	0.90	0.44	2.8	1.8
Nap1Me	0.56	0.63	0.59	0.31	0.060	0.030	0.56	0.39	2.6	1.7
Nap2Et	0.18	0.25	0.18	0.17	0.055	0.044	0.19	0.14	0.90	0.57
Nap26DMe	0.26	0.33	0.21	0.21	0.050	0.060	0.77	0.22	1.8	1.1
Nap16DMe	0.44	0.97	0.51	0.55	0.24	0.16	*	*	3.2	1.7
Nap14DMe	*	*	*	*	*	*	*	*	0.72	0.28
Nap15DMe	0.093	0.13	0.098	0.10	*	*	0.11	0.10	0.94	0.44
Nap12DMe	*	*	*	*	*	*	*	*	0.93	0.45
Nap18DMe	*	*	*	*	*	*	*	0.13	0.21	0.089
ANL	*	*	*	*	*	*	*	0.28	1.4	0.60
AN	1.1	1.9	1.2	0.93	0.69	0.45	1.7	2.0	26	12
FE	0.61	0.89	0.70	0.62	0.33	0.28	1.2	1.1	18	10
DBT	0.17	0.39	0.18	0.44	0.11	0.12	0.53	0.35	7.7	3.6
PH	1.2	2.4	1.2	2.9	0.53	0.62	3.5	2.3	38	25
AC	0.082	0.22	0.10	*	0.067	0.19	0.52	1.0	5.2	2.5
PH2Me	0.38	0.67	0.27	0.86	0.14	0.21	1.1	0.62	2.9	2.1
AC2Me	*	*	*	*	*	*	0.049	0.099	0.91	0.38
PH1Me	0.26	0.49	0.19	0.65	0.14	0.15	0.60	0.41	4.3	2.0
AC9Me	*	*	*	*	*	*	*	*	0.12	0.068
PH36DMe	*	*	*	*	*	*	0.040	0.041	0.42	0.19
FA	1.0	1.4	0.97	0.81	0.61	1.7	5.9	4.4	110	48
Pyr	0.52	1.4	0.50	0.55	0.32	5.1	9.5	12	120	58
Ret	0.19	0.19	0.12	0.18	0.063	0.061	0.21	0.21	0.22	*
BaFE	*	*	*	*	*	0.052	0.17	0.19	3.6	1.4
BbFE	*	*	*	*	*	0.061	0.21	0.21	3.6	1.3
BcFE	*	*	*	*	*	0.23	0.39	0.58	3.4	1.8
P1ME	*	*	*	0.050	*	0.19	0.36	0.62	1.1	0.53
BaA	0.082	0.14	0.070	0.074	0.041	0.10	0.31	0.32	2.0	0.79
CPedP	*	*	*	*	*	*	*	*	*	*
Tphen	0.076	0.15	0.080	0.070	0.050	0.16	0.41	0.32	1.9	0.97
CH	0.072	0.074	0.050	0.039	*	0.070	0.25	0.20	2.6	0.80
BbF	0.11	0.20	0.11	0.11	0.070	0.25	0.57	0.63	1.0	0.47
AC7 12DmeBa	*	*	*	*	*	*	*	0.035	*	*
BkF	*	*	*	*	*	0.13	0.32	0.35	0.54	0.25
BjF	*	*	*	*	*	0.12	0.32	0.36	0.54	0.22
BeP	*	0.10	*	*	*	0.16	0.35	0.44	0.47	0.21
BaP	*	*	*	*	*	0.21	0.51	0.72	0.59	0.25
IP	*	*	*	*	*	*	*	*	*	*
BghiiP	*	*	*	*	*	0.055	0.12	0.15	0.090	0.035
CO	*	*	*	*	*	*	*	*	*	*
∑62PAH	18	19	13	13	5.0	12	36	33	390	190

Table B5 cont.

	Beach 3					Beach 4				
	1	**2**	**3**	**4**	**5**	**1**	**2**	**3**	**4**	**5**
Nap	0.76	0.29	1.2	0.81	1.5	3.4	2.5	1.3	3.8	8.0
Nap2Me	*	*	0.080	0.06	0.20	0.69	0.64	0.14	1.0	0.86
Nap1Me	0.010	*	0.070	0.16	0.14	0.36	0.38	0.11	0.49	0.67
Nap2Et	0.080	0.062	0.14	0.069	0.14	0.16	0.20	0.18	0.30	0.54
Nap26DMe	0.060	*	0.13	0.16	0.18	0.42	1.1	0.23	0.57	0.37
Nap16DMe	0.22	0.14	0.40	0.42	0.42	0.44	0.68	0.48	0.78	0.95
Nap14DMe	0.040	*	*	0.10	0.059	0.064	0.089	*	*	*
Nap15DMe	*	*	0.074	0.084	0.080	0.077	0.11	*	*	0.17
Nap12DMe	*	*	*	*	*	*	*	*	*	*
Nap18DMe	*	*	*	*	*	*	*	*	*	*
ANL	*	*	*	0.20	*	*	*	*	*	*
AN	*	*	*	0.49	*	0.47	0.73	*	*	*
FE	0.13	*	0.19	0.61	0.32	0.30	0.54	0.32	0.50	0.58
DBT	0.050	0.040	0.10	0.10	0.16	0.25	0.24	0.24	0.34	0.30
PH	0.37	0.21	0.84	0.97	1.3	1.9	1.4	1.5	2.2	1.3
AC	*	*	*	0.11	*	*	*	*	*	*
PH2Me	0.071	0.11	0.20	0.16	0.35	0.79	0.61	0.46	0.91	0.36
AC2Me	*	*	*	*	*	*	*	*	*	*
PH1Me	0.057	0.089	0.17	0.15	0.25	0.52	0.36	0.34	0.62	0.30
AC9Me	0.020	*	*	*	*	*	*	*	*	*
PH36DMe	*	*	*	*	*	0.026	*	*	*	*
FA	0.11	0.080	0.16	0.38	0.18	0.18	0.22	0.11	0.35	0.23
Pyr	0.080	0.060	0.12	0.27	0.14	0.14	0.15	*	0.24	0.13
Ret	0.020	0.050	0.041	0.043	0.070	0.15	0.082	0.060	0.19	0.14
BaFE	*	*	*	*	*	*	*	*	*	*
BbFE	*	*	*	*	*	*	*	*	*	*
BcFE	*	*	*	*	*	*	*	*	*	*
P1ME	*	*	*	*	*	*	*	*	*	*
BaA	*	*	*	*	*	*	*	*	*	*
CPcdP	*	*	*	*	*	*	*	*	*	*
Tphen	*	*	*	*	*	*	*	*	*	*
CH	*	*	*	*	*	*	*	*	*	*
BbF	*	*	*	*	*	*	*	*	*	*
AC7 12DmeBa	*	*	*	*	*	*	*	*	*	*
BkF	*	*	*	*	*	*	*	*	*	*
BjF	*	*	*	*	*	*	*	*	*	*
BeP	*	*	*	*	*	*	*	*	*	*
BaP	*	*	*	*	*	*	*	*	*	*
IP	*	*	*	*	*	*	*	*	*	*
BghiiP	*	*	*	*	*	*	*	*	*	*
CO	*	*	*	*	*	*	*	*	*	*
∑62PAH	2.1	1.2	3.9	5.3	5.5	10	10	5.5	12	15

Sediment porewater concentration calculations

Calculations to determine the freely dissolved concentrations of PAHs was based on the model described by *Huckins, Petty and Booij* [11]. This model uses performance reference compounds (PRCs) to determine in-situ uptake rates of target compounds which takes into account variable environmental conditions such as wind speeds, temperatures, and humidity levels. The freely dissolved (C_w) PAH concentration is given by the following equation.

$$C_w = \frac{N_{analyte}}{V_s K_{sw}(1 - \exp\left(-\frac{R_s t}{V_s K_{sw}}\right))} \quad \text{(Eq. B1)}$$

In *Equation S1*, $N_{analyte}$ is the mass of the compound (ng) of interest present in the sampler, V_s is the sampler volume (cm^3), *t* is the duration of sampling (s), K_{sw} is the sampler-water partition coefficient, and R_s is the PRC derived sampling rates. Using individual octanol-water partition coefficients (K_{ow}), values for K_{sw}(Kg/L) were calculated according to the following empirical relationship for PAHs reported by Lohmann[173].

$$log\ K_{sw} = 1.22 * (logK_{ow}) - 1.22 \quad \text{(Eq. B2)}$$

From *Equation S2*, K_{sw} values (Kg/L) were divided by the nominal density of polyethylene (0.91 Kg/L) to achieve a unitless K_{sw} .
Temperature decreases water solubility and thus increases K_{sw}. A temperature corrected sampler-water partition coefficient ($K_{sw\ (T)}$) was determined using the Van't Hoff equation.

$$K_{sw\ (T)} = K_{sw\ (298)} * exp^{\frac{-\Delta H_{vap}}{R}\left(\frac{1}{T}-\frac{1}{298}\right)} \quad \text{(Eq. B3)}$$

where T is the average temperature of deployment and ΔH_{sw} is the enthalpy of sampler-water partition. Booij et al. determined that ΔH_{sw} values for PAHs ranged from -22KJ/mol to -46KJ/mol [174]. Adams et al. calculated ΔH_{sw} values that also fit within this range of values[175]. However, comprehensive data is lacking and for this reason *Lohmann* recommends using a ΔH_{sw}value of -25 $KJmol^{-1}$ for all PAHs[173].
Dissolved salts in aqueous solutions reduce the solubility of hydrophobic organic contaminants. The presence of dissolved ions (mainly NaCl and $MgCl_2$ in a marine system) is not expected to have an effect on the polymer itself. Therefore, we would expect that K_{sw} should increase inversely proportional to the compounds aqueous solubility which decreases in a salt water environment. The following equation was used to correct $K_{sw\ (T)}$ for salinity.

$$K_{sw\ (T,S)} = K_{sw(T)} * 10^{(K_s * M)} \quad \text{(Eq. B4)}$$

In *Equation S4*, K*s* is the Setshenow constant and is given to be 0.35 1/M as shown by Jonker and Muijs in addition to Lohmann[7, 173]. M is the total marine salt concentration in molar. In this study a value of 0.5M was estimated following Schwarzenbach [45].
Sampling rates for target analytes in water (R_{sw}) were calculated by first determining PRC sampling rates in water ($R_{sw,PRC}$) based upon PRC dissipation according to the following equation.

$$R_{sw,PRC} = -\frac{\ln(\frac{N}{N_0})}{t} K_{sw} V_s \quad \text{(Eq. B5)}$$

In *Equation S5*, N_0 and N are the amounts of PRC at the beginning and end of sampling respectively. Target sampling rates ($R_{s,analyte}$) were related to PRC sampling rates ($R_{s,PRC}$) according to the following equations.

$$R_{sw,analyte} = R_{sw,PRC} * \frac{\alpha_{analyte}}{\alpha_{PRC}} \quad \text{(Eq. B6)}$$

In *Equation S7*, α is a compound specific function of K_{ow} according to the following empirical relationship.

$$\log \alpha = 0.0130 \log K_{OW}^3 - 0.3137 \log K_{OW}^2 + 2.244 \log K_{OW} \quad \text{(Eq. B7)}$$

Quantitative risk assessment calculations

Risk assessment was performed using equations S8-S10. The benzo[a]pyrene equivalent concentration (BaP_{eq}) was used in these calculations. This was determined using:

$$\sum BaP_{eq} = \sum (C_i * RPF_i) \quad \text{(Eq. S8)}$$

C_i is the concentration of a given PAH in a clam sample, and RPF_i is the EPA's Relative Potency Factor for each PAH[88]. Average daily dose (ADD) was calculated using:

$$ADD = \frac{C * CF * IR * EF * ED}{BW * AT} \quad \text{(Eq. S9)}$$

ADD is the average daily dose, in mg/kg-day, C is the concentration in clams (ng/g), CF is a conversion factor, IR is the ingestion rate (g/d), EF is the exposure frequency (days/year), ED is the exposure duration (years), BW is body weight (kg) and AT is the averaging time. The AT includes the lifetime in years multiplied by 365 days/year. In this work, $\sum BaP_{eq}$ for a given sample was used as the concentration in clam tissue. The IR was set at 100g/day and 4.6 g/day for subsistence and average non-subsistence consumers respectively. The average adult BW was set at 70 kg, the average lifetime was set at 70 years, the EF was set at 365 days/year and ED was set at 70 years.

$$ELCR = ADD * SF \quad \text{(Eq. S10)}$$

ELCR is an estimate of excess lifetime cancer risk and SF is an oral slope factor. In this study, a SF of 7.3 mg/kg-d was used, based on the EPA's 2010 guidance [88].
There were 11 PAHs that were above the detection limits and had nonzero relative potency factors (RPFs) in clams. Thus, these were the 11 PAHs used in the carcinogenic risk assessment: benzo[c]fluorene, benzo[b]fluoranthene, fluoranthene, benzo[a]pyrene, benzo[a]anthracene, chrysene, benzo[j]fluoranthene, indeno[1,2,3-c,d]pyrene, benzo[k]fluoranthene, anthanthrene, and benzo[g,h,i]perylene

Appendix C: Supporting Information to Chapter 4 – Systematic developmental neurotoxicity assessment of a representative PAH Superfund mixture using zebrafish

Table C1. Aquatic environmental concentrations in 2010 as determined from passive sampling with LDPE. Data is reported previously with detailed methods, sampling locations, and quantification limits [132]. * PAH not in analytical method. BLOQ- values below limits of detection..

Locations	RM 7W-Jul	RM7E-Jul	RM6.5-Jul	RM7E-Aug	RM7W-Oct	RM7E-Oct
Naphthalene	3.3	1.9	19	2.5	0.38	1.0
2-Methylnaphthalene	0.74	0.41	3.7	0.45	0.55	0.71
1-Methylnaphthalene	0.49	0.30	2.2	0.36	0.33	0.49
2-Ethylnaphthalene	*	*	*	*	*	*
2,6-Dimethylnaphthalene	*	*	*	*	*	*
1,6-Dimethylnaphthalene	0.18	0.12	0.44	0.077	0.20	0.15
1,4-dimethylnaphthalene	*	*	*	*	*	*
1,5 dimethylnaphthalene	*	*	*	*	*	*
1,2-Dimethylnaphthalene	0.18	0.12	0.16	BLOQ	0.20	0.034
1,8-Dimethylnaphthalene	*	*	*	*	*	*
2,6-Diethylnaphthalene	*	*	*	*	*	*
Acenaphthylene	0.29	0.14	0.58	0.17	0.22	0.15
Acenaphthene	1.3	0.76	3.7	1.0	0.41	0.41
Fluorene	1.1	0.59	2.1	0.47	0.34	0.21
Dibenzothiophene	0.50	0.090	1.0	0.077	0.20	0.040
Phenanthrene	3.5	0.65	6.0	0.46	1.7	0.37
Anthracene	0.75	0.26	1.6	0.19	0.48	0.11
2-Methylphenanthrene	0.88	0.20	1.6	0.093	0.54	0.087
2-Methylanthracene	0.16	0.084	0.41	0.073	0.11	0.017
1-Methylphenanthrene	0.47	0.26	1.0	0.16	0.31	BLOQ
9-Methylanthracene	BLOQ	BLOQ	BLOQ	0.021	0.053	BLOQ
3,6-Dimethylphenanthrene	BLOQ	BLOQ	0.32	BLOQ	BLOQ	BLOQ
Fluoranthene	7.9	2.7	13	2.9	3.5	0.47
2,3-Dimethylanthracene	BLOQ	BLOQ	BLOQ	BLOQ	BLOQ	BLOQ
9,10-Dimethylanthracene	BLOQ	BLOQ	BLOQ	BLOQ	BLOQ	BLOQ
Pyrene	7.2	2.5	14	2.9	3.9	0.52
Retene	1.1	1.4	1.8	1.4	0.79	0.24
Benzo(a)fluorene	*	*	*	*	*	*
Benzo(b)flourene	*	*	*	*	*	*
Benzo(c)fluorene	*	*	*	*	*	*
1-Methylpyrene	0.15	0.066	0.33	0.094	0.11	0.016
Benz(a)anthracene	0.88	0.32	1.9	0.44	0.52	0.055
Cyclopenta(c,d)pyrene	*	*	*	*	*	*
Triphenylene	*	*	*	*	*	*
Chrysene	1.3	0.58	2.4	0.77	0.65	0.097
6-Methylchrysene	BLOQ	BLOQ	BLOQ	BLOQ	BLOQ	BLOQ
5-Methylchrysene	*	*	*	*	*	*
Benzo(b)fluoranthene	0.29	0.12	0.52	0.14	0.098	0.014
7,12-Dimethylbenz(a)anthracene	*	*	*	*	*	*
Benzo(k)fluoranthene	0.11	0.050	0.22	0.052	0.034	0.0050
Benzo(j)fluoranthene	*	*	*	*	*	*
Benzo(e)pyrene	0.17	BLOQ	0.27	0.047	0.093	0.016
Benzo(a)pyrene	0.079	BLOQ	0.36	0.033	0.063	0.0080
Indeno(1,2,3-c,d) pyrene	0.037	0.022	0.077	0.029	0.017	BLOQ
Dibenz(a,h)anthracene	0.013	0.011	0.022	BLOQ	BLOQ	BLOQ
Picene	*	*	*	*	*	*
Benzo(ghi)perylene	0.066	0.043	0.14	0.064	0.038	0.0070
Anthanthrene	*	*	*	*	*	*
Naptho[1,2-b]fluoranthene	*	*	*	*	*	*
Naptho[2,3-j]fluoranthene	*	*	*	*	*	*
Dibenzo(a,e)fluoroanthene	*	*	*	*	*	*
Dibenzo(a,l)pyrene	0.015	0.023	0.018	0.039	BLOQ	BLOQ
Naptho[2,3-k]fluoranthene	*	*	*	*	*	*
Naptho[2,3-e]pyrene	*	*	*	*	*	*
Dibenzo(a,e)pyrene	*	*	*	*	*	*
Coronene	*	*	*	*	*	*
Dibenzo(e,l)pyrene	*	*	*	*	*	*
Naptho[2,3-a]pyrene	*	*	*	*	*	*
Benzo(b)perylene	*	*	*	*	*	*
Dibenzo(a,i)pyrene	*	*	*	*	*	*
Dibenzo(a,h)pyrene	*	*	*	*	*	*

Table C2. Aquatic environmental concentrations in 2015 as determined from passive sampling with LDPE. Data is reported previously with detailed methods, sampling locations, and quantification limits[87]. BLOQ- values below limits of detection. .

Locations	RM11-B	RM11-T	RM7E-B	RM7E-T	RM6.5-B
Naphthalene	0.54	0.51	1.0	0.66	3.4
2-Methylnaphthalene	0.45	0.58	0.31	0.29	0.54
1-Methylnaphthalene	0.31	0.40	0.26	0.27	0.64
2-Ethylnaphthalene	0.066	0.081	0.062	0.043	0.096
2,6-Dimethylnaphthalene	0.21	0.24	0.22	0.18	0.38
1,6-Dimethylnaphthalene	0.21	0.23	0.23	0.18	0.36
1,4-dimethylnaphthalene	0.034	0.038	0.055	0.038	0.12
1,5 dimethylnaphthalene	0.036	0.043	0.062	0.042	0.096
1,2-Dimethylnaphthalene	0.043	0.053	0.062	0.048	0.12
1,8-Dimethylnaphthalene	BLOQ	BLOQ	BLOQ	BLOQ	BLOQ
2,6-Diethylnaphthalene	BLOQ	BLOQ	BLOQ	BLOQ	BLOQ
Acenaphthylene	0.079	0.11	0.13	0.15	0.76
Acenaphthene	0.34	0.44	1.6	1.2	3.8
Fluorene	0.27	0.31	0.77	0.58	1.5
Dibenzothiophene	0.018	0.019	0.050	0.034	0.29
Phenanthrene	0.35	0.39	0.65	0.48	3.0
Anthracene	0.099	0.11	0.22	0.17	0.91
2-Methylphenanthrene	0.17	0.17	0.15	0.15	1.0
2-Methylanthracene	0.050	0.058	0.063	0.061	0.30
1-Methylphenanthrene	0.10	0.11	0.13	0.10	0.50
9-Methylanthracene	0.030	0.027	0.042	0.030	0.040
3,6-Dimethylphenanthrene	0.095	0.10	0.11	0.10	0.32
Fluoranthene	1.3	1.1	2.4	2.1	8.6
2,3-Dimethylanthracene	0.037	0.044	0.037	0.039	0.15
9,10-Dimethylanthracene	BLOQ	BLOQ	BLOQ	BLOQ	BLOQ
Pyrene	1.1	1.1	1.7	1.6	11
Retene	2.2	0.59	0.93	0.80	0.92
Benzo(a)fluorene	0.11	0.12	0.18	0.19	0.71
Benzo(b)flourene	0.089	0.092	0.15	0.14	0.57
Benzo(c)fluorene	0.042	0.045	0.066	0.066	0.26
1-Methylpyrene	0.067	0.083	0.080	0.070	0.53
Benz(a)anthracene	0.12	0.13	0.23	0.20	1.6
Cyclopenta(c,d)pyrene	0.041	0.043	0.032	0.033	0.18
Triphenylene	0.10	0.10	0.13	0.13	0.55
Chrysene	0.15	0.16	0.28	0.23	1.8
6-Methylchrysene	0.014	0.021	0.034	0.016	0.058
5-Methylchrysene	BLOQ	BLOQ	BLOQ	BLOQ	BLOQ
Benzo(b)fluoranthene	0.063	0.060	0.096	0.065	0.58
7,12-	0.014	0.013	0.0097	0.0066	0.019
Benzo(k)fluoranthene	0.026	0.025	0.042	0.028	0.28
Benzo(j)fluoranthene	0.029	0.027	0.045	0.028	0.33
Benzo(e)pyrene	0.065	0.063	0.088	0.058	0.55
Benzo(a)pyrene	0.026	0.028	0.045	0.022	0.47
Indeno(1,2,3-c,d) pyrene	0.014	0.012	0.018	0.0085	0.11
Dibenz(a,h)anthracene	BLOQ	BLOQ	BLOQ	BLOQ	BLOQ
Picene	0.0071	0.0059	BLOQ	BLOQ	0.023
Benzo(ghi)perylene	0.024	0.021	0.029	0.014	0.15
Anthanthrene	0.0029	0.0025	0.0051	0.0011	0.020
Naptho[1,2-b]fluoranthene	BLOQ	BLOQ	BLOQ	BLOQ	BLOQ
Naptho[2,3-j]fluoranthene	BLOQ	BLOQ	BLOQ	BLOQ	BLOQ
Dibenzo(a,e)fluoroanthene	BLOQ	BLOQ	BLOQ	BLOQ	BLOQ
Dibenzo(a,l)pyrene	BLOQ	BLOQ	BLOQ	BLOQ	BLOQ
Naptho[2,3-k]fluoranthene	BLOQ	BLOQ	BLOQ	BLOQ	BLOQ
Naptho[2,3-e]pyrene	BLOQ	BLOQ	BLOQ	BLOQ	BLOQ
Dibenzo(a,e)pyrene	BLOQ	BLOQ	BLOQ	BLOQ	BLOQ
Coronene	0.0075	0.0061	BLOD	BLOD	0.017
Dibenzo(e,l)pyrene	BLOQ	BLOQ	BLOQ	BLOQ	BLOQ
Naptho[2,3-a]pyrene	BLOQ	BLOQ	BLOQ	BLOQ	BLOQ
Benzo(b)perylene	BLOQ	BLOQ	BLOQ	BLOQ	BLOQ
Dibenzo(a,i)pyrene	BLOQ	BLOQ	BLOQ	BLOQ	BLOQ
Dibenzo(a,h)pyrene	BLOQ	BLOQ	BLOQ	BLOQ	BLOQ

Locations	RM6.5-T1	RM6.5-T2	RM6.5-T3	RM3.5-B	RM3.5-T
Naphthalene	2.4	2.4	2.7	0.41	0.82
2-Methylnaphthalene	0.45	0.50	0.53	0.28	0.33
1-Methylnaphthalene	0.50	0.51	0.56	0.34	0.36
2-Ethylnaphthalene	0.081	0.084	0.085	0.059	0.059
2,6-Dimethylnaphthalene	0.30	0.31	0.33	0.24	0.23
1,6-Dimethylnaphthalene	0.30	0.31	0.32	0.26	0.25
1,4-dimethylnaphthalene	0.065	0.066	0.069	0.057	0.057
1,5 dimethylnaphthalene	0.0679	0.070	0.073	0.065	0.062
1,2-Dimethylnaphthalene	0.077	0.080	0.084	0.070	0.068
1,8-Dimethylnaphthalene	BLOQ	BLOQ	BLOQ	BLOQ	BLOQ
2,6-Diethylnaphthalene	BLOQ	BLOQ	BLOQ	BLOQ	BLOQ
Acenaphthylene	0.46	0.48	0.50	0.40	0.43
Acenaphthene	1.8	1.8	1.9	1.3	1.3
Fluorene	0.96	0.98	1.0	0.87	0.83
Dibenzothiophene	0.15	0.15	0.16	0.10	0.091
Phenanthrene	1.8	1.8	1.9	1.5	1.2
Anthracene	0.54	0.57	0.58	0.43	0.43
2-Methylphenanthrene	0.49	0.49	0.49	0.37	0.34
2-Methylanthracene	0.16	0.16	0.16	0.13	0.13
1-Methylphenanthrene	0.25	0.25	0.24	0.25	0.23
9-Methylanthracene	0.033	0.032	0.031	0.030	0.033
3,6-Dimethylphenanthrene	0.18	0.18	0.18	0.16	0.17
Fluoranthene	5.0	5.1	4.9	5.3	5.0
2,3-Dimethylanthracene	0.088	0.089	0.087	0.076	0.081
9,10-Dimethylanthracene	BLOQ	BLOQ	BLOQ	BLOQ	BLOQ
Pyrene	5.9	5.7	5.8	5.6	5.5
Retene	0.99	0.97	0.99	1.4	1.3
Benzo(a)fluorene	0.47	0.45	0.45	0.43	0.43
Benzo(b)flourene	0.36	0.34	0.33	0.33	0.32
Benzo(c)fluorene	0.16	0.15	0.16	0.15	0.14
1-Methylpyrene	0.25	0.25	0.24	0.21	0.21
Benz(a)anthracene	0.82	BLOQ	0.81	0.70	0.71
Cyclopenta(c,d)pyrene	0.084	0.086	0.080	0.053	0.058
Triphenylene	0.31	0.29	0.29	0.30	0.27
Chrysene	0.86	0.91	0.87	0.80	0.80
6-Methylchrysene	0.031	0.040	0.032	0.031	0.031
5-Methylchrysene	BLOQ	BLOQ	BLOQ	BLOQ	BLOQ
Benzo(b)fluoranthene	0.25	0.28	0.25	0.24	0.22
7,12-	0.012	0.013	0.012	0.011	0.010
Benzo(k)fluoranthene	0.12	0.13	0.12	0.11	0.10
Benzo(j)fluoranthene	0.13	0.15	0.13	0.13	0.11
Benzo(e)pyrene	0.21	0.24	0.21	0.21	0.19
Benzo(a)pyrene	0.16	0.18	0.15	0.13	0.13
Indeno(1,2,3-c,d) pyrene	0.030	0.048	0.030	0.037	0.031
Dibenz(a,h)anthracene	BLOQ	BLOQ	BLOQ	BLOQ	BLOQ
Picene	0.0076	0.012	0.0076	0.010	0.0081
Benzo(ghi)perylene	0.046	0.065	0.045	0.052	0.045
Anthanthrene	0.0062	0.0094	0.0061	0.0077	0.0070
Naptho[1,2-b]fluoranthene	BLOQ	BLOQ	BLOQ	BLOQ	BLOQ
Naptho[2,3-j]fluoranthene	BLOQ	BLOQ	BLOQ	BLOQ	BLOQ
Dibenzo(a,e)fluoroanthene	BLOQ	BLOQ	BLOQ	BLOQ	BLOQ
Dibenzo(a,l)pyrene	BLOQ	BLOQ	BLOQ	BLOQ	BLOQ
Naptho[2,3-k]fluoranthene	BLOQ	BLOQ	BLOQ	BLOQ	BLOQ
Naptho[2,3-e]pyrene	BLOQ	BLOQ	BLOQ	BLOQ	BLOQ
Dibenzo(a,e)pyrene	BLOQ	BLOQ	BLOQ	BLOQ	BLOQ
Coronene	0.00579	0.011	0.0053	0.0069	0.0055
Dibenzo(e,l)pyrene	BLOQ	BLOQ	BLOQ	BLOQ	BLOQ
Naptho[2,3-a]pyrene	BLOQ	BLOQ	BLOQ	BLOQ	BLOQ
Benzo(b)perylene	BLOQ	BLOQ	BLOQ	BLOQ	BLOQ
Dibenzo(a,i)pyrene	BLOQ	BLOQ	BLOQ	BLOQ	BLOQ
Dibenzo(a,h)pyrene	BLOQ	BLOQ	BLOQ	BLOQ	BLOQ

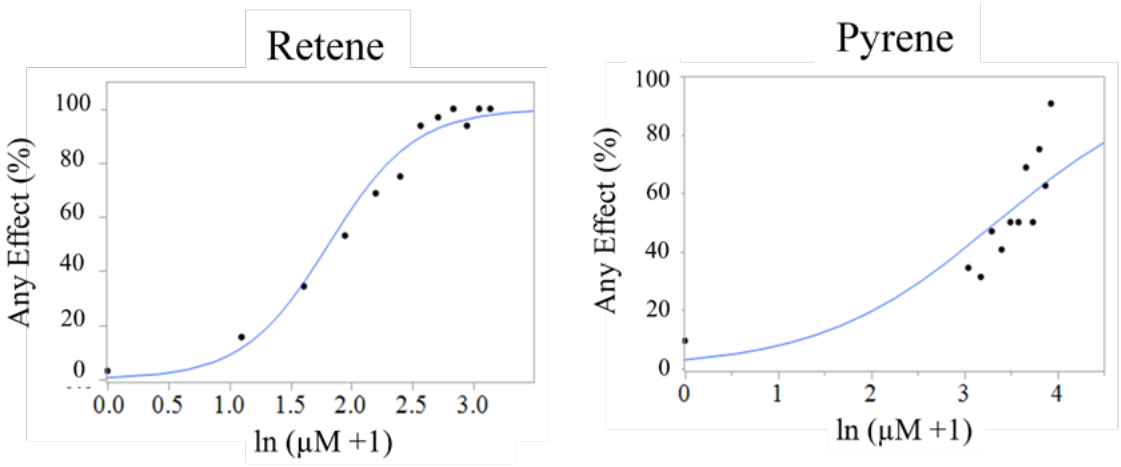

Figure C1. Individual dose response curves. N=1 replicate experiment. Each point represents n= 32 fish dosed in individual wells .

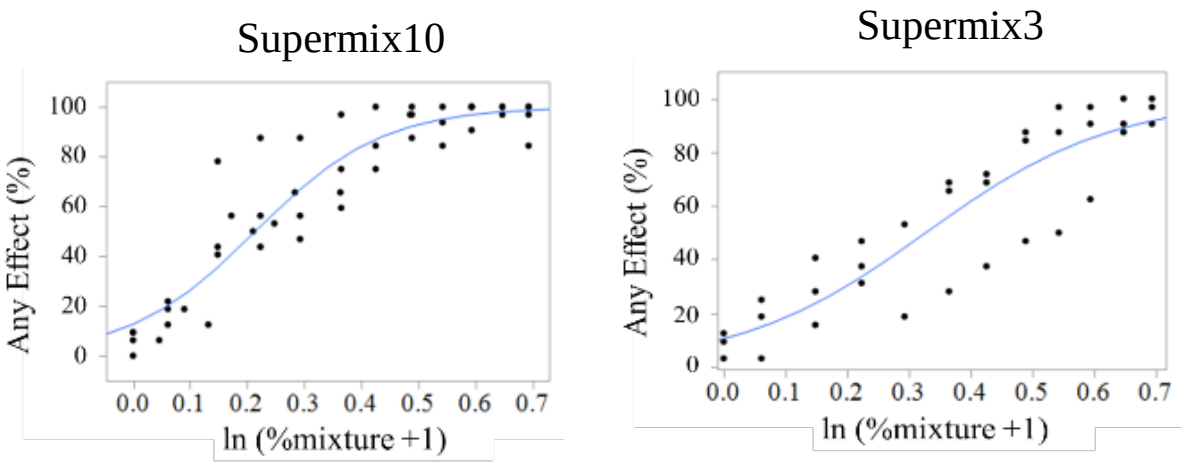

Figure C2. Mixture dose response curves. N=4 and N=3 replicate experiments for Supermix10 and Supermix3 respectively. Each point represents n=32 fish dosed in individual wells.